CO-COMBUSTION OF COAL AND OLIVE CAKE IN A FLUIDIZED BED WITH LIMESTONE ADDITION AND FREEBOARD EXTENSION

A THESIS SUBMITTED TO
THE GRADUATE SCHOOL OF NATURAL AND APPLIED SCIENCES
OF
MIDDLE EAST TECHNICAL UNIVERSITY

BY

ONUR AKPULAT

IN PARTIAL FULLFILLMENT OF THE REQUIREMENTS
FOR
THE DEGREE OF MASTER OF SCIENCE
IN
ENVIRONMENTAL ENGINEERING

SEPTEMBER 2009

Approval of the thesis:

CO-COMBUSTION OF COAL AND OLIVE CAKE IN A FLUIDIZED BED WITH LIMESTONE ADDITION AND FREEBOARD EXTENSION

submitted by **ONUR AKPULAT** in partial fulfillment of the requirements for the degree of **Master of Science in Environmental Engineering Department, Middle East Technical University** by,

Prof. Dr. Canan Özgen
Dean, Graduate School of **Natural and Applied Sciences** ____________________

Prof. Dr. Göksel Demirer
Head of Department, **Environmental Engineering** ____________________

Prof. Dr. Aysel Atımtay
Supervisor, **Environmental Engineering Dept., METU** ____________________

Examining Committee Members:

Prof. Dr. F. Dilek Sanin
Environmental Engineering Dept., METU ____________________

Prof. Dr. Aysel Atımtay
Environmental Engineering Dept., METU ____________________

Prof. Dr. Gürdal Tuncel
Environmental Engineering Dept., METU ____________________

Assoc. Prof. Dr. İpek İmamoğlu
Environmental Engineering Dept., METU ____________________

Assoc. Prof. Dr. Hayati Olgun
Energy Institute, TÜBİTAK MAM ____________________

Date: **09.09.2009**

I hereby declare that all information in this document has been obtained and presented in accordance with academic rules and ethical conduct. I also declare that, as required by these rules and conduct, I have fully cited and referenced all material and results that are not original to this work.

Name, Last name : Onur Akpulat

Signature :

ABSTRACT

CO-COMBUSTION OF COAL AND OLIVE CAKE IN A FLUIDIZED BED WITH LIMESTONE ADDITION AND FREEBOARD EXTENSION

Akpulat, Onur
M.Sc., Department of Environmental Engineering
Supervisor: Prof. Dr. Aysel Atımtay

September 2009, 151 pages

In this study, flue gas emissions and combustion efficiencies during combustion and co-combustion of olive cake and coal are investigated in a bubbling fluidized bed with an inside diameter of 102 mm and a height of 900 mm and 1900 mm. Tunçbilek lignite coal and Edremit olive cake were used in the experiments as fuels. Temperature distributions along the combustion column were continuously measured. Flue gas concentrations of O_2, CO, SO_2 and NO_x were measured during combustion experiments. Four sets of experiments were performed in order to examine the effect of fuel composition, excess air ratio, freeboard extension and limestone addition on flue gas emissions and combustion efficiency. The olive cake addition to coal were 25, 50, 75 % by wt. The bed temperature on the average was 850 ^{o}C.

The results of the experiments showed that coal combustion occurs at lower parts of the combustion column whereas olive cake combustion takes place more in the freeboard region. As olive cake percentage in the fuel mixture increased, CO emissions increased, SO_2 and NO_x emissions decreased. The reason for the decrease of NO_x emissions with increasing percentage of olive cake in the fuel mixture was due to a reducing atmosphere created in the combustion column. Mostly combustion losses resulted mainly from the unburnt carbon in the fly ash.

With the freeboard extension, noticeable decrease in CO emissions and slight increase in combustion efficiencies were observed. Among the limestones tested, Çan limestone gave the best result with Ca/S = 3 at an optimum bed temperature of 850 ^{o}C. The SO_2 reduction was 87% at this Ca/S ratio. For co-combustion experiments, it was observed that SO_2 adsorption efficiency of limestone increased with the addition of olive cake to the fuel mixture.

Key Words: Co-combustion of lignite coal and biomass, Bubbling fluidized bed combustor, Olive cake combustion, Lignite coal combustion, Freeboard extension, SO_2 removal.

ÖZ

KÖMÜR VE PRİNANIN KİREÇTAŞI EKLENEREK VE SERBEST BÖLGE UZATILARAK AKIŞKAN YATAKTA BİRLİKTE YAKILMASI

Akpulat, Onur
Yüksek Lisans, Çevre Mühendisliği Bölümü
Tez Yöneticisi: Prof. Dr. Aysel Atımtay

Eylül 2009, 151 sayfa

Bu çalışmada, prina ve kömürün ayrı ayrı ve birlikte yakılması sırasında ortaya çıkan emisyonlar ve yanma verimleri, 102 mm iç çapında, 900 mm ve 1900 mm yüksekliğinde bir kabarcıklı akışkan yatakta incelenmiştir. Deneylerde yakıt olarak Tunçbilek linyit kömürü ve Edremit prinası kullanılmıştır. Yakma kolonu boyunca sıcaklık profilleri sürekli olarak ölçülmüştür. Yakma deneyleri esnasında oluşan baca gazında O_2, CO, SO_2 ve NO_x konsantrasyonları ölçülmüştür. Yakıt karışım oranı, fazla hava oranı, yakma kolonunun yüksekliği ve kireçtaşı eklemenin emisyonlar ve yanma verimi üzerindeki etkilerini incelemek için dört set yakma deneyleri yapılmıştır. Kömüre ağırlıkça % 25, 50 ve 75 oranlarında prina katılmıştır. Ortalama yatak sıcaklığı 850 ^{o}C'dir.

Deney sonuçları, kömürün yakma kolonun alt kısımlarında, prinanın ise daha ziyade serbest bölgede yandığını göstermiştir. Yakıt karışımındaki prina yüzdesi arttıkça, CO emisyonları artmış, SO_2 ve NO_x emisyonları azalmıştır. Prinanın yakıt karışımındaki yüzdesinin artması ile NO_x emisyonlarının azalması, yakma kolonu içinde oluşan indirgen atmosfere bağlıdır. Genellikle yanma kayıplarının çoğu uçucu küldeki yanmamış karbondan kaynaklanmaktadır.

Yakma kolonunun yükseltilmesi ile birlikte, CO emisyonlarında fark edilir bir düşüş ve yanma verimlerinde hafif bir artış gözlenmiştir. Test edilen kireçtaşları arasında Çan kireçtaşı, optimum yatak sıcaklığı olan 850 ^{o}C'de en iyi adsorplama verimini Ca/S = 3 olduğu zaman vermiştir. Bu Ca/S oranında SO_2 giderimi % 87'dir. Birlikte yakma deneylerinde, yakıt karışımına prina eklenmesi ile kireçtaşının SO_2 adsorplama veriminin arttığı gözlenmiştir.

Anahtar Sözcükler: Linyit kömürü ve prinanın birlikte yakılması, Kabarcıklı akışkan yataklı yakıcı, Prina yanması, Linyit kömürü yanması, Serbest bölgenin uzatılması, SO_2 giderimi.

To My Parents

ACKNOWLEDGMENTS

First of all, I would like to express my deepest gratitude to my supervisor Prof. Dr. Aysel Atımtay for her guidance, precious comments and encouragement throughout this study.

I would also like to thank Murat Varol for his motivation, guidance and companionship during my whole study. I am grateful for his help and patience from the beginning of the experiments to the end of this thesis.

I also thank to “TÜBİTAK MAM Energy Institute, Coal and Biomass Combustion and Gasification Laboratory” research group members for their support during the experiments, in particular Assoc. Prof. Dr. Hayati Olgun.

And finally, I am indebted to my parents, Neriman and Hüseyin Akpulat, for their endless motivation, encouragement and faith in me, not only during this study but also throughout my whole life.

TABLE OF CONTENTS

CHAPTERS

APPENDICES

LIST OF TABLES

TABLES

LIST OF FIGURES

FIGURES

LIST OF SYMBOLS AND ABBREVIATIONS

Symbols:

Ash_{bottom} : Amount of bottom ash formed during combustion, kg ash/h
Ash_{fly} : Amount of fly ash formed during combustion, kg ash/h
Ca/S : Calcium to sulfur ratio (-)
$CaCO_3\%$: $CaCO_3$ percentage in limestone
C_{bottom} : Unburnt carbon content in the bottom ash, kg C/ kg ash
C_{fly} : Unburnt carbon content in the fly ash, kg C/ kg ash
$C_{SO2,th}$: Theoretical SO_2 emission concentration from combustion of Tunçbilek lignite coal, mg/Nm^3
$C_{NO,th}$: Theoretical NO emission concentration from combustion of Tunçbilek lignite coal, mg/Nm^3
d_p : Particle diameter, mm
g : Gravitational acceleration, cm/s^2
HHV : Higher heating value, kJ/kg
H_{L_Char} : Lower heating value of char, MJ/kg char
H_{L_CO} : Lower heating value of CO, MJ/Nm^3 CO
H_{L_fuel} : Lower heating value of the fuel used, MJ/kg fuel
$L_{bottom\ ash}$: Total C loss resulted from carbon in bottom ash, %
L_{CO} : Total C loss resulted from CO formation, %
$L_{fly\ ash}$: Total C loss resulted from carbon in fly ash, %
LHV : Lower heating value, kJ/kg
L_m : Height of fixed bed, cm
L_{mf} : Height of bed at minimum fluidization, cm
M_f : Fuel feeding rate, kg fuel/h
MW_X : Molecular weight of X, g/mole
m_X : Amount of X in 100 g of fuel, g/100g fuel

$N_{2,atm}$: Atmospheric nitrogen percentage (79.1%)

$n_{air,actual}$: Actual mole of air required for the combustion of 100 g of fuel, mole air/100 g fuel

$n_{air,th}$: Mole of air theoretically required for the combustion of 100 g of fuel, mole air/100 g fuel

n_{CO2} : Mole of CO_2 coming from the combustion of 100 g of Tunçbilek coal, mole/100 g fuel

$n_{fluegas,th(w.b)}$: Mole of theoretical total flue gas coming from the combustion of 100 g of Tunçbilek coal, mole/100 g fuel

$n_{fluegas,th(w.b)}$: theoretical total flue gas coming from the combustion of 100 g of coal (on wet basis), mole/100 g fuel

n_{H2O} : Mole of H_2O coming from the combustion of 100 g of coal, mole/100 g fuel

$n_{H2O,air}$: Mole of water vapor in air required for the combustion of 100 g of fuel, mole H_2O/100 g fuel

$n_{H2O,fuel}$: Mole of H_2O coming from coal, mole/100 g fuel

Nm^3 : Volume (m^3) at normal conditions (0^oC, 1 Atm)

n_{N2} : The mole of N_2 supplied for 100 g of fuel, mole N_2/100 g fuel

n_{NO} : Mole of NO coming from the combustion of 100 g of coal, mole/100 g fuel

$n_{O2,ex}$: Mole of excess O_2 supplied to the system, mole O_2/100 g fuel

$n_{O2,th}$: Mole of oxygen theoretically required for the combustion of 100 g of fuel, mole O_2/100 g fuel

n_{SO2} : Mole of SO_2 coming from the combustion of 100 g of coal, mole/100 g fuel

$O_{2,atm}$: Atmospheric oxygen percentage (20.9%)

Q_f : Total thermal capacity of the system, kW

Re : Reynolds number

RH : Relative humidity, %

S% : S percentage in fuel

u_{mf} : Minimum fluidization velocity at room temperature, m/s

u_o : Superficial gas velocity, m/s

$V_{air,actual}$: Actual volume of air required for the combustion of one kg of fuel, Nm^3/kg fuel

$V_{fluegas,actual}$: Actual amount of total flue gas formed, Nm^3/kg fuel

$V_{fluegas,th(w.b)}$: Volume of theoretical total flue gas formed on wet basis for the combustion of one kg of fuel, Nm^3/kg fuel

W : Actual mixing ratio, g H_2O/kg of air

W/A : Weight of particles / cross sectional area of the column

W_s : Saturation mixing ratio, g H_2O/kg of air

η : Overall combustion efficiency, %

λ : Excess air ratio (-)

Δp_{max} : Maximum pressure drop across the bed, mm water

ε : Void fraction of fixed bed (-)

μ : Viscosity of air at 20°C, g-cm/s

ρ_f : Air density at 20°C, g/cm^3

ε_{mf} : Void fraction at minimum fluidization (-)

ρ_s : Solid (sand) density, g/cm^3

ϕ_s : Sphericity of an average sand particle (-)

Abbreviations:

BFB : Bubbling fluidized bed

BFBC : Bubbling fluidized bed combustor

CFB : Circulating fluidized bed

CFBC : Circulating fluidized bed combustor

CH_4 : Methane

C_mH_n : Hydrocarbons

CO : Carbon monoxide

CO_2 : Carbon dioxide

COP7 : 7th Conference of Parties

EU : European Union

FAO	: Food and Agriculture Organization
FBC	: Fluidized bed combustion
HCl	: Hydrogen chloride
ICRE	: International Conference for Renewable Energies
IEA	: International Energy Agency
LCP BREF	: Reference Document on Best Available Techniques for Large Combustion Plants
LPG	: Liquefied petroleum gas
MENR	: Ministry of Energy and Natural Sources
MSW	: Municipal solid waste
MTA	: Mineral Research and Exploration
MTEP	: Million tons equivalent of petroleum
MW_e	: Mega watt electric
MW_{th}	: Mega watt thermal
N_2O	: Nitrous oxide
NH_3	: Ammonia
NMVOC	: Non-Methane Volatile Organic Components
NO	: Nitric oxide
NO_2	: Nitrogen dioxide
NO_x	: Nitrogen oxides
O_3	: (Ground level) Ozone
OC	: Olive cake
OGRI	: Olive Growing Research Institute
PAH	: Polycyclic Aromatic Hydrocarbons
PCDD/F	: Polychlorinated dioxins and furans
RCAPIS	: Turkish Regulation for Control of Air Pollution from Industrial Sources
REC	: Regional Environmental Center
SO_2	: Sulfur dioxide
SO_x	: Sulfur oxides
SS	: Sewage sludge
TC	: Thermocouple

TSI : Turkish Statistical Institute
UNFCCC : United Nations Framework Convention on Climate Change
VM : Volatile Matter

CHAPTER 1

INTRODUCTION

1.1. General

Global energy needs have been growing rapidly as the world population increases. Nowadays most of this energy demand is met by fossil fuels. Not only developing countries but also developed countries are still using fossil fuels. However, fossil fuels are finite in resources and eventually they will be consumed away. Moreover, their consumption leads to irrecoverable damages (greenhouse gases, air pollution, water and soil contamination etc.) on the environment. At this point, renewable energy has come into question as a supplementary or alternative resource for energy production. Renewable energy sources such as solar, wind, geothermal, hydropower and biomass energy have much lower impacts on environment than conventional energy sources. Since usage of indigenous supply is so important for developing countries such as Turkey, renewable energy utilization will be very crucial also in decreasing reliance on energy imports. Therefore, renewable energy should be attached much more importance in order to reduce environmental effects of fossil fuels and increase sustainable energy production.

Modern biomass is seen as one of the most promising renewable energy sources in the near future. The utilization of biomass within the European Union (EU) has strongly increased over the last decades, and the ambitions of the EU for the use of biomass are high (Junginger et al., 2006). Biomass energy is one of the advantageous renewable energy sources and defined as the biological material that can be used as fuel or for industrial production. Agricultural residues, animal wastes, forestry and wood processing residues, municipal and industrial wastes are the major types of biomass. Both greenhouse gas emissions and air pollutants can be reduced by biomass utilization. The basic idea of using biomass as a renewable energy resource is that CO_2 emitted to the atmosphere as a result of the biomass combustion is captured as carbon from ambient CO_2 in growing biomass by photosynthesis. As a result of this, "almost zero net CO_2" emission is added into the atmosphere. As well as reducing $CO_{2,}$ one of the major greenhouse gases, low sulfur and nitrogen content of the of biomass leads to lower SO_2 and NO_x emissions when it is compared with fossil fuels.

On the other hand, there are some doubts whether biomass fuels are CO_2 neutral or not. Some opposite views claim that extra energy is needed to produce fertilizers and pesticides, farm and harvest the crop and transport the biomass to a power plant and most of this energy comes from fossil fuels, which emit CO_2. However unlike other sources, biomass can actually absorb CO_2 released by burning fossil fuels also. According to Thomas (2007), 20 percent of CO_2 released by fossil fuels could be absorbed by planting energy crops. In addition to the additional CO_2 sources, oppositions claim that there will be some interval of time between the release of CO_2 into the atmosphere when the biomass is burned, and the removal of a corresponding amount of CO_2 when replacement plants are grown. However, if biomass fuels are produced in a responsible and sustainable way, they can compensate this time difference and be carbon neutral sources (Thomas, 2007).

The Kyoto Protocol

The decision No: 26 of 7th Conference of Parties (COP7) to the United Nations Framework Convention on Climate Change (UNFCCC), convened in Marrakesh in 2001, invited Parties to recognize the special circumstances of Turkey, which place Turkey, after becoming a Party, in a situation different from that of other

Parties included in Annex I to the Convention. Thus, Turkey acceded as the 189th Party to the UNFCCC on 24 May 2004, ten years after its entry into force (REC Turkey, 2008). Turkey has today signed the Kyoto Protocol four years after it came into force in 2005. By complying this protocol which aims to mitigate the emissions of greenhouse gases to the 1990's level, Turkey will become part of the construction of a new global climate change regime. Now in a position to shape the post-2012 debates, Turkey must be ready to take up its responsibilities (REC, 2009).

The aim of the European Commission is to increase the share of the renewable energy sources in overall energy consumption to 20% by 2020. This was set as a binding target by the European Commission in its energy package in spring 2007. Additionally, within the Biomass Action Plan which was published at the end of 2005, the European Commission encourages the EU member States to harness the potential of all cost effective forms of electricity generation from biomass. Co-combustion of biomass is one of the promising technologies. It is an important technology for CO_2-neutral electricity generation. In many countries biomass co-combustion is one of the most economic ways to save CO_2. The major advantages of co-combustion are the common utilization of existing plants, the fuel flexibility, a wide range of usable fuels and the attainment of higher overall efficiencies for power generation from biomass (VGB Powertech, 2008). Co-combustion can be achieved in various ways for several purposes.

Fluidized bed is one of the most promising methods for combustion today. Its application to boilers is recognized primarily for its low sensitivity to fuel quality and its capacity to limit air pollution. This technology is being used for co-combustion of coal and waste fuels (Patumsawad, 2001).

1.2. Energy Review of Turkey

According to the total primary energy production and supply data provided by Ministry of Energy and Natural Sources, Turkey met **74.49%** of its energy from imports in 2007. Considering this percentage, it is very obvious that Turkey is an energy importing country. As it is represented in Figure 1.1, Turkey's energy importation has been increasing year by year, as a result of low increase in production and high increase in demand. Total primary energy supply, which was approximately **108 MTEP** in 2007, is projected to be **222 MTEP** in 2020. As the difference between energy production and supply increases in that way and if necessary precautions are not taken, our dependence on foreign sources will increase more and more in the future (MENR, 2009).

The increase of energy imports between 1985 and 2007 can be seen in detail from Table 1.1 and Figure 1.1. Shares of energy production and net energy imports in the total energy supply are represented in the table as units of MTEP (million tons equivalent of petroleum) and as percentages. In addition to this, energy production and supply projections for Turkey between 2010 and 2020 are given in Table 1.2.

Table 1.1 Energy situation of Turkey between 1985 and 2007 (MENR, 2009)

	Total Production, MTEP	**Total Net Import, MTEP**	**Total Supply, MTEP**	**Total Production, %**	**Total Net Import, %**
1985	21.94	17.46	39.40	55.68%	44.32%
1990	25.48	27.51	52.99	48.08%	51.92%
1995	26.72	36.96	63.68	41.96%	58.04%
1999	27.66	46.62	74.28	37.24%	62.76%
2000	26.05	54.45	80.50	32.36%	67.64%
2001	24.58	50.83	75.40	32.59%	67.41%
2002	24.28	54.05	78.33	31.00%	69.00%
2003	23.78	60.04	83.83	28.37%	71.63%
2004	24.33	63.49	87.82	27.71%	72.29%
2005	24.55	66.52	91.07	26.96%	73.04%
2006	26.76	73.06	99.82	26.81%	73.19%
2007	27.45	80.17	107.62	**25.51%**	**74.49%**

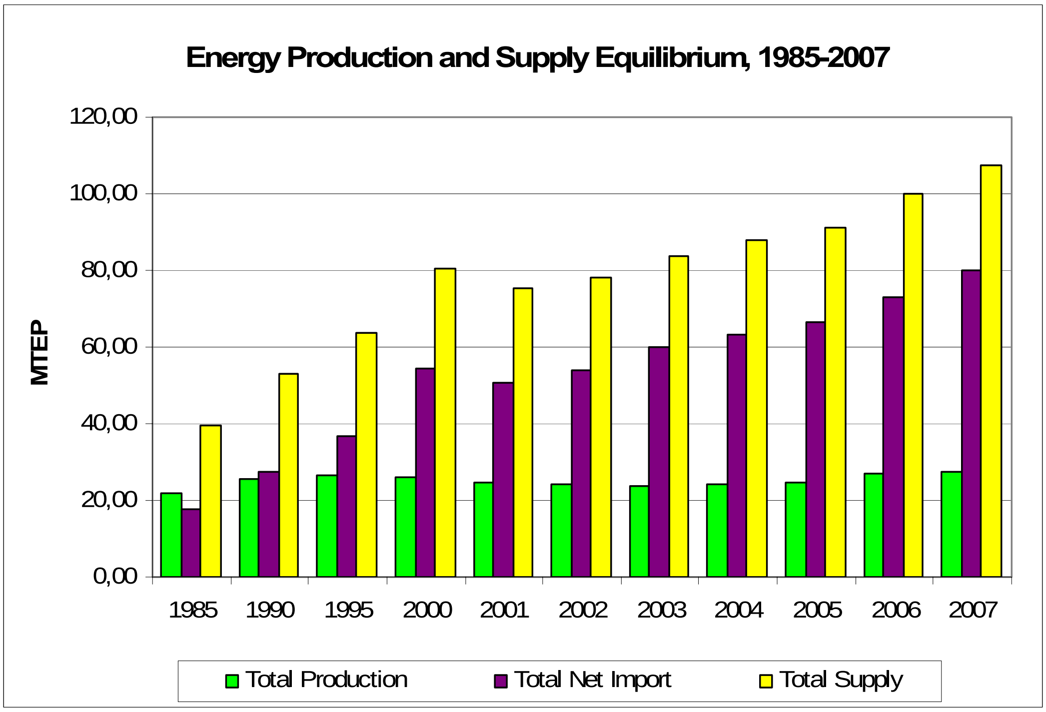

Figure 1.1 Energy production and supply equilibrium between 1985 and 2007 in Turkey (MENR, 2009)

Table 1.2 Projections for energy situation of Turkey between 2010 and 2020 (MENR, 2009)

	Total Production, MTEP	**Total Net Import, MTEP**	**Total Supply, MTEP**
2010	37.52	88.76	126.27
2015	54.51	115.64	170,15
2020	66.09	156.33	**222.42**

According to the last data collected in 2007, the total primary energy production of Turkey is 27.45 MTEP which meets only 25.51 % of the total primary energy supply. As it can be seen from Figure 1.1, while net energy imported is increasing continuously, our energy production stays nearly constant. Therefore, total primary energy supply has been always showing an increasing trend between

1985 and 2007 except for the decrease in year 2001. The reason of this decrease is the economical crisis broken out in that year.

The share of imported energy has reached to 74.49% in 2007 while it is 44.32% in 1985. This sharp increase in imported energy between 1985 and 2007 is clearly seen in Figure 1.2. In 2007, Turkey imported 80.17 MTEP of energy from foreign sources.

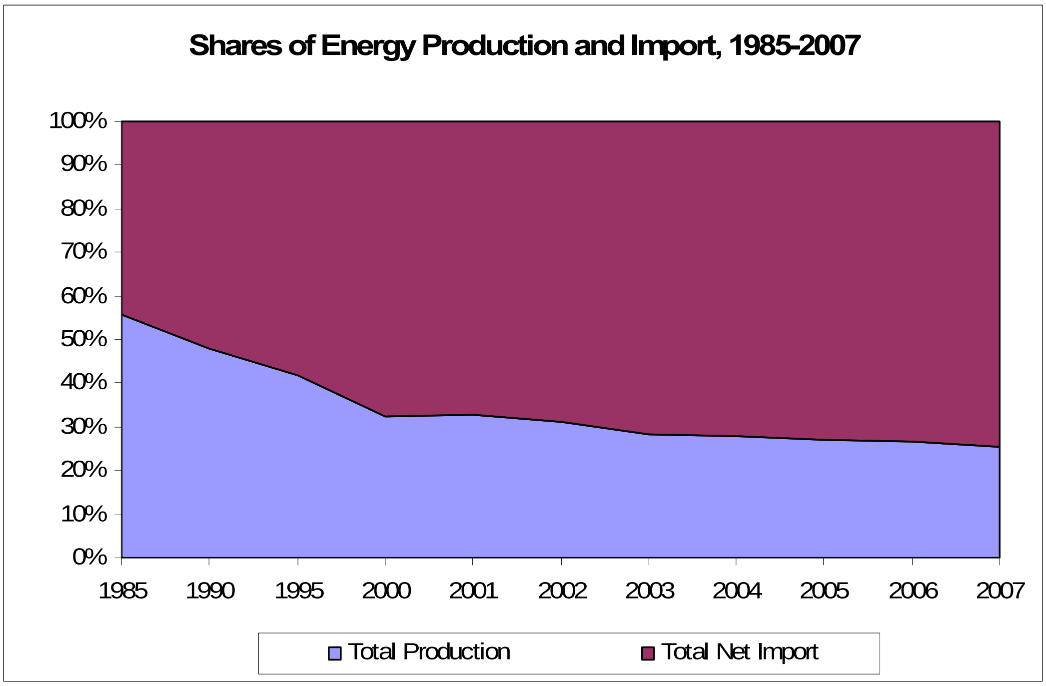

Figure 1.2 Shares of energy production and net imports in Turkey between 1985 and 2007 (MENR, 2009)

Figure 1.3 represents the evolution of total primary energy supply in Turkey between 1985 and 2007. Coal, oil and natural gas usage have increased almost every year. However the most dramatic increase is observed in natural gas usage. Natural gas share in total primary energy supply was not even 1% in 1985 however this number has reached to 31.55% (usage of 33.95 MTEP) in 2007.

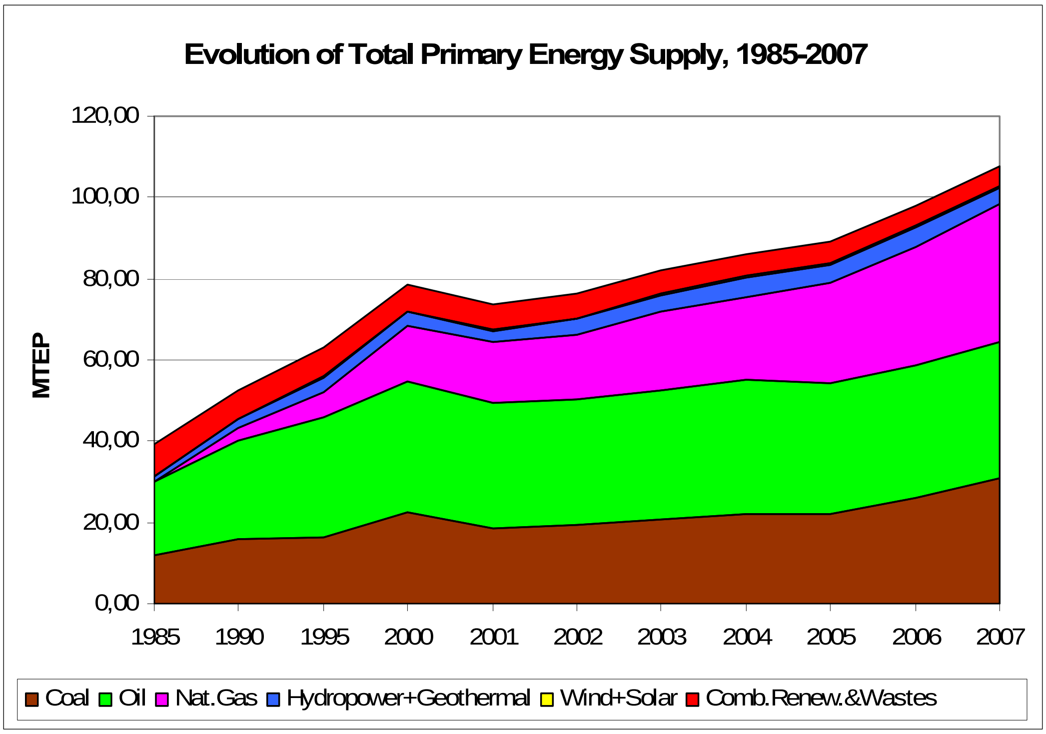

Figure 1.3 Evolution of total primary energy supply between 1985 and 2007 in Turkey (MENR, 2009)

When Figure 1.4 is looked over, it is clearly seen that oil, natural gas and coal constitute the biggest portion of the total primary energy supply of Turkey in 2007. The rest contains energy obtained from renewable sources (combustible renewables and wastes, hydropower, geothermal, solar and wind) which has reached to 9.58 MTEP (with a total share of 8.91%) in 2007.

Total energy production in Turkey in 2007 is given in Figure 1.5. At first glance coal stands out with a big portion in the figure. More than half (53.92%) of the Turkey's total energy production is met by coal. Another big share is constituted by the combustible renewables and wastes. Especially in rural areas, high energy is obtained from uncontrolled combustion of those wastes. Therefore, these amounts of energy can not be disregarded. Their share in the total primary energy production is 19.32% in 2007. Hydropower + geothermal energy is another important energy resource and has a share of 15.05% in 2007 total primary energy production of Turkey.

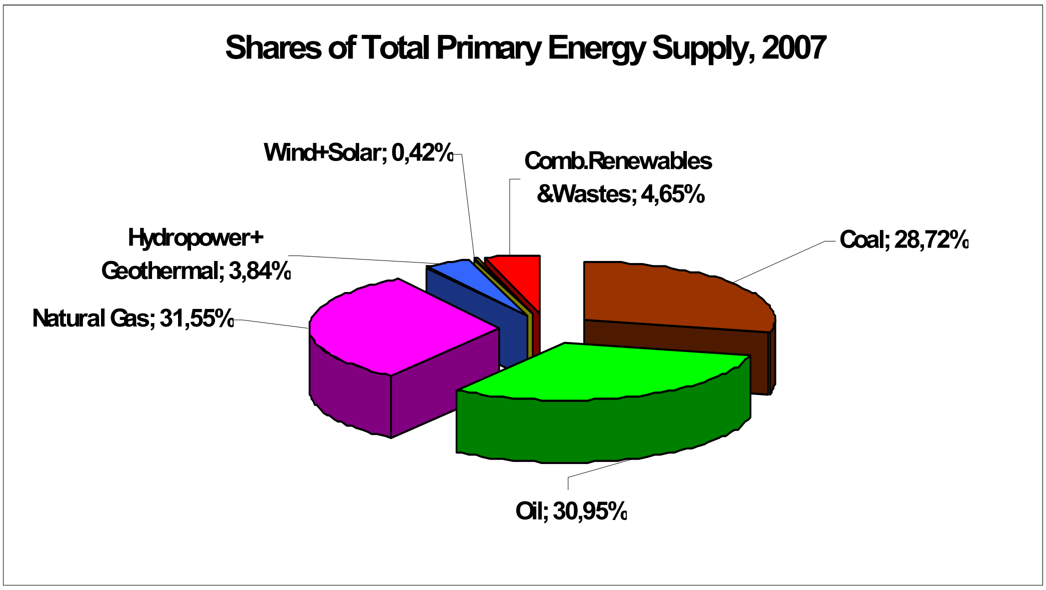

Figure 1.4 Shares of total primary energy supply of Turkey in 2007 (MENR, 2009)

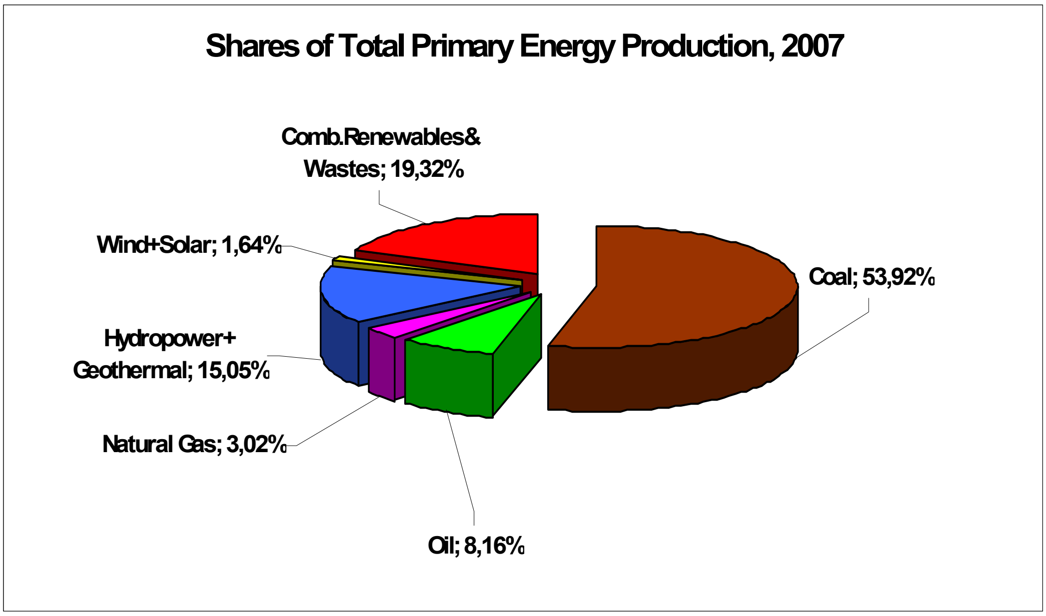

Figure 1.5 Shares of total primary energy production of Turkey in 2007 (MENR, 2009)

1.3. Biomass Energy Potential of Turkey

In Turkey, there is a use of conventional biomass in the form of wood and dried dung; however, modern biomass use is limited related to energy crops. The technical potential of conventional biomass is about 10 MTEP while the currently available potential is about 7 MTEP/year in Turkey. However, it would be more agreeable to use the technical potential of modern biomass instead of conventional biomass. In this regard, the technical potential of Turkey is about 40 MTEP and the currently available potential is about 25 MTEP/year (Table 1.3). The amount of vegetable waste (in dry form) from grain plants in Turkey is about 55–70 million tons. The available part of this waste, which could be used in several areas including power plants, is about 37–48 million tons (Ozgur, 2008).

Table 1.3 Biomass Energy Potential of Turkey (Ozgur, 2008)

Usage Kind of Energy	Natural Potential	Technical Potential	Economic Potential
Fuel (classic) (MTEP/year)	30	10	7
Fuel (modern) (MTEP/year)	90	40	25

1.3.1. Olive and Olive Cake Production in Turkey

In Turkish economy, agriculture as well as the production and exportation of industrial products based on agriculture have a significant contribution in country’s economy. These agricultural products mainly include olive and olive oil. The importance of olive production sector in Turkey is so great that can not be disregarded (Kayali et al., 2008). According to the data gathered from Turkish Statistical Institute (TSI), in 2009, Turkey has harvested approximately 106 million bearing olive trees on an area of 774,000 hectares. This makes 3.16% of the total agricultural area of Turkey (approx. 25 million hectares).

Olive production throughout the world, between 2004 and 2007 are given in Table 1.4. In most of the countries, olive production highly varies with the fluctuation of high crop and low crop years. Due to these big differences in the production, last 11 years’ average olive production quantities and shares of countries in total world production are given in this table. Distribution of olive production quantities is clearly seen from the graphical representation of the country shares in Figure 1.6.

Table 1.4 World olive production between 2004 and 2007, last 11-years' average and shares of countries (FAO, 2008)

	Olive Production Quantity (tons)					**Shares of Countries, % (1997-2007)**
	2004	**2005**	**2006**	**2007**	**1997-2007 Average**	
Spain	5,200,029	4,021,720	5,472,500	5,787,600	5,252,331	32.65
Italy	4,534,231	3,774,812	3,415,683	3,481,379	3,429,585	21.32
Greece	2,204,020	2,646,447	2,410,467	2,600,000	2,355,926	14.64
Turkey	***1,600,000***	***1,200,000***	***1,766,749***	***1,525,005***	***1,263,796***	***7.86***
Tunisia	650,000	600,000	1,050,000	900,000	747,727	4.65
Syria	1,027,200	501,000	510,000	550,000	639,334	3.97
Morocco	500,000	750,000	631,210	657,000	576,855	3.59
Portugal	312,124	211,873	373,400	375,000	289,512	1.80
Egypt	315,193	310,000	315,000	318,000	278,371	1.73
Algeria	468,800	316,489	264,733	300,000	266,722	1.66
Libya	180,000	180,000	160,000	165,000	178,636	1.11
Others	1,015,099	959,101	825,964	797,506	810,019	5.03
World	18,006,696	15,471,442	17,195,706	17,456,490	16,088,815	100.00

As it is seen in Table 1.4 and Figure 1.6, Turkey has the 4th place in world olive production with 7.86% share. According to the last 11-years' average (1997-2007), Turkey produced 1,263,796 tons of olive per year.

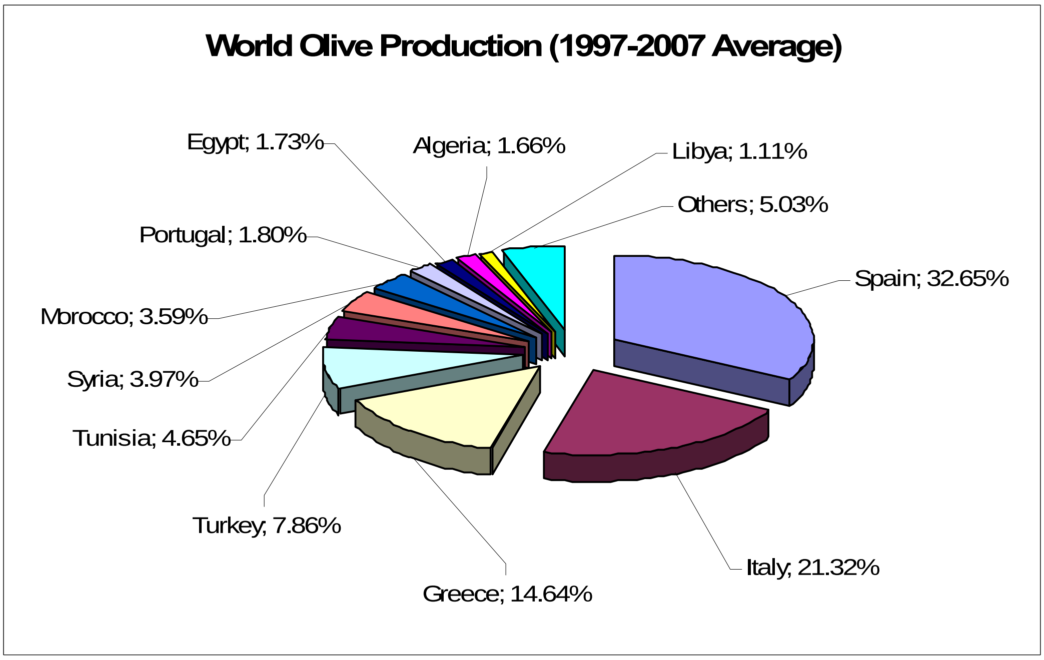

Figure 1.6 Graphical representation of country shares in world olive production between 1997 and 2007 (FAO, 2008)

Olive and olive cake production of Turkey between 2000 and 2008 are given in Table 1.5. Since olive cake is the residual product remaining after processing of olives for olive oil production, olive used for oil production is also given in this table. Olive cake and dry olive cake production amounts for Turkey between 2000 and 2008 are calculated based on the data taken from Olive Growing Research Institute (OGRI). According to OGRI, 35-45 kg of olive cake remains from 100 kg of olive and 60-70 kg dry olive cake can be obtained from 100 kg olive cake (OGRI, 2008). In order to calculate the amount of olive cake, olive amounts are multiplied by 0.40 and to calculate dry olive cake amounts, olive cake amounts are multiplied by 0.65.

Total olive and dry olive cake production of Turkey between 2000 and 2008 are also represented graphically in Figure 1.7.

Table 1.5 Olive and olive cake production in Turkey between 2000 and 2008 (TSI, 2009)

	Production (1000 tons)								
	2000	**2001**	**2002**	**2003**	**2004**	**2005**	**2006**	**2007**	**2008**
Olive	1,800	600	1,800	850	1,600	1,200	1,766.7	1,075.9	1,464.2
Olive for Oil	1,310	365	1,350	500	1,200	800	1,211	620.5	952.1
Olive Cake*	524	146	540	200	480	320	484.4	248.2	380.9
Dry Olive Cake**	340.6	94.9	351	130	312	208	314.9	161.3	247.6

* 35-45 kg olive cake can be obtained from 100 kg olive.

**60-70 kg dry olive cake can be obtained from 100 kg olive cake.

Between 2000 and 2008, average production amount of dry olive cake in Turkey is calculated as 240,033 tons/year. Lower heating value of olive cake is around 20 MJ/kg. With a simple calculation, it is clearly seen that 4.8 PJ energy can be obtained from olive cake per year. This amount of energy can not be disregarded and should be taken into consideration.

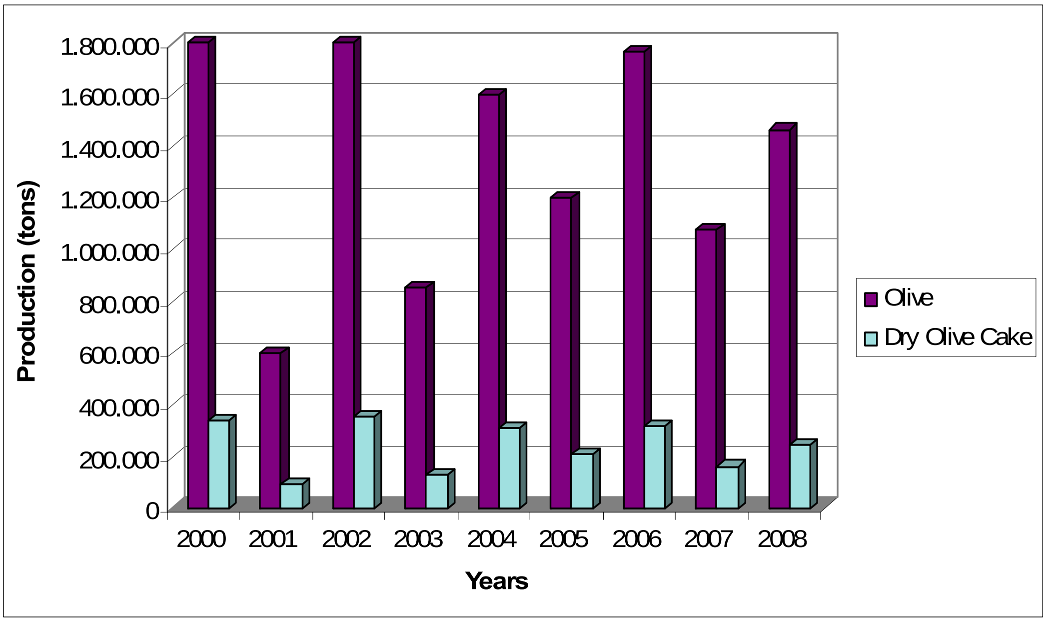

Figure 1.7 Olive and dry olive cake production in Turkey between 2000 and 2008 (TSI, 2009)

1.4. Aim of the Study

The aim of this study is to investigate co-combustion of coal and biomass in a bubbling fluidized bed in order to make use of the biomass potential in energy production. Turkey is rich in lignite coals. However, the quality of the coal is poor (high ash, high sulfur and low calorific value). Therefore, biomass and coal can be burned together in order to produce heat and electrical energy in the country. Since biomass is considered as CO_2 neutral, replacement of coal with biomass in energy production will provide carbon credits in the CO_2 budget of the country. Olive cake has high production potential in Turkey especially in the Mediterranean Region. Thus olive cake was chosen as a biofuel to investigate in this study. Throughout this research, studies have been made to burn lignite coal and olive cake together in a bubbling fluidized bed in order to maximize combustion efficiency and minimize the emissions generated. Therefore, the results of this work can be used for local and regional heating, cogeneration and disposal of biowastes which otherwise create environmental problems.

Specifically, the effect of freeboard height on combustion efficiency and emissions were investigated for the fluidized bed combustor. Because when biomass is burned in a fluidized bed combustor, volatile matters releasing from the biomass mostly burn in the freeboard region. Therefore, the height of the freeboard is important.

Additionally, three limestones were used to reduce SO_2 emissions and various Ca/S ratios were tested to comply with the Turkish and EU regulations. When coal, biomass and limestone burned together, there may be some synergistic effects during combustion and emissions may be affected. This point is also worth further investigation in this study.

CHAPTER 2

THEORETICAL BACKGROUND

2.1. Biomass Energy

“Biomass is a biological material derived from living, or recently living organisms. In the context of biomass for energy this is often used to mean plant based material, but biomass can equally apply to both animal and vegetable derived material” (Khan et al., 2009). In this work, “biomass” term will be generally used as plant based biomass.

Plant based biomass is defined by McKendry (2002) as the plant material derived from the reaction between CO_2 in the air, water and sunlight, through photosynthesis in order to form carbohydrates that constitute the basic elements of biomass. “The basic idea of utilizing biomass as a renewable energy resource consists of the capture of solar energy and carbon from ambient CO_2 in growing biomass, which is converted to other fuels (biofuels, synfuels, hydrogen) or is used directly as a source of thermal energy or is converted to chemicals or chemical intermediates” (Klass, 2004). The role of biomass in the natural carbon cycle process is demonstrated in Figure 2.1.

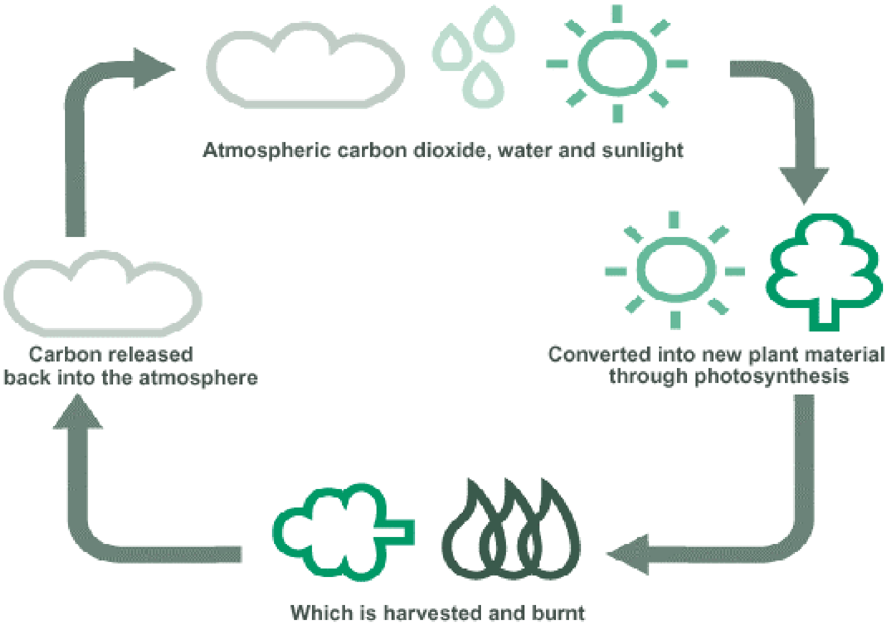

Figure 2.1 Biomass in the carbon cycle (SYW, 2009)

After coal and oil, biomass makes up the third largest primary energy resource in the world. Almost 14% of the world's annual energy consumption is provided by biomass forms. Providing 35% of all the energy requirements, biomass is a major source of energy in developing countries. Biomass energy use is also significant in developed countries. Since biomass combustion has the potential to be CO_2 neutral, biomass usage as a partial substitution for fossil fuels, has an additional importance regarding global warming. This is mainly the case concerning agricultural residues or energy plants, which are periodically planted and harvested. During their growth, these plants remove CO_2 from the atmosphere for photosynthesis then CO_2 is released again during combustion (Werther et al., 2000).

Additionally, air polluting emissions such as oxides of sulfur (SO_x) and nitrogen (NO_x) generated from fossil fuels are as important as the greenhouse gas CO_2. These emissions cause acid rain and ozone depletion. Because of its low sulfur and nitrogen content, SO_2 and NO_x emissions can be also reduced using biomass as a substitute of fossil fuels.

Biomass energy can be utilized in a wide selection of fields such as electricity generation, residential heating, fuel supply for vehicles and process heat for industries.

2.1.1. Biomass Types

According to ICRE (2004), biomass resources can be classified as in the list below:

- Vegetable/plant biomass
    - Woody
    - Non-woody
    - Processed waste
    - Processed fuel
- Animal biomass
- Municipal solid waste

Forestry plantations, natural forests, woodlands and forestry waste make up most woody biomass, while most non-woody biomass and processed waste originates from agricultural residues and agro-industrial activities. Types and examples of plant biomass are shown in Table 2.1 (ICRE, 2004). While animal biomass is mainly composed by manures of stock farm animals such as cattle, pigs and chickens municipal solid waste contains household waste like paper, plastic, paper-based cartons and food waste.

Table 2.1 Types and examples of plant biomass (ICRE, 2004)

Woody biomass	Non-woody biomass	Processed waste	Processed fuels
• Trees • Shrubs and scrub • Bushes such as coffee and tea • Sweepings from forest floor • Bamboo • Palms	• Energy crops such as sugarcane • Cereal straw • Cotton, cassava, tobacco stems and roots • Grass • Bananas, plantains and the like • Soft stems such as pulses and potatoes • Swamp and water plants	• Cereal husks and corn cobs • Bagasse • Wastes from pineapple and other fruits • Nut shells, flesh and the like • Plant oil cake • Sawmill wastes • Industrial wood bark and logging wastes • Black liquor from pulp mills • Municipal Waste	• Charcoal from wood and residues • Briquette and densified biomass • Methanol and ethanol • Plant oils from palm, rape, sunflower and the like • Producer gas • Biogas

2.1.2. Advantages of Biomass Energy

As it was stated above biomass energy has brought various advantages. They are summarized in the following list.

- Biomass sources are sustainable and easily grown.
- They can be used as a substitute for fossil fuels which are depleted rapidly.
- Due to its lower sulfur and nitrogen content, they help to reduce air pollutants such as SO_2 and NO_x. As a result of lowering SO_2 and NO_x emissions, they help to prevent acid rain and ozone depletion problem.
- They are much cheaper than current fossil fuels.
- Biomass usage results in almost zero net CO_2 which is a greenhouse gas causing global warming.
- With biomass production, unused areas such as deforested areas can be reused and new job opportunities can be created.

2.1.3. Biomass Fuel Properties

The most important fuel properties which provide the basic information of a fuel specie are determined by proximate analysis, ultimate analysis and heating value. While proximate analysis gives fixed carbon, volatile matter, moisture and ash content of the fuel, ultimate analysis provides percentages of elemental C, S, H, N, and O. Proximate and ultimate analysis of some biomass fuels and bituminous coal are shown in Table 2.2 and Table 2.3. It can be seen that the values vary in wide ranges. As shown in these two tables, biomass fuels generally contain less carbon, more oxygen, less sulfur, higher moisture, less fixed carbon and higher volatile content when it is compared with coal. In Table 2.4 ash analysis of some biomass fuels and bituminous coal are presented. According to this table, biomass fuels have more potassium, calcium and magnesium and less aluminum and iron than bituminous coal. Additionally, from Table 2.5 it is seen that biomass fuels have lower heating values in comparison with bituminous coal. Since biomass fuels have high volatile content and highly reactive char, they show high reactivity. On the other hand they have much lower carbon and high oxygen content resulting in low heating values. These characteristic properties of biomass are discussed below in detail (Khan et al., 2009).

Table 2.2 Proximate analysis of some biomass fuels and bituminous coal (Khan et al., 2009)

Fuels	**Moisture (wt %)**	**VM (wt %)**	**FC (wt %)**	**Ash (wt %)**
Wood pellets (pine)	4.9	80.4	14.5	0.2
Demolition wood pellets	9.1	69.6	19.7	1.7
Pepper plant residue	6.5	60.5	19.5	13.5
Greenhouse residue	2.5	61.0	5.5	31.0
Wheat straw*	13.9	77.9	21.5	6.8
Sunflower pellets	11.2	65.2	19.5	4.1
Olive cake pellets	11.9	64.2	15.7	8.2
Sewage sludge	6.9	44.6	7.0	41.5
Bituminous coal*	4.9	32.3	48.1	14.7

* Ashing at 815°C

Table 2.3 Ultimate analysis of some biomass fuels and bituminous coal (Khan et al., 2009)

Fuels	**C (wt %)**	**H (wt %)**	**O** (wt %)**	**N (wt %)**	**S (wt %)**
Wood pellets (pine)	45.5	6.6	47.7	<LDL	<LDL
Demolition wood pellets	45.7	6.3	36.2	0.9	<LDL
Pepper plant residue	33.8	4.0	39.1	2.5	0.5
Greenhouse residue	47.1	7.4	10.9	1.0	<LDL
Wheat straw*	56.7	6.7	48.8	1.0	0.2
Sunflower pellets	44.1	5.17	34.6	0.5	0.1
Olive cake pellets	42.1	4.99	31.0	1.3	0.1
Sewage sludge	52.0	6.3	32.1	6.3	3.1
Bituminous coal*	65.7	5.6	7.7	1.2	0.5

* Ashing at 815°C, ** by difference, <LDL: below the lower detection limit

Table 2.4 Ash analysis of some biomass fuels and bituminous coal (Khan et al., 2009)

Fuels	**SiO_2 (wt %)**	**Al_2O_3 (wt %)**	**Fe_2O_3 (wt %)**	**MgO (wt %)**	**CaO (wt %)**	**K_2O (wt %)**	**P_2O_5 (wt %)**
Wood pellets (pine)	4.3	1.3	1.5	8.5	55.9	16.8	3.9
Demolition wood pellets	20.4	3.5	2.2	7.5	27.5	10.5	11.1
Pepper plant residue	12.6	4.9	2.0	7.4	32.2	24.6	5.2
Greenhouse residue	28.4	3.9	18.4	5.7	25.8	9.7	3.8
Wheat straw*	2.9	0.6	0.8	21.6	21.6	22.8	15.2
Sunflower pellets	12.8	2.9	3.0	4.9	17.5	47.9	6.0
Olive cake pellets	53.1	3.6	1.2	3.0	17.7	30.0	4.1
Sewage Sludge	38.3	0.8	12.5	2.8	9.1	2.2	15.4
Bituminous coal*	59.7	20.3	7.0	1.9	1.8	2.3	0.1

* Ashing at 815°C

Table 2.5 Heating values of some biomass fuels and bituminous coal (McKendry, 2002)

Fuels	**HHV (MJ/kg)***
Fir	21.0
Danish pine	21.2
Willow	20.0
Poplar	18.5
Cereal straw	17.3
Miscanthus	18.5
Bagasse	19.4
Switchgrass	17.4
Bituminous coal	26.2

* Dry Basis

2.2. Combustion of Biomass

Combustion is defined in LCP BREF (2006) as the rapid chemical reaction of oxygen with the combustible elements of a fuel. Carbon, hydrogen and sulfur are three crucial combustible chemical elements. Sulfur has usually a small contribution as a source of heat as compared to other ones.

Although biomass fuels have some properties (high moisture content, high volatile matter content, low bulk density, low ash melting point etc.) complicating the combustion process, due to its low costs and high reliability, combustion is the most frequently used process for biomass fuels (IEA, 2009). “Combustion is the most common way of converting biomass into energy, - both heat and electricity - and worldwide, it already provides over 90% of the energy generated from biomass. It is well understood, relatively straightforward, commercially available, and can be regarded as a proven technology. Compared to other thermo-chemical primary conversion technologies (gasification, pyrolysis etc.) it is the simplest and most established technology, and it can easily be integrated within existing infrastructures” (Clini et al., 2008).

The most important combustion technologies are fixed-bed combustion and fluidized bed combustion. Properties of the biomass fuel (moisture content, ash content, particle sizes etc.) and capacity of the system are the main factors in the choice of the most suitable method (Clini et al., 2008).

2.2.1. Stages of Biomass Combustion

A single particle of solid fuel undergoes through a series of interrelated processes during combustion. These are heating up and drying, devolatilization and the combustion of char. Figure 2.2 shows a schematic representation of these processes (Werther et al., 2000). During first stage which is heating up and drying, the biomass gives up its moisture at temperatures up to 100°C, using the heat from other particles that release their heat value. For the period of devolatilization, as the dried particle heats up, volatile gases containing hydrocarbons, CO, CH_4 and other gaseous components are released. These components released during devolatilization period make up approximately 70% of the heating value of the biomass. At the last stage, char oxidation occurs finally and only ash remains from the solid fuel particle as a residue (IEA, 2009).

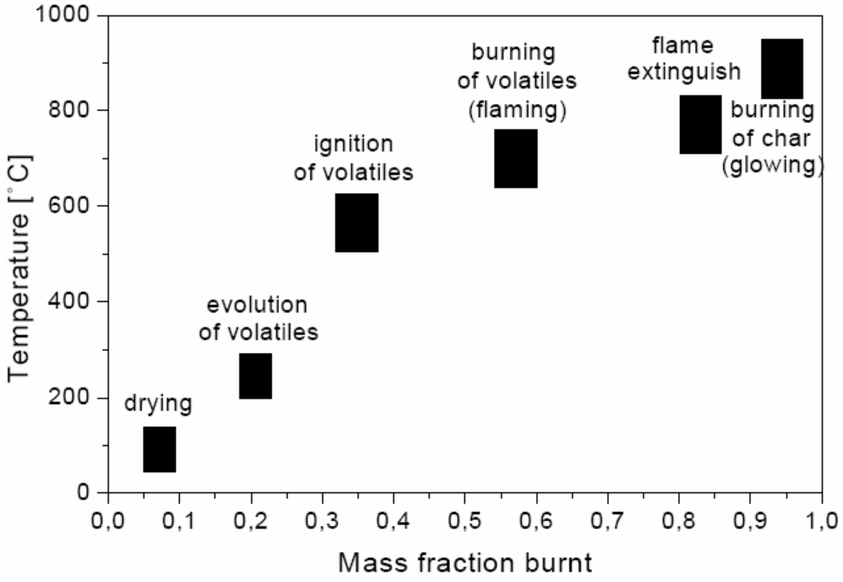

Figure 2.2 Stages of biomass combustion (Werther et al., 2000)

2.2.2. Emissions from Biomass Combustion

This section of "Emissions from Biomass Combustion" was arranged using the book by Van Loo and Koppejan (2008) as a reference material.

Emissions from biomass combustion are divided into two main groups as emissions from complete combustion and emissions from incomplete combustion. They are presented in the two subsections below.

2.2.2.1. Emissions from Complete Combustion

The following components in Table 2.6 originate from complete combustion of biomass.

Table 2.6 Emissions from complete combustion (Van Loo and Koppejan, 2008)

Emissions from complete combustion	**Notes**
Carbon dioxide (CO_2)	• Major combustion product from all biomass fuels • Regarded as being CO_2-neutral for biomass combustion
Nitrogen oxides (NO_x)	• Formed both in the gas phase combustion and in char combustion • Mainly emitted as nitric oxide (NO) then converted to NO_2 in the atmosphere
Nitrous oxide (N_2O)	• Formed in very low amounts during biomass combustion • High global warming potential factor (296 for 100 years) • Contribution to the ozone depletion in stratosphere
Sulfur oxides (SO_x)	• Divided as combustible sulfur and non-combustible sulfur (sulfur in the ash) • Mainly emitted as SO_2 (> 95 percent)
Hydrogen chloride (HCl)	• Significant amounts from biomass fuels containing higher amounts of chlorine, such as miscanthus, grass and straw
Particles	• Mainly emitted as fly ash from complete combustion • Coarse fly-ashes (particles with a diameter > 1 μm) and aerosols (particles with a diameter < 1 μm) • Aerosols can cause severe problems due to their low melting temperatures
Heavy metals	• All virgin biomass fuels contain heavy metals to some degree • The most important ones are Cu, Pb, Cd, Hg • Remain in the ash or evaporate

2.2.2.2. Emissions from Incomplete Combustion

Emissions resulted from incomplete combustion are mainly the result of inadequate mixing of combustion air and fuel in the combustion chamber, an overall lack of available oxygen, too low combustion temperatures, too short residence times or too low radical concentrations (Van Loo and Koppejan, 2008).

The following components in Table 2.7 originate from incomplete combustion of biomass.

Table 2.7 Emissions from incomplete combustion (Van Loo and Koppejan, 2008)

Emissions from incomplete combustion	**Notes**
Carbon monoxide (CO)	• The most important final intermediate through conversion of fuel carbon to CO_2 • Can be regarded as a good indicator of the combustion quality • Sufficient residence time and oxygen supply are important to achieve low CO emission levels
Methane (CH_4)	• Direct greenhouse gas • An important intermediate in the conversion of fuel carbon to CO_2 and fuel hydrogen to H_2O
Non-Methane Volatile Organic Components (NMVOC)	• Include all hydrocarbons except CH_4, PAH (polycyclic aromatic hydrocarbons) and other heavy hydrocarbons which condense and form particle emissions
Polycyclic Aromatic Hydrocarbons (PAH)	• Carcinogenic effects
Particles	• Found as soot, char or condensed heavy hydrocarbons (tar)
Polychlorinated dioxins and furans (PCDD/PCDF = PCDD/F)	• A group of highly toxic components • Found in the temperature window between 180°C and 500°C • Can be formed in very small amounts from all biomass fuels containing chlorine
Ammonia (NH_3)	• Small amounts emitted • Secondary NO_x reduction measures may contribute to the NH_3 emission level
(Ground level) Ozone (O_3)	• Secondary pollutant formed due to photochemical atmospheric reactions including CO, CH_4, NMVOC and NO_x • Direct greenhouse gas • Very strong oxidant

2.3. Co-combustion of Biomass

According to Leckner (2007), co-combustion is the simultaneous combustion of two or more fuels in the same plant for energy production. It is probably the least complicated and one of the most advantageous methods of utilizing biomass and waste as a substitute to fossil fuels for stationary energy conversion. The interest for this type of combustion has been raised recently although it has been applied for many years (Leckner, 2007).

Co-combustion can be performed in various means to serve different purposes. A simple categorization including new plants and existing plants is given in the following list:

1) in order to dispose of waste or to replace coal by biomass, a small amount of biomass is fired with coal in a combustor which is initially designed for coal
2) in order to obtain the desired combustion temperature, a small amount of fuel with a high heating value is fired with a biomass fuel having a lower heating value
3) utilization of various fuels in any ratio, depending on cost, accessibility and supply conditions (Leckner, 2007).

2.3.1. Advantages and Disadvantages of Co-combustion

Co-combustion has several advantages and they are listed below:

- conversion of biomass and waste fuels to the energy with high efficiency,
- reduction of CO_2 emissions originated from fossil fuels,
- increased usage of indigenous fuels,
- compensation of seasonal variations of biomass fuels,
- less complicated and accordingly cheaper than other conversion methods for biomass fuels and
- possible positive synergistic effects between different fuels.

There are also some disadvantages:

- the extra cost of some additional equipment or treatment processes,
- the risk of harmful effects originated from the additional fuel on the plant,
- possible negative synergistic effects if the additional fuel has extreme properties and
- lack of experience about two of the items above (Leckner, 2007).

2.4. Fluidized Bed Technology

2.4.1. Fluidization

According to Kunii and Levenspiel (1991), fluidization is a process where solid particles are converted from a solid-like state into a dynamic fluid-like state through suspension in a gas or liquid. Different forms of fluidization are presented in Figure 2.3.

"If a fluid is passed upward through a bed of fine particles at a low rate, the fluid merely percolates through the void spaces between stationary particles. This is a *fixed bed*. With an increase in flow rate, particles move apart and a few vibrate. This is the *expanded bed.* At a still higher velocity, a point is reached where all the particles are just suspended by the upward-flowing gas or liquid. The bed is considered to be just fluidized and is referred to as *incipiently fluidized bed* or a bed at *minimum fluidization*" (Kunii and Levenspiel, 1991).

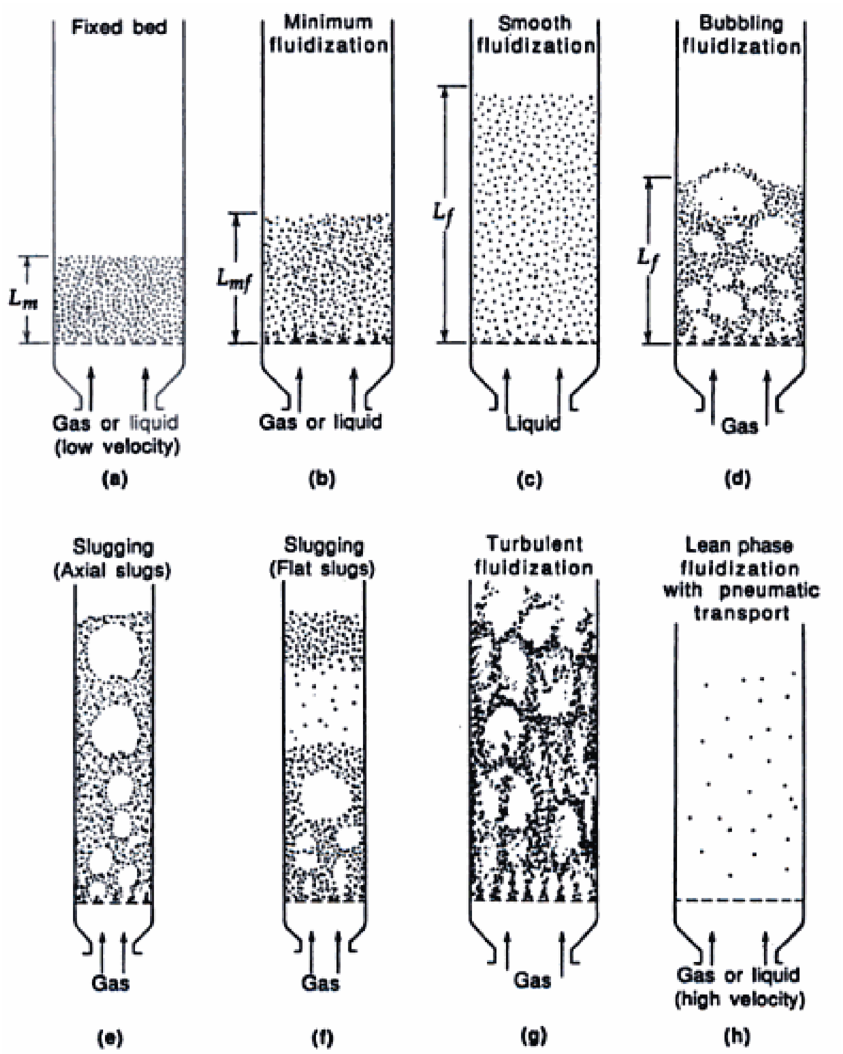

Figure 2.3 Different forms of fluidization (Kunii and Levenspiel, 1991)

"With an increase in flow rate beyond minimum fluidization, large instabilities with bubbling and channeling of gas are observed. At higher flow rates, agitation becomes more violent and the movement of solids becomes more vigorous. In addition to this, the bed does not expand much beyond its volume at minimum fluidization. Such a bed is called as an *aggregative fluidized bed*, a *heterogeneous fluidized bed,* or a *bubbling fluidized bed* " (Kunii and Levenspiel, 1991).

2.4.2. Fluidized Bed Combustion

Fluidized bed combustion (FBC) applications have been utilized for combustion of municipal and industrial wastes since 1960. More than 300 commercial installations have been built worldwide up till now. Bubbling fluidized beds (BFB) and circulating fluidized beds (CFB) have to be separated concerning their technological applications (Van Loo and Koppejan, 2008). BFB and CFB combustions are explained in detail in sections 2.4.2.2 and 2.4.2.3 respectively.

A fluidized bed includes a cylindrical column with a perforated bottom plate filled with a hot, inert and granular material in suspension. Silica sand and dolomite are widely used bed materials. The bed material makes up 90-98% of the fuel - bed material mixture. Primary combustion air enters the column from bottom through the distributor plate and fluidizes the bed. High heat transfer and good mixing provides necessary conditions for complete combustion with low excess air demand (λ = 1.1-1.2 for CFB and λ = 1.2-1.3 for BFB). In order to prevent ash sintering in the bed, combustion temperature is kept low (650-900°C) by internal heat exchangers, by flue gas recirculation, by water injection or by sub-stoichiometric bed operation (Van Loo and Koppejan, 2008).

In FBC plants, various fuel mixtures can be flexibly utilized since good mixing is achieved. As a result of good air staging, good mixing and a low requirement of excess air, low NO_x emissions can also be obtained. Furthermore, the addition of adsorbents such as limestone for sulfur capture is proved to be useful due to the good mixing behavior. With low excess air quantities, combustion efficiency can be increased whereas the flue gas volume can be reduced. This makes FBC systems especially attractive for large-scale applications (normal boiler capacity > 20 MW_{th}) (Van Loo and Koppejan, 2008).

2.4.2.1. Development of Fluidized Bed Combustion

The development of the FBC started with the Winkler patent for gasification of lignite in 1922 and this technology has been applied for different purposes since then. In the beginning, three coal firing test units were designed in the 1960s. Then, the first BFB test facility was established in 1965 in order to control emissions of sulfur dioxide. Moreover, the Atmospheric FBC Program was started in the USA in the same year. Without the use of auxiliary equipment FBC could comply with the new SO_2 and NO_x emission standards. In addition to the development in the USA, the UK, Finland, Germany and China also started programs to develop FBC, because they wanted to establish a new technology, which was able to burn low-grade fuels with low emissions (Koornneef et al., 2007).

Like the UK and the USA, China and Germany have abundant amounts of low-grade coals with high sulfur content which was the main driver for starting the FBC development programs. On the other hand, in early stage of its development Finland were particularly applied the technology as burning low-grade fuels like peat, wood waste and sludge (Koornneef et al., 2007).

The number of installed FBCs with respect to years is shown in Figure 2.4. As it is seen from the figure, BFB shows a more steady growth than CFB. In the early 1990s, number of installed BFB units increases rapidly however it reaches to a steady level after year 2000. On the other hand, CFB has a constant increase which starts in the late 1990s (Koornneef et al., 2007).

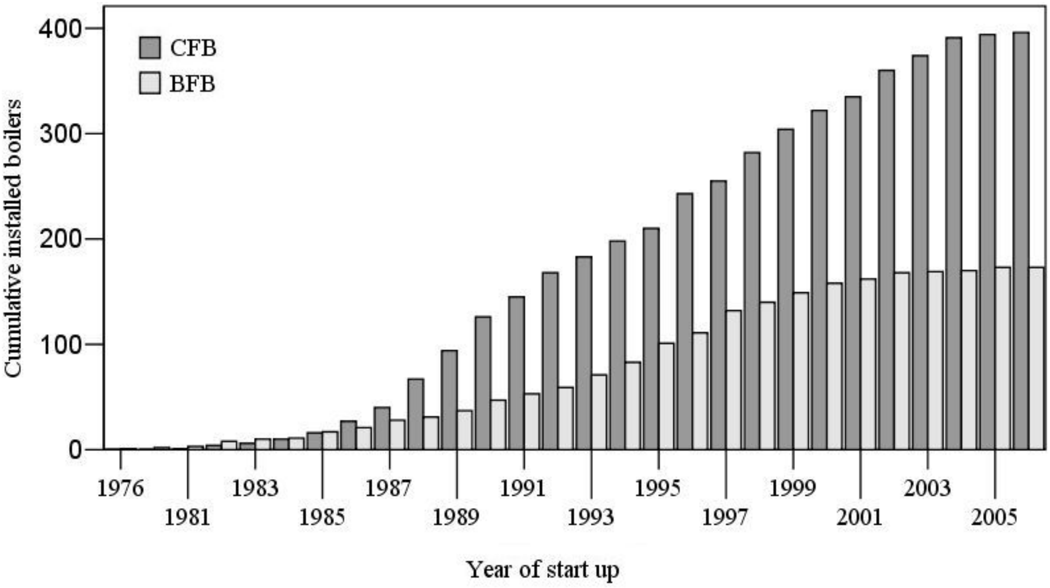

Figure 2.4 The number of installed FBCs with respect to years (Koornneef et al., 2007)

2.4.2.2. Bubbling Fluidized Bed (BFB) Combustion

BFB furnaces start to draw attention for plants with a boiler capacity of over 20 MW_{th}. A typical BFB furnace is shown in Figure 2.5. In BFB furnaces, the primary air is supplied through a distributor plate from below and fluidizes the bed material. Silica sand with a diameter between 0.5-1.0 mm is used as the bed material. The fluidization velocity of the air varies between 1.0-2.0 m/s. Secondary air is injected from several ports throughout the freeboard to reduce NO_x emissions by air staging. The biomass fuel should not be fed onto, but into, the bed because of the higher reactivity of biomass as compared with coal. The fuel amounts are only 1-2% of the bed material. Additionally, the bed material should be heated before the fuel is fed into the combustor (Van Loo and Koppejan, 2008).

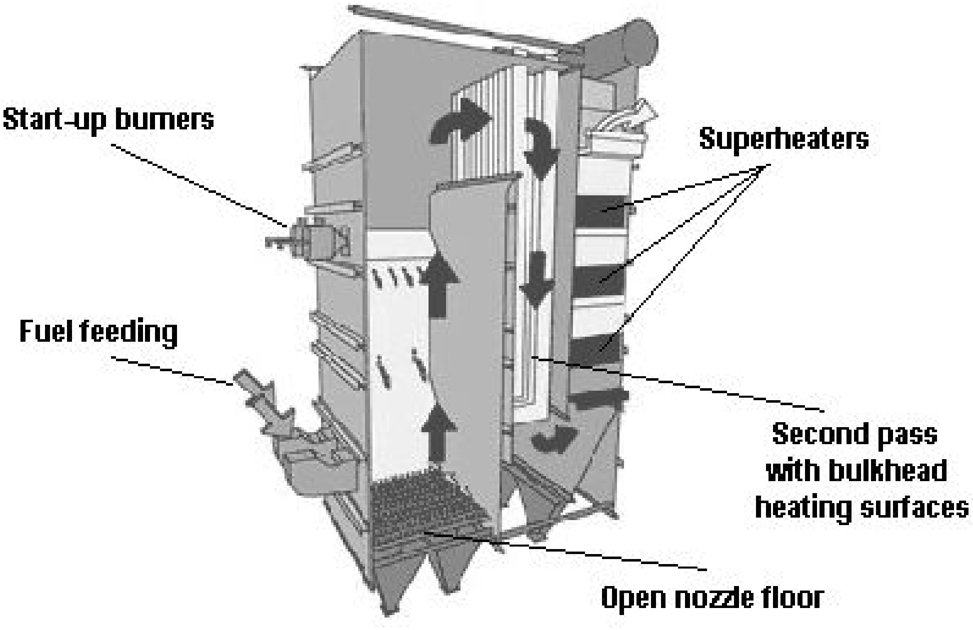

Figure 2.5 A typical BFB furnace (Van Loo and Koppejan, 2008)

Flexibility is the main advantage of BFB furnaces with regard to particle size and moisture content of the biomass fuels. It is also possible to burn mixtures of different biomass types or to co-fire them with other fuels. Additionally, in modern BFB furnaces a sub-stoichiometric condition ($\lambda \approx 0.35$) is possible, which provides bed temperature in the range of 650-850°C. Therefore, fuels having low ash-melting temperature can also be burned (Van Loo and Koppejan, 2008).

2.4.2.3. Circulating Fluidized Bed (CFB) Combustion

In CFB furnaces, the fluidization velocity varies between 5-10 m/s and smaller sand particles (0.2-0.4 mm in diameter) are used as the bed material. The sand particles carried upwards with the flue gas are separated in a hot cyclone and fed back into the combustor. A typical CFB furnace is shown in Figure 2.6. The bed temperature is kept between 750-900°C by external heat exchangers or by water-cooled walls. Better heat transfer and homogeneous bed temperature can be provided with the higher turbulence in CFB furnaces which assists for stable combustion conditions and the control of air staging. Considering their high specific heat transfer capacity, CFB furnaces start to be the focus of attention for plants of more than 30 MW_{th}, because of their higher combustion efficiency and the lower flue gas flow (Van Loo and Koppejan, 2008).

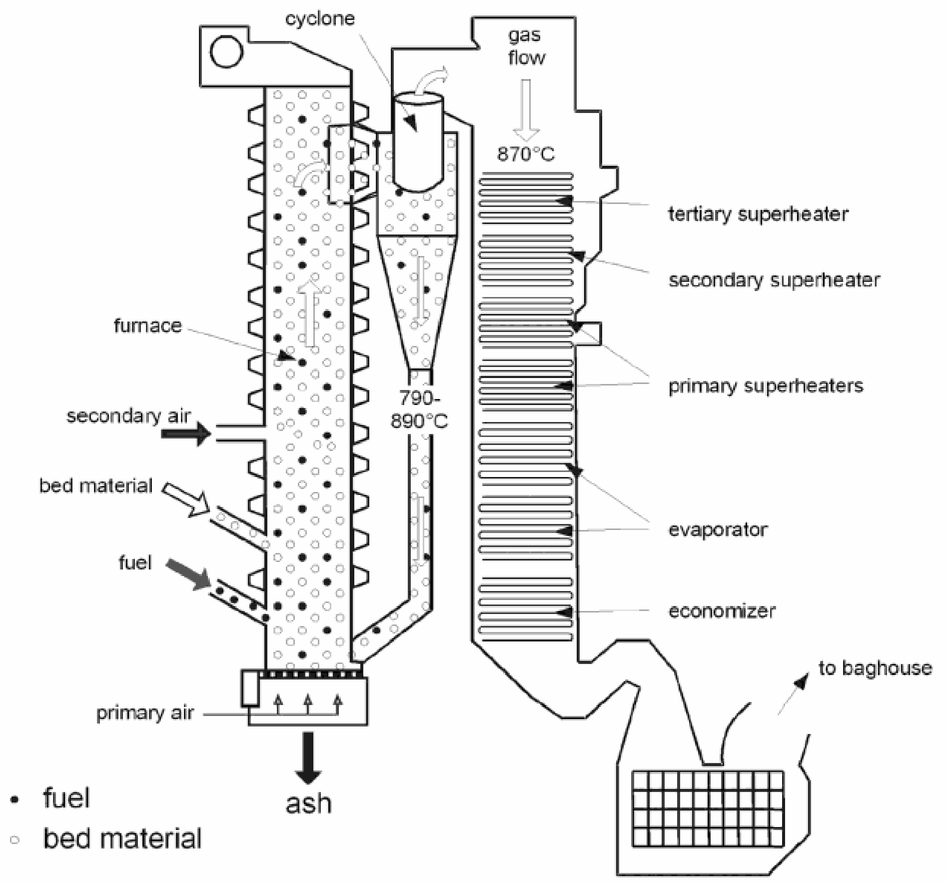

Figure 2.6 A typical CFB furnace (Van Loo and Koppejan, 2008)

2.4.3. Advantages and Disadvantages Fluidized Bed Combustion

“Due to its numerous advantages over other thermo-chemical conversion technologies (gasification, pyrolysis etc.), nowadays the most suitable option for combustion and co-combustion of biomass seems to be the fluidized bed technology ” (Nowak and Kobylecki, 2009). Despite its several advantages, there are some disadvantages of this technology and they are both listed below.

Advantages

- high fuel flexibility with regard to calorific value, moisture content, and ash content,
- low NO_x emissions due to low bed temperature,
- high specific heat transfer capacity (due to high turbulence) leading to stable combustion with low CO emissions,
- removal of SO_2 by direct limestone addition into the system,
- homogenous combustion conditions in the combustor if several fuel injectors are used and
- higher efficiency and lower flue gas flow due to low excess oxygen (1-4%) (Van Loo and Koppejan, 2008).

Disadvantages

- high operating and investment costs for BFB plants > $20MW_{th}$ and CFB plants > $30MW_{th}$
- low particle size flexibility,
- bed agglomeration, slagging and fouling on boiler walls and tubes during combustion of high alkali content biomass fuels,.
- flue gas with high dust load and
- loss of some bed material and unburned carbon content with the ash (Van Loo and Koppejan, 2008).

2.5. EU Directives and Turkish Regulations about Biomass Energy

Since Turkey is an accession country for the European Union (EU), Turkey will be responsible for the regulations, legislations and directives prepared by EU. Standards and limits included in these instruments should be complied with as soon as possible in this adaptation process. There are certain limits for flue gas emissions not only in EU Directives but also in Turkish Regulations.

In EU member countries, two distinct directives cover the flue gas emissions: Emissions from Large Combustion Plants (2001/80/EC) and Waste Incineration Directive (2000/76/EC). Directive 2001/80/EC applies for biomass, defined as vegetable waste from agriculture and forestry, vegetable waste from the food processing industry, fibrous vegetable waste from virgin pulp production and from production of paper from pulp, untreated wood waste and cork waste while directive 2000/76/EC applies to the incineration of all other types of waste (Van Loo and Koppejan, 2008). In Table 2.8, emission limits are listed for coal, olive cake and their mixtures. Since olive cake is a vegetable waste from agriculture, emission limits of Directive 2001/80/EC are taken into consideration. Furthermore, emission limits of Turkish Regulation for Control of Air Pollution from Industrial Sources (RCAPIS) are also included in this table.

For co-combustion of coal and biomass, emission limits are revised according to “mixing rules”. As said by European Union, emission limits for fuel mixtures are calculated based on Waste Incineration Directive (2000/76/EC). In this directive, mixing rule is defined like that: emission limit of each fuel is multiplied by a weighted factor which is the flue gas volume produced during mono-combustion of either fuels. Then obtained values are summed up and divided to the total flue gas volume of the fuels. The emission limit (EL_{mix}) resulting from co-firing is calculated by the formula below (Leckner, 2007).

$$EL_{mix} = [(V_{bf}*EL_{bf})+(V_{wf}*EL_{wf})]/(V_{bf}+V_{wf}) \quad (2.1)$$

where;

EL_{bf}: emission limit of base fuel

V_{bf}: flue gas volume resulting from base fuel

EL_{wf}: emission limit of waste fuel

V_{wf}: flue gas volume resulting from waste fuel

On the other hand, emission limits for fuel mixtures are calculated a little different in Turkish Regulation for Control of Air Pollution from Industrial Sources (RCAPIS, 2009). In this case, the weighted factor is the thermal power gained from each fuel. The rest of the calculation is the same with Waste Incineration Directive (2000/76/EC) and the formula is given below.

$$EL_{mix} = [(TP_{bf}*EL_{bf})+(TP_{wf}*EL_{wf})]/(TP_{bf}+TP_{wf}) \quad (2.2)$$

where;

EL_{bf}: emission limit of base fuel

TP_{bf}: thermal power gained from base fuel

EL_{wf}: emission limit of waste fuel

TP_{wf}: thermal power gained from waste fuel

Table 2.8 Emission limits for NO_x, SO_2, CO (2001/80/EC and RCAPIS, 2009)

		Emissions, mg/Nm^3 (based on 6% O_2)		
Regulation	**Fuel Share (wt %)**	**NO_x**	**SO_2**	**CO**
2001/80/EC (EU Regulation)	100% coal	600^a	2000^b	-
	100% biomass	400^b	200^b	-
	75% coal + 25% biomass	540	1458	-
	50% coal + 50% biomass	487	985	-
	25% coal + 75% biomass	441	569	-
RCAPIS (Turkish Regulation)	100% coal	800^c	2000^d	200
	100% biomass	400^c	200^e	460^e
	75% coal + 25% biomass	680	1459	278
	50% coal + 50% biomass	575	987	346
	25% coal + 75% biomass	482	570	407

[a] 50 to 500 MW, [b] 50 to 100 MW, [c] >50 MW, [d] <100 MW, [e] 0,5 to 15 MW

* Since the thermal power of the system used in this study is approximately 5 kW and this value is smaller than most of the limits given in two mentioned regulations, the emission limits presented in the Table 2.6 are the ones corresponding to minimum thermal power intervals.

CHAPTER 3

LITERATURE SURVEY

Renewable energy has come into question with increasing greenhouse gas emissions and need for sustainable energy. Biomass which is one of the renewable energy sources has a very high energy and low emission potential. Combustion of biomass and co-combustion of biomass with coal are the most common ways of converting biomass to energy. Hence, in order to meet increasing energy demand and minimize environmental pollution, many studies and research were conducted on biomass usage in energy generation.

In the early 1960s, Douglas Elliott recognized the advantage of burning coal in fluidized beds for steam generation by installing boiler tubes in it. He supported the use of fluidized beds to generate steam with the British Coal Utilization Research Association and the National Coal Board of the U.K. After Elliott's investigation, an active program started at the Central Electricity Generation Laboratory, Marchwood in order to develop fluidized bed combustion. In the meantime, investigations on bubbling fluidized bed (BFB) boilers were carried out in the U.S.A. and China. In 1982, probably first steam generation from biomass-fired BFB boilers started with the establishment of a 10 t/h rice husk-fired BFB boiler in India. From that day on, several types of bubbling fluidized bed boilers, using a variety of fuels, have been developed and commercialized around the world. The BFB boilers have significantly started to replace the old stoker-fired boilers used in the past (Basu, 2006).

On the other hand, in 1982, the first circulating fluidized bed (CFB) boiler which was completely designed to generate steam and heat was built in the Vereingte

Aluminum Werke at Luenen, Germany. By burning low-grade coal processing wastes with limestone, this plant generated 84 MW total energy (9 MW electricity, 31 MW process steam, 44 MW molten salt melt). Moreover, in the late 1960s, the Ahlstrom group in Finland started to develop BFB boilers. In order to improve the performance of their bubbling fluidized bed, Ahlstrom tried a hot cyclone to capture fine particles leaving the bed and recycle them back to the system. After a series of experiments, they established the first commercial CFB boiler in Pihlava, Finland. This was a 15 MW_{th} boiler transformed from an existing oil-fired boiler in order to replace expensive oil with peat. In the beginning, Ahlstrom built the circulating fluidized bed boilers for burning primarily multifuel or low-grade fuels such as bark, peat, and wood waste. Afterwards boilers were completely designed for coal (Basu, 2006).

In this chapter, some example studies in the literature on coal or biomass combustion and coal + biomass co-combustion in fluidized bed combustors are presented.

Liu and Gibbs (1998) investigated the influence of limestone addition at different positions on gaseous emissions in a coal-fired circulating fluidized bed combustor with a riser of diameter 161 mm and length 6.2 m. Limestone was added at two different positions in the riser, one at the bottom of the riser and the other above the secondary air injection ports. Gaseous emissions, including SO_2, N_2O, NO/NO_x, and CO were measured. In addition to reducing SO_2 emissions, limestone addition at either of two positions always resulted in decreases in N_2O and CO emissions and increases in NO/NO_x emissions. Limestone addition above the secondary air injection ports resulted in larger reductions in N_2O and CO emissions but also greater increases in NO/NO_x, emissions than limestone addition at the bottom of the riser. However, it was stated that the effect of limestone injection position on sulfur capture was negligible. From this study it was concluded that limestone addition at either of the positions was not an effective method for reducing N_2O emissions. Relatively small N_2O reduction (20% or less) and associated increases in NO/NO_x emissions obtained by limestone addition at the typical Ca/S molar ratios used for sulfur capture led to this conclusion.

Khraisha et al. (1999) carried out combustion experiments with olive cake using fluidized bed. A stainless steel fluidized bed combustor of 0.146 m diameter and 1 m length was used to burn olive cake. In order to obtain fluidization, firstly the system was operated under cold conditions using a sand with particle size in the range of 500 to 710 microns. Effects of bed temperature, olive cake feed rate, fluidization velocity, and particle size on combustion efficiency and flue gas composition were investigated during the continuous combustion experiments. It was found that the combustion efficiency increased with the increase in bed temperature and particle size while it decreased with the increase in feed rate and fluidization velocity. Additionally, small amounts of SO_2 and CO were observed at the end of the analysis of gases carried out using a gas chromatography analyzer. Finally, the temperature distribution along the bed indicated that the temperature throughout the bed was fairly uniform, demonstrating a good mixing of reactants, which was important for efficient combustion. Therefore, it was concluded that olive cake, which had a high heating value and free of sulfur content could be continuously burned like most solid fuels and was a rather promising source of energy.

Cliffe and Patumsawad (2001) investigated co-combustion of waste from olive oil production with coal in a fluidized bed in order to study the feasibility of using this waste as an energy source. The combustion efficiency and CO emission were investigated and compared to those of burning 100% of coal. From the study, it was concluded that olive oil waste with up to 20% mass concentration could be co-fired with coal in a fluidized bed combustor designed for coal combustion with a maximum drop of efficiency of 5%. CO emission from 10% olive oil waste mixture was found lower than 100% coal firing because of improved combustion in the freeboard region. On the other hand CO emission from 20% olive oil waste mixture was observed higher than both 100% coal firing and 10% olive oil waste mixture. However, the combustion efficiency was higher than the 10% olive oil waste mixture due to lower elutriation from the bed.

Özkan and Doğu (2002) studied combustion of a high ash and sulfur containing lignite in a 50 kW pilot circulating fluidized bed combustor and its pollution characteristics. Beypazarı lignite containing 45% ash and 3.72% sulfur was mixed with limestone and was burnt in this combustor. For different Ca/S mole ratios, emission characteristics were investigated. SO_2 removal efficiencies were observed to reach values of 98%. NO_x emission levels were found to be around 300 ppm at an average bed temperature of 850°C. However, CO emissions were around 1466 ppm. It was stated that CO emission could be lowered at higher velocity regimes and higher bed lengths. Temperature variation along the combustor (of 1.8 m in height) was found to be about 140 and 90°C for two different feed points located at 0.17 and 0.52 m above the distributor and two different feedback points located at 0.37 and 0.17 m above the distributor, respectively. In this study, it was shown that lignites with low calorific value and high ash content could be successfully burned in a circulating fluidized bed combustor with rather high combustion efficiencies.

Armesto et al. (2003) studied co-combustion of coal and olive oil industry residues in fluidized bed. Two different Spanish coals were used in this study: a lignite and an anthracite. The combustion tests were carried out in the CIEMAT bubbling fluidized bed pilot plant. The system is composed of a riser 0.2 m i.d. and 3 m high, two high-efficiency cyclones in series, a heat exchanger and the bag filter. Different operating conditions such as furnace temperature, share of foot cake in the mixtures and coal type were used in the experiments in order to study the effect of different parameters on the emissions and combustion efficiency. No significant effect of the presence of foot cake in the mixtures was observed on the combustion efficiency. When the amount of foot cake in the mixtures increased, SO_2 and NO_x emissions decreased but N_2O emission increased. It was noted that N_2O increase could be due to the decreasing of the flame temperature caused by high moisture content in the foot cake. As a conclusion it was stated that the combustion of foot cake/lignite or anthracite coal mixtures in bubbling fluidized bed combustor was a way to utilize this biomass residue in energy generation.

Suksankraisorn et al. (2003) studied the combustion of three high moisture content waste materials in a fluidized bed combustor. Co-combustion of these materials was compared with combustion of coal in the same combustor. Waste materials burnt were olive oil waste, municipal solid waste (MSW) and potato. In order to study the effect of moisture content originating from the food waste component in the MSW on the combustion with coal, potato was used as a vegetable substitute instead increasing moisture content using water. It was found that above 20% moisture content in the waste was too high to sustain combustion without addition of coal. CO, NO_x, SO_2 emissions and temperatures were measured and the carbon combustion efficiency evaluated. Co-firing with coal resulted in markedly higher combustion efficiencies with an increase of approximately 10–80% than the simulated MSW. However, this was much lower than the coal combustion efficiency of 93%. It was also much lower than the co-firing efficiency of potato and olive oil waste with coal (average 90%). It was concluded that the high ash content of the simulated MSW (26%), compared with 5% in the other two waste materials resulted in slower burning rate. Therefore, the char particles were elutriated from the bed without being fully burnt. CO emission was observed not to change too much with waste fraction. It was stated that due to the low S content of the fuel, SO_2 emission could be reduced when the waste fraction increased. On the other hand, emissions of NO and N_2O increased slightly with increasing MSW fraction.

Toraman et al. (2004) investigated emission characteristics of co-combustion of sewage sludge (SS) with olive cake (OC) and lignite coal in a circulating fluidized bed (CFB) of 125mm diameter and 1800mm height. SS + OC, and SS + coal mixtures were burned separately. Various sludge to lignite coal and sludge to olive cake ratios (5/95, 10/90, 15/85, 20/80) were tried. On-line concentrations of major components (O_2, SO_2, CO_2, CO, NO_x, C_mH_n) were measured in the flue gas, as well as temperature and pressure distributions along the bed. Combustion efficiencies of SS + OC and SS + coal mixtures were calculated, and the optimum conditions for operating parameters were discussed. The results showed that the combustion mainly took place in the upper regions of the main column where the temperature reached 900°C. SS + coal were burned in the CFB with an efficiency of 95.14% to 96.18%, which was considered to be quite good. When burning sludge mixed with olive cake, appreciable amounts of CO and unburned hydrocarbons were formed and the combustion efficiency dropped to 92.93%. CO and C_mH_n emissions were found to be lower for SS + coal co-combustion than the emissions of the coal combustion. As the %SS was increased in the fuel mixture, the SO_2 emission decreased. NO_x emissions were slightly higher. When burning sludge mixed with olive cake, SO_2 and NO_x emissions were slightly higher. CO and C_mH_n emissions decreased sharply when 5wt% SS was mixed with olive cake. With increasing sludge ratio these emissions increased due to the unburned hydrocarbons. As a result of this study, it was believed that SS could be burned effectively in a CFBC together with other fuels, especially with olive cake. Additionally, it was stated that OC would be a good additive fuel for the combustion of lower quality fuels.

Llorente et al. (2006) carried out combustion tests in a 1 MW_{th} bubbling fluidized bed (BFB) with bed material of limestone in order to reduce the biomass ash agglomeration and sintering. Instead of traditional silica sand, limestone was used as bed material. Mass balances of the inorganic elements and ash characterization with respect to bed agglomeration, fouling and emissions were performed in the BFB combustion pilot plant. Limestone bed material with particle sizes between 0.25 and 2 mm, corresponding to a mean fluidization velocity of 1.2 m/s and at a mean bed temperature of 775°C, were chosen. It was stated that the limestone bed material was a sink of lignocellulosic biomass ash and its elements, even with elements considered to be volatile (sulfur and chlorine). The calcium particles escaped from the limestone bed material were observed to adhere on heat exchangers and reduced the sintering of ash deposits on the tubes. In this study, it was proven that the limestone bed material eliminated the bed agglomeration with biomasses of thistle and almond shell which produced agglomerates in BFB combustor tests with silica as bed material under the same operational conditions.

Scala and Chirone (2006) studied the fluidized bed combustion of a biomass residue (olive husk) common in the Mediterranean area in a bench-scale reactor. The focus of the study was the high propensity of this fuel to have bed agglomeration problems during combustion as a consequence of the high potassium content of the ash. Bed defluidization characteristic times were measured, together with the temperature/pressure profiles within the bed at different operating conditions. Results showed that during the experimental runs both the temperature and pressure profiles changed because of the decrease of mixing and the ash accumulation in the bed. While excess air did not affect ash accumulation, bed temperature, sand size, and the type of husk had all strong effects on this quantity. A diagnostic tool based on the measurement of the dynamic pressure signal inside the bed was tested for its ability to predict bed agglomeration. This technique was fairly accurate under the present operating conditions. Mechanisms of the fuel ash-bed particle interaction and agglomerate formation were analyzed and found that the most likely ash transfer mechanism relies on collisions of sand with burning char particles.

Varol and Atimtay (2007) investigated combustion performances and emission characteristics of olive cake and coal in a bubbling fluidized bed. Flue gas concentrations of O_2, CO, SO_2, NO_x, and total hydrocarbons (C_mH_n) were measured during combustion experiments. By changing operational parameters (excess air ratio (λ), secondary air injection), variation of pollutant concentrations and combustion efficiency were studied. The temperature profiles measured along the combustor column was found higher in the freeboard for olive cake than coal due to combustion of hydrocarbons mostly in the freeboard. Combustion efficiencies in the range of 83.6–90.1% were obtained for olive cake with λ of 1.12–2.30. It was seen that the major indicators responsible for the decrease in the combustion efficiency were combustion losses due to the formation of CO and hydrocarbons, leaving the system unburnt. The efficiency of coal combustion under the same conditions was found to be 98.4–99.8%. Therefore secondary air injection into the freeboard suggested being a useful solution to decrease the CO and hydrocarbon emissions and to increase the combustion efficiency. For the setup used in this study, the optimum operating conditions with respect to NO_x and SO_2 emissions were found as 1.2 for λ, and 50 L/min for secondary air flow rate for the combustion of olive cake.

Xie et al. (2007) investigated the emissions of SO_2, NO and N_2O in a 30 kWth bench scale circulating fluidized bed combustor for coal combustion and co-firing coal and biomass (rice husk). The influence of the excess air, the degree of the air staging, the biomass share and the feeding position of the fuels on the emissions of SO_2, NO and N_2O were studied. Probably due to the high volatile content of the biomass, an increase in the biomass shares resulted in an increase of the CO concentration in the flue gas. On the other hand emissions of NO and N_2O significantly decreased by increasing the biomass share during coal-biomass co-firing. In co-firing, the emission of SO_2 increased with increasing biomass share slightly. Air staging significantly decreased the NO emission without raising the SO_2 level. When the fuel feeding position was changed from riser to downer, NO emission level decreased however no obvious change was observed for the SO_2 level. Additionally, no obvious influence of excess air on N_2O and SO_2 emission could be found not only for coal combustion, but also for co-firing. It was also observed that the emission of CO decreased with the increase of excess air during co-firing. NO emission during co-firing was found lower than that during coal combustion at higher excess air.

Gogebakan et al. (2008) carried out experimental studies in order to observe the effect of biomass share on gaseous pollutant emissions from fluidized bed co-firing of olive residue with low calorific value lignite coals having high ash and sulfur contents. O_2, CO_2, CO, SO_2, NO, N_2O emissions were investigated in a 0.3 MW_{th} Atmospheric Bubbling Fluidized Bed Combustor with an internal cross-section of 0.45 x 0.45m and 5 m height. In the experiments, olive residues at 0, 15, 30 and 50 wt% shares were tried and ash of lignite coal was used as bed material. Additionally, sulfur retention efficiencies were studied with the addition of limestone as sorbent. It was observed that combustion efficiency increased with co-firing but remained constant around 98% for all tests. While NO_x, O_2 and CO_2 concentrations were not affected by the change in the biomass share, CO concentrations were observed to increase with increasing olive residue share in fuel mixture. On the other hand, N_2O and SO_2 concentrations were reduced considerably with the increase in olive residue share. Sulfur retention efficiencies were obtained between 84-89 % for different Ca/S ratios. Finally it was concluded that olive residue can be co-fired with high ash and sulfur containing lignite without any operational problems.

Ghani et al. (2009) studied co-combustion of agricultural residues with coal in a fluidized bed combustor. Rice husk and palm kernel were co-fired with coal in a 0.15 m diameter and 2.3 m high fluidized bed combustor in order to explain the behavior of biomass-fired fluidized bed combustor. Combustion efficiencies and carbon monoxide emissions were studied and the results were compared with those for 100% coal combustion. Carbon monoxide levels were observed to change between 200 and 900 ppm with the addition of coal. Additionally, the effects of biomass properties (such as particle size, particle density and volatility) and the influences of operating parameters (such as the effect of fluidizing velocity and the amount of excess air on axial temperature profile, the combustion efficiencies, and the CO emissions) were also investigated. Combustion efficiencies ranged between 67% and 75% for burning 100% rice husk, 80–83% for burning 100% palm kernel shell, and 83–88% and 86–92% for burning coal equally mixed with rice husk and palm kernel shell, respectively. It was shown that addition of a 50% mass fraction of coal could increase the carbon combustion efficiency up to 20% and CO emissions less than 2500 ppm. It was stated that combustion efficiency was mainly influenced by the loss of carbon in the elutriated solids, and the loss of carbon as CO due to incomplete combustion. Furthermore in this study, it was observed that the operating parameters such as percentage of excess air, fluidizing velocity and bed temperatures played an important role in the co-combustion process.

According to the results of investigations and research on biomass and coal combustion studies, it is believed that the most suitable technology for coal or biomass combustion and coal + biomass co-combustion is the fluidized bed technology because of its many advantages such as fuel flexibility, easy desulfurization, lower emissions (e.g. SO_2, NO_x) and higher combustion efficiency than conventional systems. Therefore, in this study combustion and co-combustion of coal and biomass will be further investigated.

CHAPTER 4

MATERIALS AND METHODS

4.1. Experimental Setup

In this study, a bubbling fluidized bed combustor (BFBC) is used for the combustion of coal, olive cake and co-combustion of olive cake with coal at various mixing ratios. Mainly, the experimental setup includes a bubbling fluidized bed column with two modules, an ash hopper, a fuel feeding system, and a cyclone. The schematic diagram of the setup and a photograph of the setup are given in Figure 4.1 and Figure 4.2, respectively. The bed column is made of Inconel steel with an inside diameter of 102 mm and a height of 900 mm. A second column (a second module) of 1000 mm can be added on the first column and the total height of the combustor column becomes 1900 mm. A stainless steel distributor plate is located between the bed column and the air box. The holes on the distributor plate have a diameter of 1.5 mm. There are one fuel feeding pipe and two overflow pipes on the column. Nine thermocouple ports are located at different heights on the column in order to observe the temperature profile along the column continuously. Type K (chromel-alumel) thermocouples are used in the experiments. These thermocouples are located at 40 mm (TC#1), 110 mm (TC#2), 190 mm (TC#3), 330 mm (TC#4), 490 mm (TC#5) and 660 mm (TC#6), 920 mm (TC#7), 1290 mm (TC#8), 1700 mm (TC#9). Additionally, flue gas temperature can be measured from a thermocouple located at 1920 mm (TC#10) above the distributor plate. Temperatures measured with thermocouples are continuously stored by the Agilent Model-3970A, Data Acquisition Switch Unit with Agilent Benchlink Data Logger software.

The pressure drops in the distributor plate and in the bed are measured with manometers. Air is given to the system by means of a blower and distributed homogenously into the column through the distributor plate. This air supplied to the column serves not only as the fluidization air but also as the combustion air. Besides, the system is completely isolated from outside with kaowool having a thickness of about 30 mm.

LPG (liquefied petroleum gas) is used to pre-heat the system. The LPG is fed (from port no. 2 in Fig. 4.1) to the combustor column by mixing it with the ambient air. A rotameter is used in order to control and measure the flow rate of the LPG. The air + fuel mixture is distributed homogenously along the combustor column by the distributor plate and ignited by an igniter (from no. 19 in Fig. 4.1). Detailed experimental procedure for a combustion test is explained in Section 4.2.

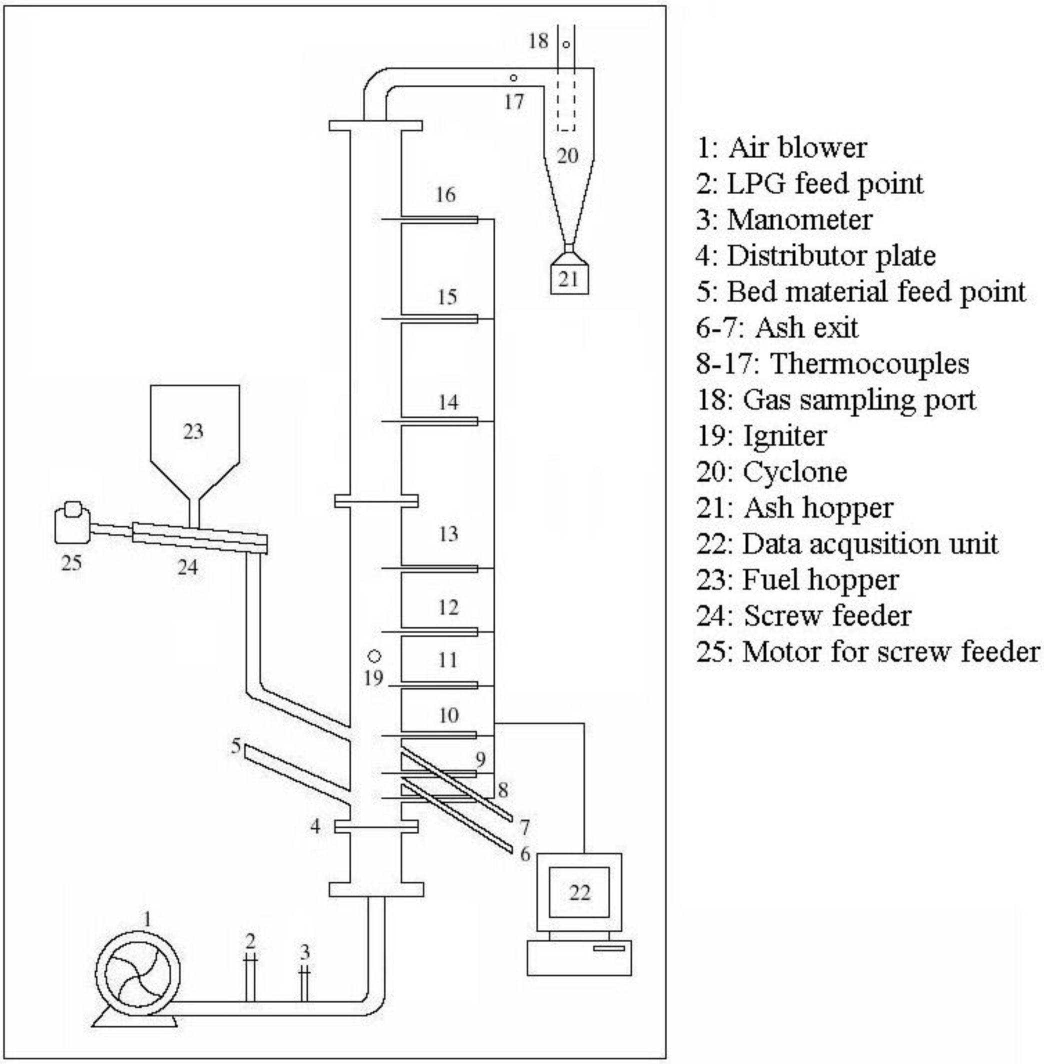

Figure 4.1 Schematic diagram of the experimental setup

Figure 4.2 Photograph of the experimental setup

In the experiments, sand is used as the bed material. Particle size of the sand used is between 0.5-2.0 mm and average particle diameter of the sand is 0.67 mm. For each experiment the bed height is kept at 100 mm. In order to do this 1339 g of sand is fed into the column. Coal and olive cake are used as solid fuels in the experiments. Olive cake, coal or a mixture of coal and olive cake at different ratios are stored in a fuel hopper (port no. 21 in Fig. 4.1). A screw feeder installed below the fuel hopper (port no. 24 in Fig. 4.1) feeds the fuel into the combustor column. A cyclone is placed at the outlet of combustor column in order to remove fly ash particles in the flue gas. Particles coming from the cyclone are collected in an ash hopper installed at the bottom of the cyclone.

Emissions are measured from the sampling port at the outlet of the cyclone (port no. 18 in Fig. 4.1) by TESTO 360 and Gasmet DX-4000 flue gas analyzers. Concentrations of O_2, CO, SO_2 and NO_x in the flue gas are continuously measured.

4.2. Experimental Procedure for a Combustion Test

Initially, the bed material (sand) is weighed (1339 g) and fed into the combustor column. Previously prepared fuel (olive cake, coal or olive cake + coal mixture) is stored in the fuel hopper. Air flow rate is adjusted to the value corresponding to the fluidization velocity required. This is checked with the pressure drop at the orifice. Then, LPG is mixed with air and supplied into the combustor column through the distributor plate. The gas mixture is ignited from the ignition port and pre-heating is started. The flow rate of LPG is controlled with a rotameter. Approximately in one hour, temperature of the bed material in the column reaches 700^{o}C. After the required temperature is reached, the fuel is started to be fed into the column and LPG flow is gradually decreased. When the combustion is observed to be self-sustained, LPG flow is shut down. Solid fuel in the hopper is fed to the combustor column by the help of a screw feeder. Fuel is fed with the rate of 22 g/min in the experiments. Calculations and calibration curves for the fuel feeding system are given in Appendix A.

Temperatures along the combustion column are continuously controlled and recorded by Agilent Bench Link Data Logger software. In order to measure flue gas concentrations, analyzer probe is placed at the outlet of the cyclone when the system reaches steady-state condition. The steady state condition here means constant temperature profile and constant flue gas concentrations. Flue gas composition is measured with TESTO 360 and Gasmet DX-4000 gas analyzers. The data obtained are recorded by the software of the gas analyzer. For every five seconds concentrations are measured and recorded. This means that in a period of one minute, 12 data are collected. Measurements are performed between five to ten minutes. Thus, for each point shown in the graphs in Chapter 5, 60-120 data measurements are averaged out.

After a combustion test is completed, the ash collected in the ash hopper and in the bed are taken out and weighed. In order to find the amount of unburnt carbon content, collected ash is analyzed. The unburnt carbon analysis is carried out by heating the ash samples at 950 ^{o}C until constant weight is reached. The difference in weight gives the unburnt carbon in the ash sample.

Occasionally, some operational problems were observed throughout the experiments. At high temperatures ($\geq$ 950 ^{o}C) agglomeration of bed material was encountered due to the adhesion of fine ash particles in the bed. Additionally, for low excess air ratios (1.2-1.3) defluidization sometimes occurred because of the lower fluidization air supplied to the system. Lastly, excessive volatiles burn in the freeboard due to the segregation of the olive cake particles and bed material originating from density difference.

4.3. Characterization of Bed Material, Fuels and Adsorbents

4.3.1. Physical Properties

Silica sand obtained from Siltaş Sand Mine in Şile - İstanbul was used as bed material. The size of silica sand was in the range of 0.5 - 2.0 mm. The weighed average particle size (d_p) of the silica sand was found as 0.67 mm and dry bulk density of sand was determined as 1,640 kg/m^3. Porosity of the sand was also measured as 0.36.

Tunçbilek lignite coal and Edremit olive cake (dried) were used in the experiments as fuels. The size of these fuel particles used in the experiments was between 1.0 - 2.0 mm. The weighed average particle sizes of coal and olive cake were found as 1.43 mm and 1.52 mm, respectively.

Three different limestones obtained from Çan - Çanakkale, Çumra – Konya and Sedef - İstanbul were used in the experiments as adsorbents for SO_2. The particle size of these limestones was between 1.0 - 2.0 mm. The weighed average particle sizes of Çan, Çumra and Sedef limestones were found as 1.11 mm, 1.23 mm, and 1.29 mm, respectively. Additionally, dry bulk densities of Çan, Çumra and Sedef limestones were determined as 1,670 kg/m^3, 1,860 kg/m^3 and 2,178 kg/m^3, respectively.

The cumulative size distributions of silica sand, fuels and adsorbents are given below in Figure 4.3 and Figure 4.4 respectively.

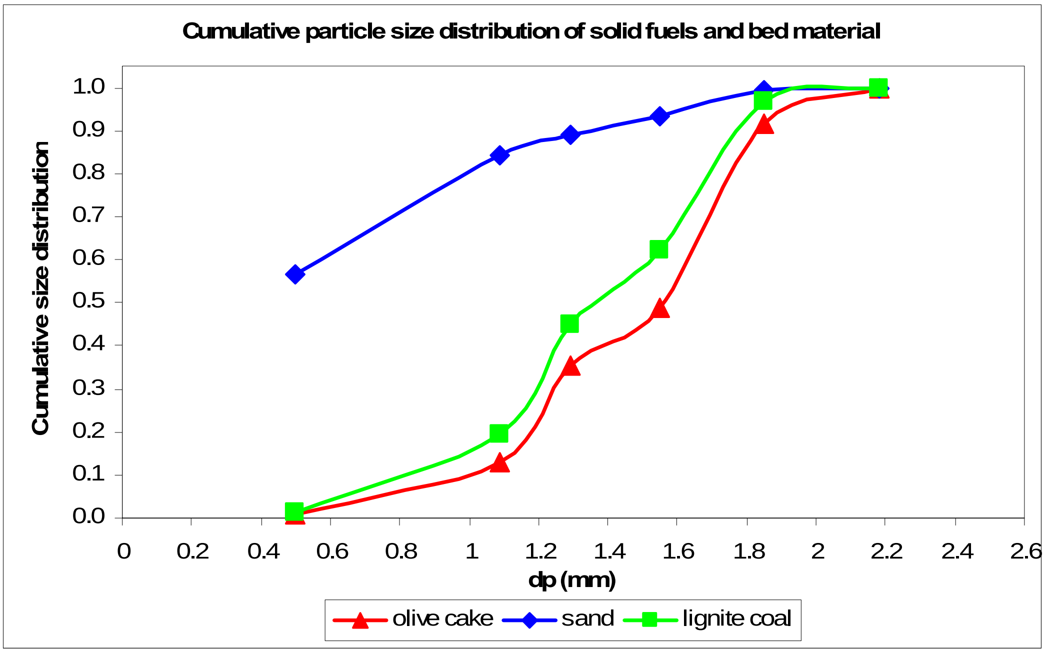

Figure 4.3 Cumulative particle size distribution of coal, olive cake and silica sand

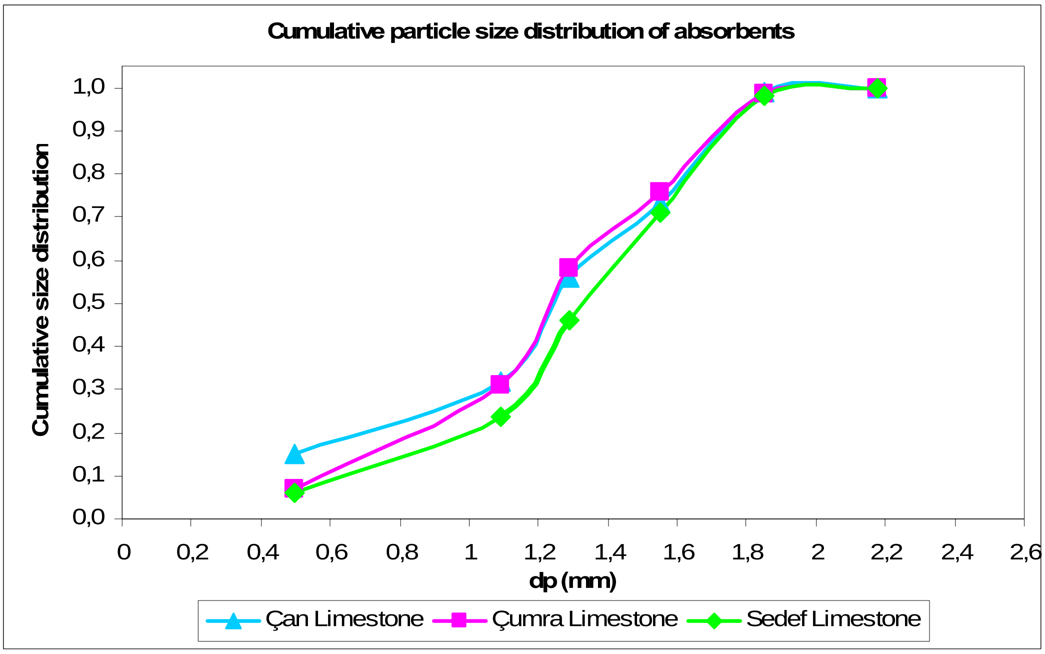

Figure 4.4 Cumulative particle size distributions of adsorbents

4.3.2. Proximate and Ultimate Analyses of the Fuels

The proximate and ultimate analyses of Tunçbilek lignite coal and Edremit olive cake were carried out by the Analysis Laboratories of the General Directorate of Mineral Research and Exploration (MTA) and they are presented in Table 4.1 and Table 4.2, respectively. Additionally, standard test methods used in these analyses are given in Table 4.3.

As it is seen from Table 4.1 lignite coal has very high ash content and olive cake has very high volatile matter content. Additionally, heating value of olive cake is higher when it is compared with lignite coal. According to the ultimate analysis results given in Table 4.2, combustible sulfur content of olive cake is zero.

Table 4.1 Proximate analyses of Tunçbilek lignite coal and Edremit olive cake

	Tunçbilek lignite coal		**Edremit olive cake**	
Analysis Type	**Wet Basis**	**Dry Basis**	**Wet Basis**	**Dry Basis**
Total Moisture, wt% (TS4745, TS690/ISO589)	10.15	-	13.49	-
Ash, wt% (TS330, TS1042)	44.30	49.31	6.32	7.30
Volatile Matter, wt% (TS711/ISO562)	24.47	27.24	62.48	72.23
Fixed Carbon, wt% **-**	21.08	23.45	17.71	20.47
Lower Heating Value, kcal/kg (TS2678)	2901	3295	3735	4408
Higher Heating Value, kcal/kg -	3099	3449	4084	4721

Table 4.2 Ultimate analyses of Tunçbilek lignite coal and Edremit olive cake

	Tunçbilek lignite coal		**Edremit olive cake**	
Element	**Wet Basis**	**Dry Basis**	**Wet Basis**	**Dry Basis**
C, wt% (ASTM 5373)	33.32	37.08	43.35	50.11
H, wt% (ASTM 5373)	2.64	2.93	5.15	5.95
N, wt% (ASTM 5373)	1.02	1.14	1.29	1.50
O, wt% (ASTM 5373)	7.98	8.89	30.40	35.13
S (Comb.), % (ASTM 5373)	0.59	0.66	0.00	0.00
S (Total), % (ASTM D4239)	1.07	1.19	0.10	0.11

Table 4.3 List of standards used in the analyses

Standard	**Date**	**Title**	**Parameter**
TS 4745	1986	Brown Coals and Lignites- Determination of Moisture Content- Indirect Gravimetric Method	Moisture
TS 690/ISO 589	2002	Hardcoal - Determination of total moisture	Moisture
TS 711/ISO 562	2002	Hard coal and coke - Determination of volatile matter	Volatile Matter
TS 2678	1977	Determination of Gross Calorific Values By The Calorimetric Bomb Method and Calculation of Net Calorific Values	HHV-LHV
TS 330	1966	Determination of Ash of Hard Coal	Ash
TS 1042	1971	Determination of Ash of Brown Coals and Lignites	Ash
ASTM D5373	2008	Standard Test Methods for Instrumental Determination of Carbon, Hydrogen, and Nitrogen in Laboratory Samples of Coal	Carbon Hydrogen Nitrogen
ASTM D4239	2008	Standard Test Methods for Sulfur in the Analysis Sample of Coal and Coke Using High-Temperature Tube Furnace Combustion Methods	Total Sulfur

4.3.3. Total Porosity, Multipoint BET, and Chemical Analyses of the Limestones

Total porosity and multipoint BET analyses of the limestones were carried out by Central Laboratory of METU while chemical analyses were performed by TÜBİTAK MRC Chemistry and Environment Institute and result are given in Table 4.4 and Table 4.5, respectively.

As it is seen from Table 4.4, total porosity and total surface area of the limestones are very low before calcination. In other words, these limestones almost have a non-porous structure. However, after calcination at 900 ^{o}C, total porosity and total surface area of limestones increase with the CO_2 leaving the limestone. Çumra limestone has the highest total porosity and total surface area after calcination.

Table 4.4 Total Porosity and Multipoint BET analyses of the limestones

Limestone	Total Porosity	Multipoint BET
	%	m^2/g
Çan	3.16	0.31
Çan after calcination @ 900^{o}C	29.88	14.93
Çumra	1.40	0.09
Çumra after calcination @ 900^{o}C	36.99	41.87
Sedef	3.77	2.70
Sedef- after calcination @ 900^{o}C	30.47	21.74

According to the chemical analyses of limestones in Table 4.5, $CaCO_3$ is the highest for all limestones. $CaCO_3$ percentage of Sedef limestone is higher than other two limestones.

Table 4.5 Chemical analyses of the limestones

Chemical Analysis (wet)	Çan	Çumra	Sedef
	original sample, wt %		
Moisture	0.395	0.070	0.065
$CaCO_3$	91.110	93.320	98.850
$MgCO_3$	0.420	0.210	0.410
SiO_2	0.772	0.062	0.125
Na_2O	0.022	0.123	0.120
K_2O	0.152	0.008	0.004
Al_2O_3	0.200	0.029	0.023
Fe_2O_3	0.485	0.020	0.075
LOI	43.662	43.666	43.712

4.4. Calibration of the Fuel Feeding System

The fuel feeding system was calibrated for olive cake and coal. Feeding rates were calculated for different on-off modes. In order to calculate the feeding rates, formulas obtained from calibration curves were used. Calibration curves of the feeding system for olive cake and coal are given in Figure A.1 and Figure A.2, respectively in Appendix A. Calculated feeding rates and corresponding on-off modes can be also seen from Table A.1 in Appendix A.

4.5. Determination of Minimum Fluidization Velocity

At the start of the experiments, the orifice was calibrated in order to see the pressure drops corresponding to different velocities and then corresponding velocities in the column were calculated. After this, two different cold experiments were performed in order to find minimum fluidization velocity (u_{mf}). Firstly, the pressure drops at the orifice and the distributor plate were measured with two manometers while the column was empty. Then these pressure drop values are matched with the velocities obtained from the orifice calibration. Secondly, 1339 g of sand (corresponding to 10 cm-bed height) was loaded into the combustor column and the same procedure for pressure measurements was carried out for the loaded column. Pressure drops through the bed were calculated by subtracting the pressure drops caused by distributor plate (empty bed) from the pressure drops caused by distributor plate + bed (loaded bed). In order to find the minimum fluidization velocity, the pressure drop in the bed versus air velocity was plotted. The velocity at minimum fluidization was found as 0.27 m/sec from this curve. Calculations for minimum fluidization velocity and more detailed explanations are given in Appendix B.

4.6. Flue Gas Analysis

During the experiments, emissions were measured with TESTO 360 and Gasmet DX-4000 flue gas analyzers. CO, SO_2, NO, and O_2 emissions were continuously measured from the sampling port at the outlet of cyclone. Calibrations of the flue gas analyzers were done with certified calibration gases. Both of the analyzers were ensured to measure the same values from calibration gases and flue gas. In order to prevent the condensation of water vapor, flue gas sample was passed through the heated sample lines of the analyzers. Measured data were recorded by analyzers of TESTO 360 and Gasmet DX-4000. Emissions were reported on dry basis (O_2 emission values can be obtained both on dry and wet basis) by the software of TESTO 360 and on wet basis by the software of Gasmet DX-4000. The specifications of TESTO 360 and Gasmet DX-4000 are given in Table 4.6.

The hydrocarbon concentration in the flue gas was not measured. However, it was measured in the previous studies carried out by Varol and Atimtay (2007, 2009). The amount of hydrocarbons in the flue gas is very small in the O_2 rich environment and the loss of C efficiency due to hydrocarbon emissions is about 1-2%. Therefore, this measurement was not done in the flue gas.

Table 4.6 Technical specifications of TESTO 360 and Gasmet DX-4000 flue gas analyzers

	Parameter	**Measurement Method**	**Measurement Sensitivity**	**Measurement Range**
TESTO 360	O_2	Electrochemical	± 0.1 vol%	0-21 vol. %
	NO	Electrochemical	± 1 ppmv	0-3000 ppm
	SO_2	Electrochemical	± 1 ppmv	0-5000 ppm
	CO	Electrochemical	± 1 ppmv	0-10000 ppm
Gasmet DX-4000	O_2	FTIR	± 0.01 vol%	0-25 vol. %
	NO	FTIR	± 0.01 ppmv	0-1000 ppm
	SO_2	FTIR	± 0.01 ppmv	0-2000 ppm
	CO	FTIR	± 0.01 ppmv	0-10000 ppm

4.7. Parameters Investigated

In this study, combustion and co-combustion of coal and olive cake in a bubbling fluidized bed combustor were investigated. Four sets of combustion experiments were performed in order to examine the effect of fuel share, excess air ratio, freeboard extension and limestone addition on flue gas emissions and combustion efficiency. As it was stated above, emissions were measured with TESTO 360 and Gasmet DX-4000 flue gas analyzers during the experiments.

The main focus of the experiments as explained before was to see how the freeboard height will affect the emissions and combustion efficiency. Especially, when biomass which is rich in volatile matter is burned in a BFBC, the volatile matters are released from the fuel and burn in the freeboard. The recommendations made in the previous studies of Varol and Atimtay, (2007, 2009) were to have a longer freeboard in the combustor to increase the residence time of the volatiles for efficient combustion in the bed, thus have lower CO emission and higher combustion efficiency.

Experiments were done first in 1 m - column, then they were repeated, in the 2 m - column for comparison. Parameters investigated in this study are listed below.

Set 1 - Combustion and co-combustion of coal and olive cake in 1 m - combustion column

Effect of excess air ratio and fuel share on;

- Temperature distributions
- Flue gas emissions
- Combustion efficiencies

Set 2 - Combustion and co-combustion of coal and olive cake in 2 m - combustion column

Effect of freeboard extension on;

- Temperature distributions
- CO emissions
- Combustion efficiencies

Set 3 - Combustion and co-combustion of coal and olive cake with limestone addition in 1 m - combustion column

Effect of addition of different limestones and different Ca/S ratios on;

- SO_2 emissions
- SO_2 removal efficiencies
- Combustion efficiencies

Set 4 - Co-combustion of coal and olive cake with limestone addition in 2 m - combustion column

Effect of freeboard extension and different Ca/S ratios on;

- SO_2 emissions
- SO_2 removal efficiencies
- Combustion efficiencies

CHAPTER 5

RESULTS AND DISCUSSION

The results obtained for the combustion and co-combustion of coal and olive cake in a bubbling fluidized bed of 1 m and 2 m high are presented and discussed in this chapter. In the first set of experiments, the effect of biomass share in the fuel mixture and excess air ratio on temperature distribution along the combustion column, flue gas emissions (CO, NO_x and SO_2) and combustion efficiency were tested in the 1 m - combustion column. In the second set of experiments, the effect of biomass share in the fuel mixture and excess air ratio on temperature distribution along the combustion column, flue gas emissions and combustion efficiency were tested in 2 m - combustion column. Furthermore, the effect of freeboard extension on CO emissions and combustion efficiency was discussed. In the third set of experiments, the effect of addition of different limestones on SO_2 emissions and combustion efficiency was explained. The reactivities of three different limestones for SO_2 adsorption were tested. In this set, different Ca/S ratios were tried for combustion of coal and co-combustion of coal and olive cake. Finally in the last set, the effect of freeboard extension on SO_2 emissions and combustion efficiency were investigated. Test runs conducted are listed in Table 5.1. A total of 40 runs were made. For each run the feeding rate of the fuel was 22 g/min. Superficial velocity was 1.03 m/s (corresponding to $\approx 4\ u_{mf}$) for average bed temperature of 850 ^{o}C.

Table 5.1 Test runs conducted for the combustion experiments

<table>
<tr><th colspan="2">Set 1 (Combustion Column Height = 1 m)</th></tr>
<tr><th>Run No.</th><th>Fuel</th></tr>
<tr><td>r-1</td><td>Coal 100 wt%</td></tr>
<tr><td>r-2</td><td>Coal 75 wt% + Olive Cake 25 wt%</td></tr>
<tr><td>r-3</td><td>Coal 50 wt% + Olive Cake 50 wt%</td></tr>
<tr><td>r-4</td><td>Coal 25 wt% + Olive Cake 75 wt%</td></tr>
<tr><td>r-5</td><td>Olive Cake100 wt%</td></tr>
<tr><th colspan="2">Set 2 (Combustion Column Height = 2 m)</th></tr>
<tr><th>Run No.</th><th>Fuel</th></tr>
<tr><td>r-6</td><td>Coal 100 wt%</td></tr>
<tr><td>r-7</td><td>Coal 75 wt% + Olive Cake 25 wt%</td></tr>
<tr><td>r-8</td><td>Coal 50 wt% + Olive Cake 50 wt%</td></tr>
<tr><td>r-9</td><td>Coal 25 wt% + Olive Cake 75 wt%</td></tr>
<tr><td>r-10</td><td>Olive Cake100 wt%</td></tr>
<tr><th colspan="2">Set 3 (Combustion Column Height = 1 m)</th></tr>
<tr><th>Run No.</th><th>Fuel + Adsorbent</th></tr>
<tr><td>r-11</td><td>Coal 100 wt% + Çan Ls. (Ca/S=1.5)</td></tr>
<tr><td>r-12</td><td>Coal 100 wt% + Çan Ls. (Ca/S=2.0)</td></tr>
<tr><td>r-13</td><td>Coal 100 wt% + Çan Ls. (Ca/S=2.5)</td></tr>
<tr><td>r-14</td><td>Coal 100 wt% + Çan Ls. (Ca/S=3.0)</td></tr>
<tr><td>r-15</td><td>Coal 100 wt% + Çan Ls. (Ca/S=3.5)</td></tr>
<tr><td>r-16</td><td>Coal 100 wt% + Çumra Ls. (Ca/S=1.5)</td></tr>
<tr><td>r-17</td><td>Coal 100 wt% + Çumra Ls. (Ca/S=2.0)</td></tr>
<tr><td>r-18</td><td>Coal 100 wt% + Çumra Ls. (Ca/S=2.5)</td></tr>
<tr><td>r-19</td><td>Coal 100 wt% + Çumra Ls. (Ca/S=3.0)</td></tr>
<tr><td>r-20</td><td>Coal 100 wt% + Çumra Ls. (Ca/S=3.5)</td></tr>
<tr><td>r-21</td><td>Coal 100 wt% + Sedef Ls. (Ca/S=1.5)</td></tr>
<tr><td>r-22</td><td>Coal 100 wt% + Sedef Ls. (Ca/S=2.0)</td></tr>
<tr><td>r-23</td><td>Coal 100 wt% + Sedef Ls. (Ca/S=2.5)</td></tr>
<tr><td>r-24</td><td>Coal 100 wt% + Sedef Ls. (Ca/S=3.0)</td></tr>
<tr><td>r-25</td><td>Coal 100 wt% + Sedef Ls. (Ca/S=3.5)</td></tr>
<tr><td>r-26</td><td>Coal 50 wt% + Olive Cake 50 wt% + Çan Ls. (Ca/S=1.5)</td></tr>
<tr><td>r-27</td><td>Coal 50 wt% + Olive Cake 50 wt% + Çan Ls. (Ca/S=2.0)</td></tr>
<tr><td>r-28</td><td>Coal 50 wt% + Olive Cake 50 wt% + Çan Ls. (Ca/S=2.5)</td></tr>
<tr><td>r-29</td><td>Coal 50 wt% + Olive Cake 50 wt% + Çan Ls. (Ca/S=3.0)</td></tr>
<tr><td>r-30</td><td>Coal 50 wt% + Olive Cake 50 wt% + Çumra Ls. (Ca/S=1.5)</td></tr>
<tr><td>r-31</td><td>Coal 50 wt% + Olive Cake 50 wt% + Çumra Ls. (Ca/S=2.0)</td></tr>
<tr><td>r-32</td><td>Coal 50 wt% + Olive Cake 50 wt% + Çumra Ls. (Ca/S=2.5)</td></tr>
<tr><td>r-33</td><td>Coal 50 wt% + Olive Cake 50 wt% + Çumra Ls. (Ca/S=3.0)</td></tr>
<tr><td>r-34</td><td>Coal 50 wt% + Olive Cake 50 wt% + Sedef Ls. (Ca/S=1.5)</td></tr>
<tr><td>r-35</td><td>Coal 50 wt% + Olive Cake 50 wt% + Sedef Ls. (Ca/S=2.0)</td></tr>
<tr><td>r-36</td><td>Coal 50 wt% + Olive Cake 50 wt% + Sedef Ls. (Ca/S=2.5)</td></tr>
<tr><td>r-37</td><td>Coal 50 wt% + Olive Cake 50 wt% + Sedef Ls. (Ca/S=3.0)</td></tr>
<tr><th colspan="2">Set 4 (Combustion Column Height = 2 m)</th></tr>
<tr><th>Run No.</th><th>Fuel + Adsorbent</th></tr>
<tr><td>r-38</td><td>Coal 50 wt% + Olive Cake 50 wt% + Çan Ls. (Ca/S=2.0)</td></tr>
<tr><td>r-39</td><td>Coal 50 wt% + Olive Cake 50 wt% + Çan Ls. (Ca/S=2.5)</td></tr>
<tr><td>r-40</td><td>Coal 50 wt% + Olive Cake 50 wt% + Çan Ls. (Ca/S=3.0)</td></tr>
</table>

5.1. Combustion and Co-combustion of Coal and Olive cake in 1 m - Combustion Column

5.1.1. Temperature Profiles

While combustion tests were performed, temperature distribution along the combustion column was continuously measured by six thermocouples. Temperature data and corresponding excess air ratios are given in detail in Appendix F. Figure 5.1 shows average temperature profiles along the column for excess air ratio (λ) of 1.9 during combustion of coal and olive cake alone. Average bed temperature is about 850 ^{o}C which is the required operation temperature for combustion tests. The temperatures were observed to increase along the bed height and then decrease along the freeboard after reaching a maximum value. For coal combustion maximum temperature (≈ 860 ^{o}C) was obtained at about 110 mm above the distributor plate. But for olive cake combustion, the maximum temperature (≈ 880 ^{o}C) was obtained at about 330 mm above the distributor plate. As it is seen from Figure 5.1, temperature profile of coal combustion has a much smoother trend as compared to the olive cake combustion.

Average temperature profiles along the column during co-combustion of coal and olive cake for excess air ratio (λ) of 1.9 are given in Figure 5.2. Maximum temperatures (≈ 870 ^{o}C and ≈ 860 ^{o}C) were obtained at about 110 mm above the distributed plate for the co-combustion of 75 wt% coal + 25 wt% OC and 50 wt% coal + 50 wt% OC, respectively. On the other hand, for the co-combustion of 25 wt% coal + 75 wt% OC the maximum temperature (≈ 860 ^{o}C) was obtained at about 330 mm above the distributor plate.

It is seen from Figure 5.2 that as the percentage of olive cake in the fuel mixture was increased, temperature profiles showed an irregular trend. Temperatures in the bed decreased while temperatures in the freeboard increased with increasing olive cake percentage in the fuel mixture. This change can be explained with difference in densities and ignition temperatures of olive cake and coal. As soon as the olive cake particles enter the bed, they are heated up, ignited and the volatile matter is released. The volatile matter content of the olive cake (72.23 wt% on dry basis) is much higher than that of coal (27.24 wt% on dry basis). After the release of volatile matter, the combustion of volatile matter continues in the freeboard and the temperature reaches to about 860 - 880 °C which is above the average bed temperature. On the other hand, coal particles ignite later. Char particles remaining after devolatilization of coal particles keep on burning within the bed. This ongoing combustion of coal particles is the result of their higher fixed carbon content. Besides, coal combustion occurs at lower parts of the combustion column for a long period of time whereas olive cake combustion takes place rapidly more in the freeboard region.

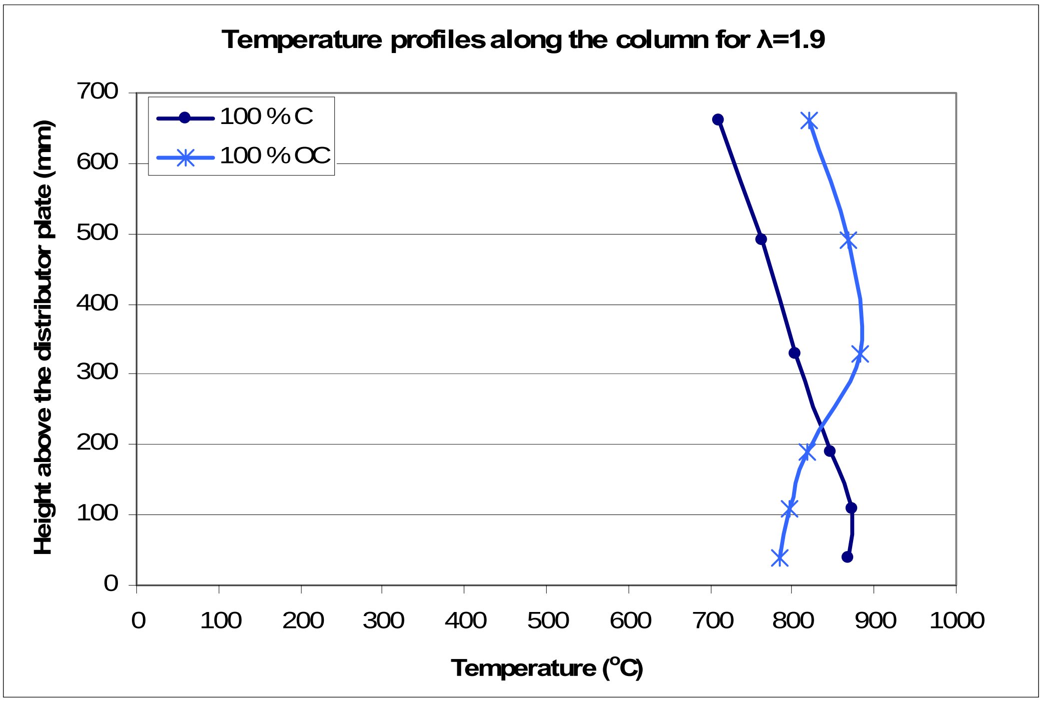

Figure 5.1 Comparison of temperature profiles along 1 m - column for the combustion of coal and olive cake (λ = 1.9)

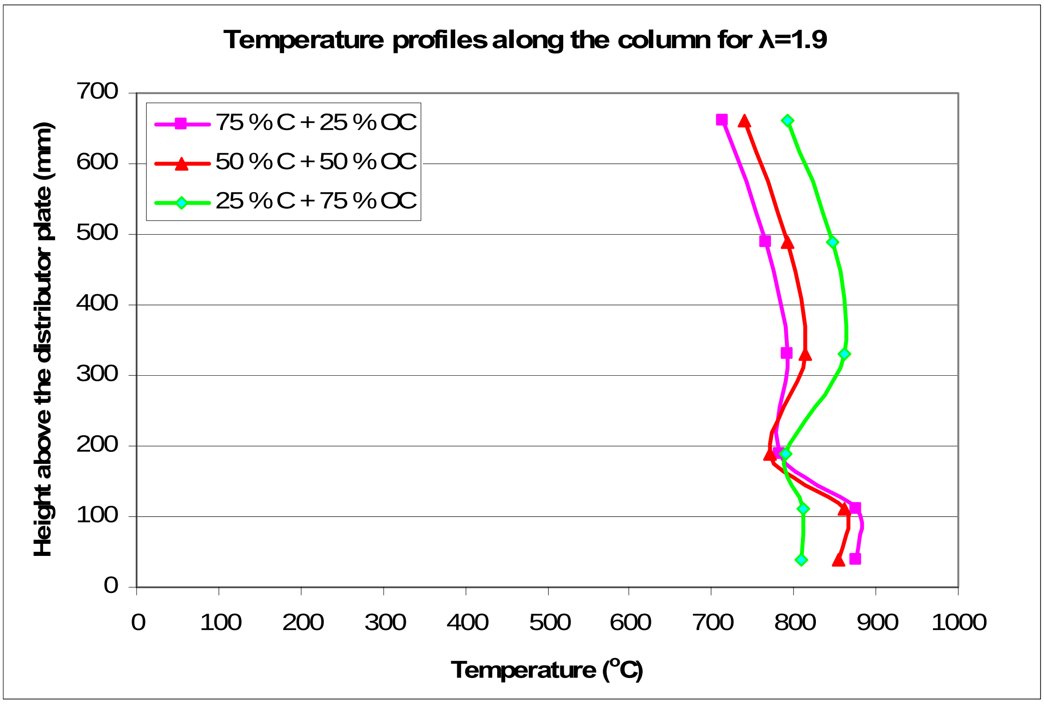

Figure 5.2 Comparison of temperature profiles along 1 m - column for the co-combustion of coal and olive cake (λ = 1.9)

5.1.2. Flue Gas Emissions

For all experiments, concentrations of the pollutants in the gas phase were measured and expressed in mg/Nm^3 at normal temperature (0 ^{o}C) and pressure (1 atm) in order to compare with Turkish and EU regulations (Turkish Regulation for Control of Air Pollution from Industrial Sources (RCAPIS) and Directive of Emissions from Large Combustion Plants (2001/80/EC)). Additionally, concentrations are based on 6 vol% O_2 in the flue gas as required in these regulations. Excess air ratios (λ) were measured in the interval of 1.2-2.5 for combustion and co-combustion experiments.

Effect of fuel share on flue gas emissions

Flue gas emissions for combustion and co-combustion experiments at an average bed temperature of 850 ^{o}C are given in Table 5.2. As it is seen from this table, for the combustion of olive cake, SO_2 emissions were found to be low (442.0 mg/Nm^3) due to very low sulfur content (0.11 wt% on dry basis) of olive cake. On the other hand for the combustion of coal, SO_2 emissions were measured much higher (2,544.1 mg/Nm^3) than the SO_2 emissions for olive cake combustion due to high sulfur content (1.19 wt% on dry basis) of coal. CO emissions for olive cake combustion (6240.4 mg/Nm^3) were found to be much higher than the ones for coal combustion (185.9 mg/Nm^3) due to the escape of high unburnt volatile matter of olive cake from the combustor. For coal combustion NO_x concentrations (2247.0 mg/Nm^3) are about two times more than the ones for olive cake combustion (1011.4 mg/Nm^3).

For the co-combustion experiments SO_2 emissions are observed to decrease with increasing olive cake percentage since sulfur content of olive cake is very low. On the other hand, as olive cake percentage in the fuel mixture was increased, CO emissions increased because of higher volatile matter content of olive cake in comparison with coal. Most of this volatile matter leaves the combustor as CO without burning completely. NO_x concentrations are observed to decrease with increasing olive cake percentage in the fuel mixture. This can be explained by quick release of volatiles in olive cake particles which causes high levels of hydrocarbon radicals and CO formation. A reducing atmosphere in the freeboard region is formed. This will cause a reduction in the amount of NO_x. This kind of reduction in NO_x emissions were also encountered by Armesto et al. (2003).

Additionally, effect of olive cake content on SO_2 emissions are discussed in detail in Appendix E.

Table 5.2 Flue gas emissions for the combustion and co-combustion of coal and olive cake in 1 m - combustion column (average bed temperature ≅ 850 °C)

Run No.	**Fuel**	**CO**	**SO_2**	**NO_x**
		(mg/Nm^3 based on 6% O_2)		
r-1	Coal 100 wt%	185.9	2544.1	2247.0
r-2	Coal 75 wt% + Olive Cake 25 wt%	167.8	2064.9	2063.6
r-3	Coal 50 wt% + Olive Cake 50 wt%	1033.4	1573.6	1439.0
r-4	Coal 25 wt% + Olive Cake 75 wt%	2379.2	703.7	1145.4
r-5	Olive Cake 100 wt%	6240.4	442.0	1011.4

Effect of excess air ratio on flue gas emissions

The effect of excess air ratio on **CO emissions** for the combustion and co-combustion of coal and olive cake is given in Figure 5.3. CO emissions are observed to decrease with increasing excess air ratios as expected. The reason for this decrease is more oxygen supply for the fuel for better combustion of volatiles. If enough oxygen is not provided in the combustion medium, the volatiles can not burn efficiently and escape from the combustion column as partially oxidized. Furthermore, increase in CO emissions is clearly seen with the gradual increase in olive cake percentage in the fuel mixture. As it was explained before, this increase in CO emissions results due to higher volatile matter content of olive cake. As olive cake percentage in the fuel mixture increases, higher amount of volatiles are released per unit weight of fuel mixture. In Figure 5.3 it is seen that highest amounts of CO concentrations are seen when the fuel is 100 wt% olive cake. This is the reason to use secondary air in the combustion column in the freeboard region to burn the volatiles and decrease the CO and hydrocarbon emissions. This was shown successfully in the previous studies by Varol and Atimtay (2009).

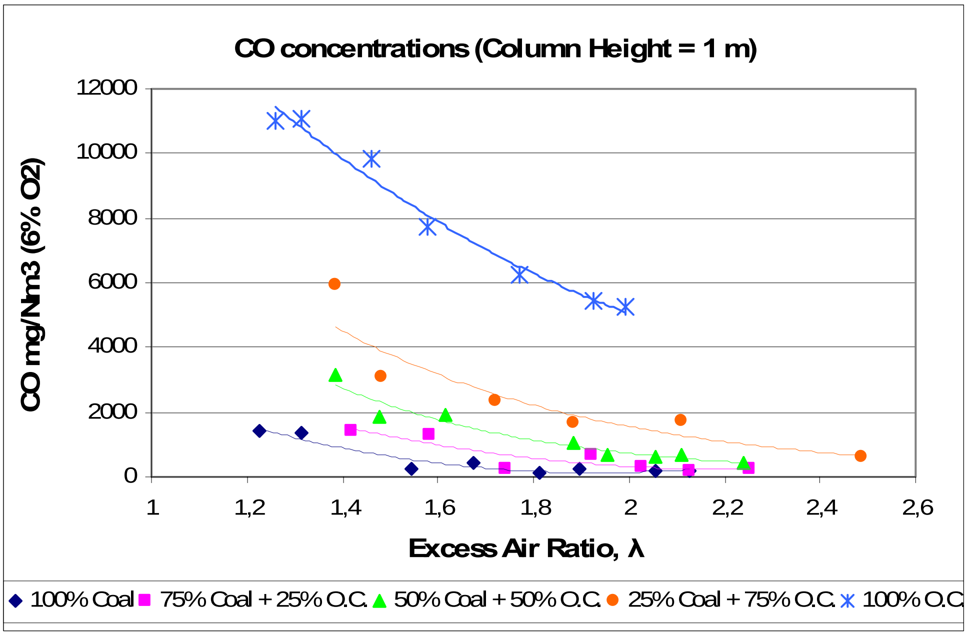

Figure 5.3 Effect of excess air ratio on CO emissions for the combustion and co-combustion of coal and olive cake in 1 m - combustion column

The effect of excess air ratio on **SO_2 emissions** for the combustion and co-combustion of coal and olive cake is given in Figure 5.4. Since temperatures (900-950 ^{o}C) are so high for lower excess air ratios (1.2-1.5), SO_2 formation is higher for this interval. As the excess air ratio is increased, emissions start to decrease because of dilution of flue gases and decrease in temperature. Moreover, SO_2 emissions are observed to decrease with increasing olive cake percentage since the sulfur content of olive cake is much lower than coal. According to Figure 5.4, the highest amounts of SO_2 concentrations are seen when the fuel is 100 wt% coal.

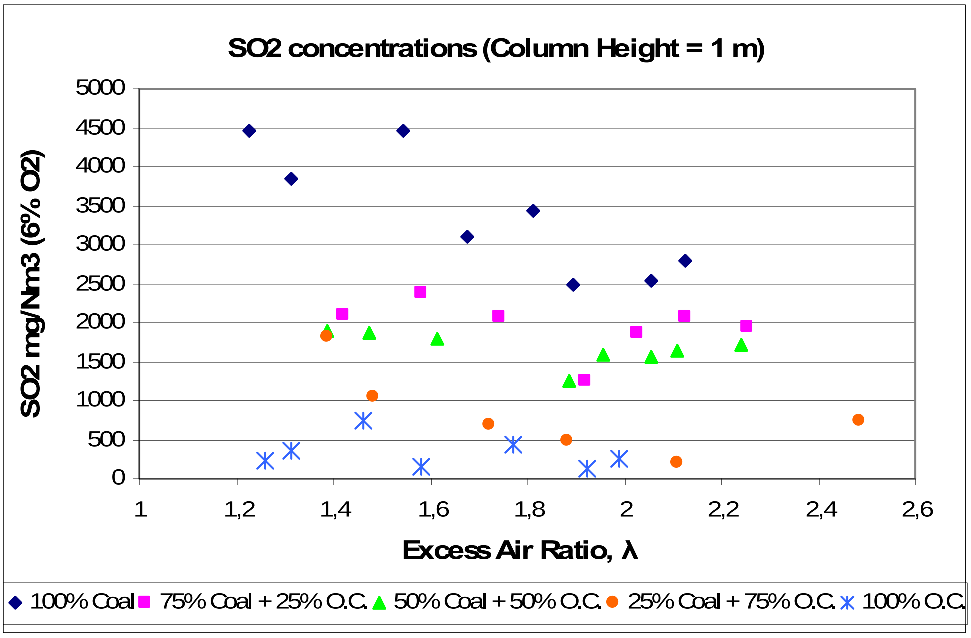

Figure 5.4 Effect of excess air ratio on SO_2 emissions for the combustion and co-combustion of coal and olive cake in 1 m - combustion column

The effect of excess air ratio on **NO_x emissions** for the combustion and co-combustion of coal and olive cake is given in Figure 5.5. According to this figure, NO_x emissions show an increasing trend with increasing excess air ratios. This may be due to higher amounts of O_2 supplied. On the other hand, at low excess air ratios CO emissions are much higher as it is seen in Figure 5.3. In this reducing atmosphere, NO_x emissions might be reduced to N_2. It is also seen from the figure that with increasing olive cake percentage in the fuel mixture, NO_x concentrations decrease. This may result from high levels of hydrocarbon radicals and CO formation (a reducing atmosphere) in the freeboard region for low excess air ratios. According to Figure 5.5, the highest amounts of NO_x concentrations are seen when the fuel is 100 wt% coal.

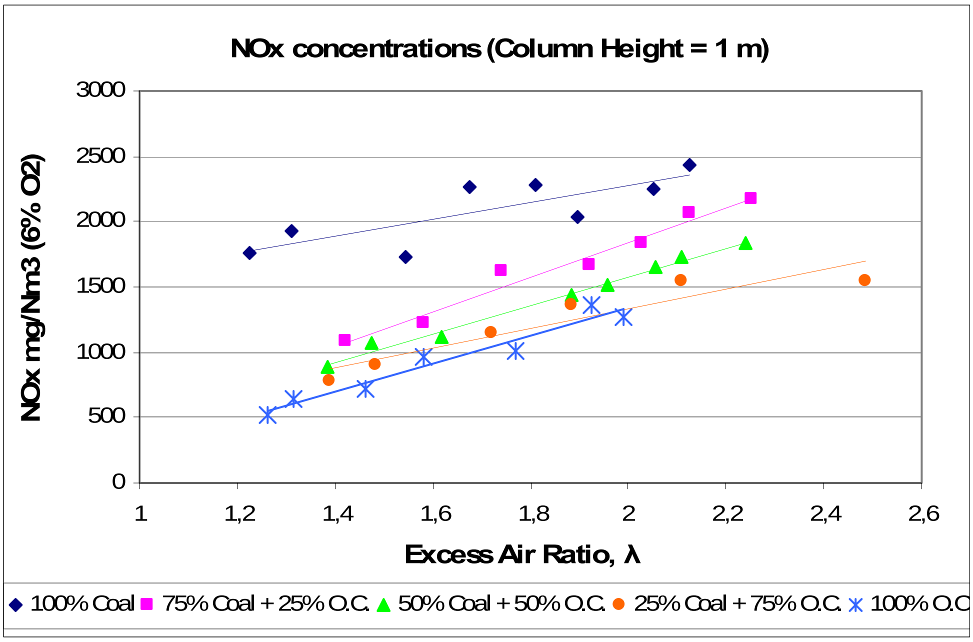

Figure 5.5 Effect of excess air ratio on NO_x emissions for the combustion and co-combustion of coal and olive cake in 1 m - combustion column

In this study hydrocarbon emissions were not measured. According to Van Loo and Koppejan (2008), hydrocarbons are in general earlier intermediates than CO; therefore they have lower concentrations in the flue gas than CO. Additionally, amounts of hydrocarbon emissions and their contribution to the total combustion losses was found to be low by Varol (2006).

5.1.3. Combustion Efficiencies

Combustion losses for BFBs are relatively high, in the range of 5 to 20%, depending upon the rank of coal. They mostly originate from CO formation (L_{CO}) and unburnt carbon in the fly ash and bottom ash ($L_{\text{fly ash}}$, $L_{\text{bottom ash}}$). $L_{\text{bottom ash}}$ may typically contain up to 3% unburnt carbon while $L_{\text{fly ash}}$ may have up to 10% (Basu, 2006). The addition of L_{CO}, $L_{\text{fly ash}}$ and $L_{\text{bottom ash}}$ gives the total % loss in combustion. Therefore net combustion efficiency is $\eta = 100 - L_{\text{total}}$.

Combustion losses and efficiencies for the combustion of coal, olive cake and co-combustion of olive cake + coal mixtures are shown in Table 5.3. In this study, combustion loss resulting from the fly ash generally has the largest portion in the total combustion loss. As can be seen from this table, combustion losses due to CO formation increases as the fuels shift from coal to olive cake. Just for 100 wt% olive cake combustion, the effect of L_{CO} is much higher than the other losses and it decreases the overall combustion efficiency Additionally, $L_{fly\ ash}$ and $L_{bottom\ ash}$ decrease gradually with increasing olive cake percentage in the fuel mixture since olive cake has much lower ash content as compared to coal.

Table 5.3 Combustion losses and efficiencies for the combustion and co-combustion of olive cake and coal in 1 m - combustion column

Run No	**Fuel**	**L_{CO} (%)**	**$L_{bottom\ ash}$ (%)**	**$L_{fly\ ash}$ (%)**	**η (%)**
r-1	Coal 100 wt%	**0.23**	**1.09**	**2.53**	**96.15**
r-2	Coal 75 wt% + O.C. 25 wt%	**0.27**	**0.71**	**2.03**	**96.99**
r-3	Coal 50 wt% + O.C. 50 wt%	**0.56**	**0.12**	**1.51**	**97.81**
r-4	Coal 25 wt% + O.C. 75 wt%	**1.11**	**0.06**	**0.76**	**98.08**
r-5	O.C. 100 wt%	**3.53**	**0.14**	**0.01**	**96.32**

The effect of excess air ratio on combustion efficiencies for the combustion and co-combustion of olive cake and coal is shown in Figure 5.6. As the coal percentage increases in the fuel mixture, combustion efficiencies decrease due to the leading effect of $L_{fly\ ash}$. On the other hand, since CO emissions are higher for lower excess air ratios, the effect of L_{CO} on the total combustion loss increases. This effect is especially observed as the olive cake percentage increases in the fuel mixture. After a certain λ value, overall efficiencies become almost stable for all fuel mixtures since CO emissions start to decrease.

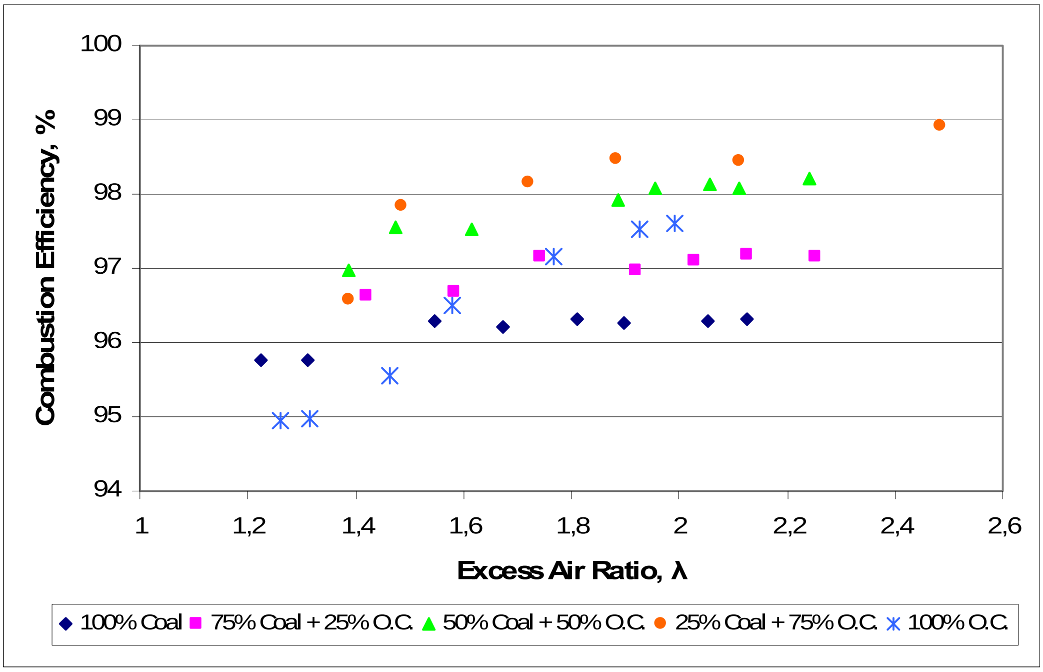

Figure 5.6 Effect of excess air ratio on combustion efficiencies for the combustion and co-combustion of olive cake and coal in 1 m - combustion column

5.2. Combustion and Co-combustion of Coal and Olive Cake in 2 m - Combustion Column

In order to see the effect of increasing the freeboard height from 90 cm to 190 cm on the combustion efficiency and the flue gas emissions, similar experiments as explained in Section 5.1 have been conducted. The results are presented in this section.

5.2.1. Temperature Profiles

In the second set of experiments, temperature distribution along the combustion column was continuously measured by nine thermocouples. Temperature data and corresponding excess air ratios are given in detail in Appendix F. Figure 5.7

shows average temperature profiles along the column for excess air ratio (λ) of 1.9 during combustion of coal and olive cake alone. Average bed temperature is about 850 °C. The temperatures were observed to increase along the bed height and then decrease along the freeboard after reaching a maximum value. For coal combustion maximum temperature (≈ 870 °C) was obtained at about 190 mm above the distributor plate. But for olive cake combustion, the maximum temperature (≈ 900 °C) was obtained at about 330 mm above the distributor plate. As it is seen from Figure 5.7, temperature profile of coal combustion has a much smoother trend as compared to the olive cake combustion**.**

Average temperature profiles along the column during co-combustion of coal and olive cake for excess air ratio (λ) of 1.9 are given in Figure 5.8. Maximum temperatures (≈ 860 °C) were obtained at about 110 mm above the distributed plate for the co-combustion of 25 wt% coal + 75 wt% OC and 50 wt% coal + 50 wt% OC. On the other hand, for the co-combustion of 75 wt% coal + 25 wt% OC the maximum temperature (≈ 850 °C) was obtained at about 330 mm above the distributor plate.

It is seen from Figure 5.8 that as the percentage of olive cake in the fuel mixture was increased, temperature profiles showed an irregular trend. Temperatures in the bed decreased while temperatures in the freeboard increased with increasing olive cake percentage in the fuel mixture. This change was explained in detail in the previous section (see section 5.1.1). As it was seen in 1 m - combustion column tests, coal combustion occurs at lower parts of the combustion column for a long period of time whereas olive cake combustion takes place rapidly more in the freeboard region. The freeboard temperature is about 130 °C higher when olive cake is burned as compared to coal.

As it is seen from Figure 5.7 and 5.8, temperature profiles obtained in the tests with 2 m - combustion column are much smoother as compared to the temperature profiles obtained in the tests with 1 m - combustion column (see Figure 5.1 and 5.2). Although temperatures at the top of the combustor decreased up to 600 °C, temperature distribution is much smoother along the 2 m - combustion column as compared to the 1 m - column. Better temperature distribution along the column height brings much better combustion efficiencies throughout the tests. However, exit temperatures of the flue gas from the combustor is lower in 2 m - column than 1 m - column as expected (500-600 °C as opposed to 700-800 °C)

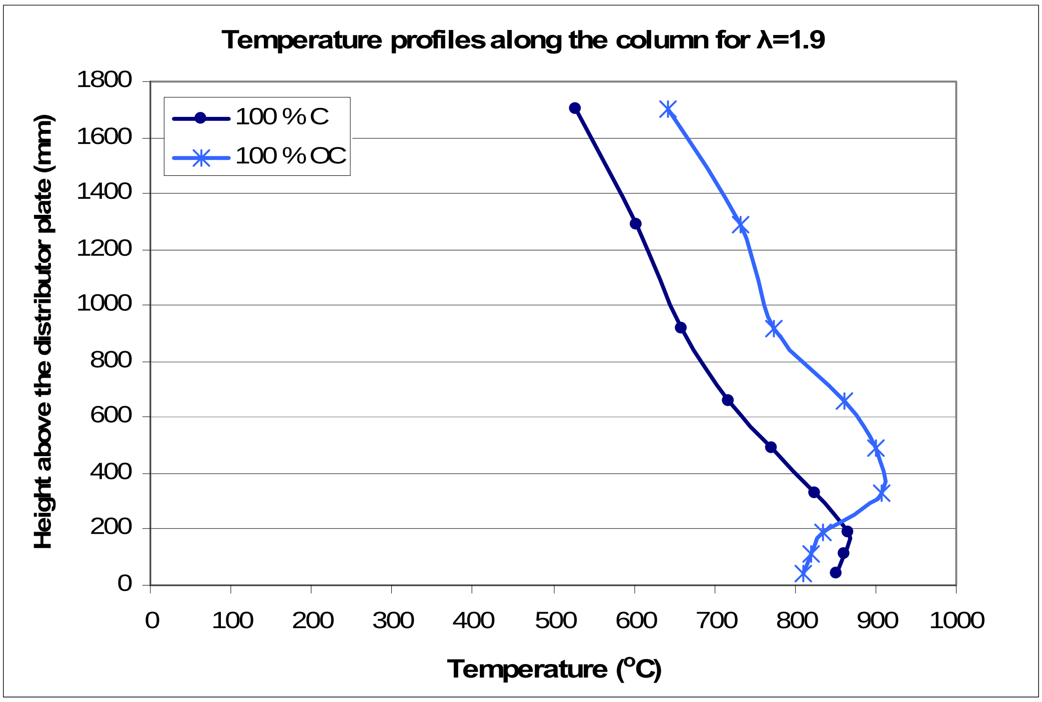

Figure 5.7 Comparison of temperature profiles along 2 m - column for the combustion coal and olive cake ($\lambda = 1.9$)

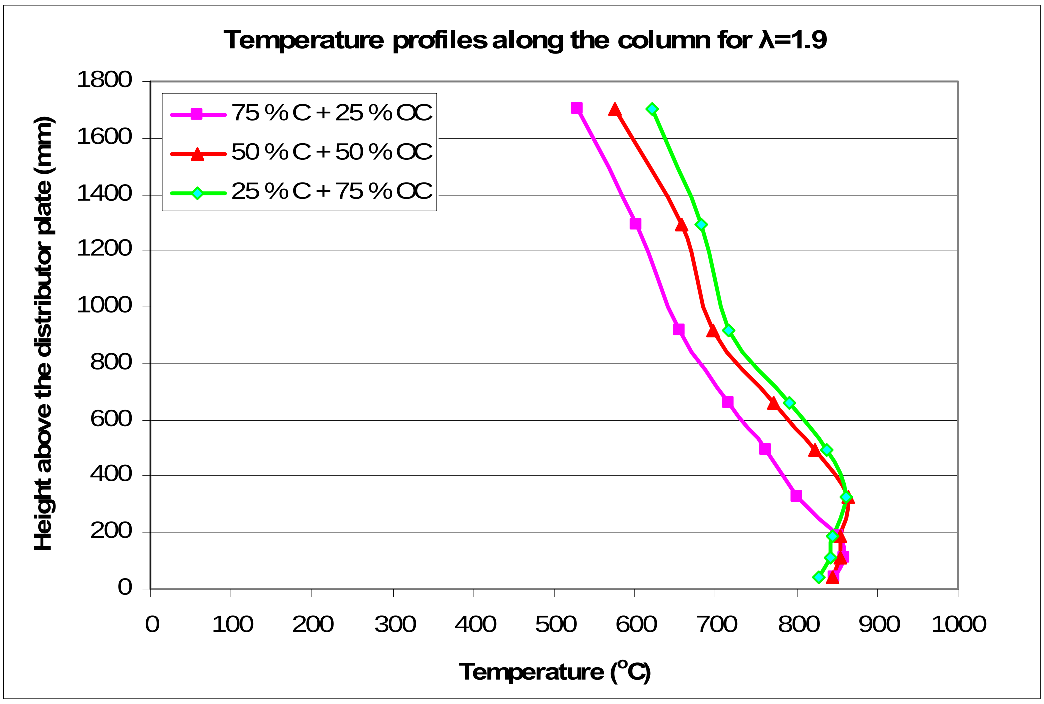

Figure 5.8 Comparison of temperature profiles along 2 m - column for the co-combustion of coal and olive cake (λ = 1.9)

5.2.2. Flue Gas Emissions

In this set of experiments, emission concentrations were measured for the corresponding excess air ratios between 1.2 and 2.5.

Effect of fuel share on flue gas emissions

Flue gas emissions for combustion and co-combustion experiments at an average bed temperature of 850 °C are given in Table 5.4. Just as in the 1 m – combustion column tests, for the combustion of olive cake, SO_2 emissions were found to be low (193.1 mg/Nm^3) since olive cake has a very low sulfur content. But for the combustion of coal, SO_2 emissions were measured much higher (2,371.8 mg/Nm^3) than the SO_2 emissions for olive cake combustion due to high sulfur content of coal. CO emissions for olive cake combustion (4593.1 mg/Nm^3) were found to be much higher than the ones for coal combustion (350.0 mg/Nm^3) due to higher volatile matter of olive cake. For coal combustion NO_x concentrations (2071.3 mg/Nm^3) are about two times more than the ones for olive cake combustion (838.9 mg/Nm^3).

Similar to 1 m - combustion column tests, for the co-combustion experiments SO_2 emissions are observed to decrease with increasing olive cake percentage in the fuel mixture since sulfur content of olive cake is very low. As olive cake percentage in the fuel mixture increased, CO emissions increased because of higher volatile matter content of olive cake in comparison with coal. NO_x concentrations are observed to decrease with increasing olive cake percentage in the fuel mixture due to the similar reasons explained in Section 5.1.2.

If overall emission results of 2 m - combustion column tests are compared with that of 1 m - combustion column tests, it is clearly seen that CO, SO_2 and NO_x emission values were lower than the ones obtained in 1 m - combustion column. Percentage decreases in the flue gas emissions with the freeboard extension are given in Table 5.5. This improvement shows the positive effect of increasing the freeboard height on the emissions.

Table 5.4 Flue gas emissions for the combustion and co-combustion of coal and olive cake in 2 m - combustion column (average bed temperature ≅ 850 °C)

Run No.	**Fuel**	**CO**	**SO_2**	**NO_x**
		(mg/Nm^3 based on 6% O_2)		
r-6	Coal 100 wt%	350.0	2371.8	2071.3
r-7	Coal 75 wt% + Olive Cake 25 wt%	261.0	1616.5	1830.1
r-8	Coal 50 wt% + Olive Cake 50 wt%	383.8	909.8	1604.6
r-9	Coal 25 wt% + Olive Cake 75 wt%	1350.9	261.0	1027.6
r-10	Olive Cake 100 wt%	4593.1	193.1	838.9

Table 5.5 Percentage decreases in the flue gas emissions with the freeboard extension (average bed temperature ≅ 850 ^{o}C)

Run No.	**Fuel**	**CO**	**SO_2**	**NO_x**
		% decrease		
r-6	Coal 100 wt%	ND	6.7	7.8
r-7	Coal 75 wt% + Olive Cake 25 wt%	ND	21.7	11.3
r-8	Coal 50 wt% + Olive Cake 50 wt%	62.9	26.8	ND
r-9	Coal 25 wt% + Olive Cake 75 wt%	43.2	62.9	10.2
r-10	Olive Cake 100 wt%	26.4	56.3	17.1

*ND - No decrease was observed

Effect of excess air ratio on flue gas emissions

The effect of excess air ratio on **CO emissions** for the combustion and co-combustion of coal and olive cake is given in Figure 5.9. As it was in the 1 m - combustion column tests, CO emissions are observed to decrease with increasing excess air ratios as expected. The reason for this decrease is more oxygen supply for the fuel for better combustion of volatiles. If enough oxygen is not provided to the combustor, the fuels can not burn efficiently and incomplete combustion products, like CO, escape from the combustion column unburnt. Furthermore, increase in CO emissions is clearly seen with the gradual increase in olive cake percentage in the fuel mixture. Higher amount of volatiles in olive cake are released per unit weight of fuel mixture as the olive cake percentage in the fuel mixture increases. As it was expected, it is seen from Figure 5.9 that highest amounts of CO concentrations are observed when the fuel is 100 wt% olive cake.

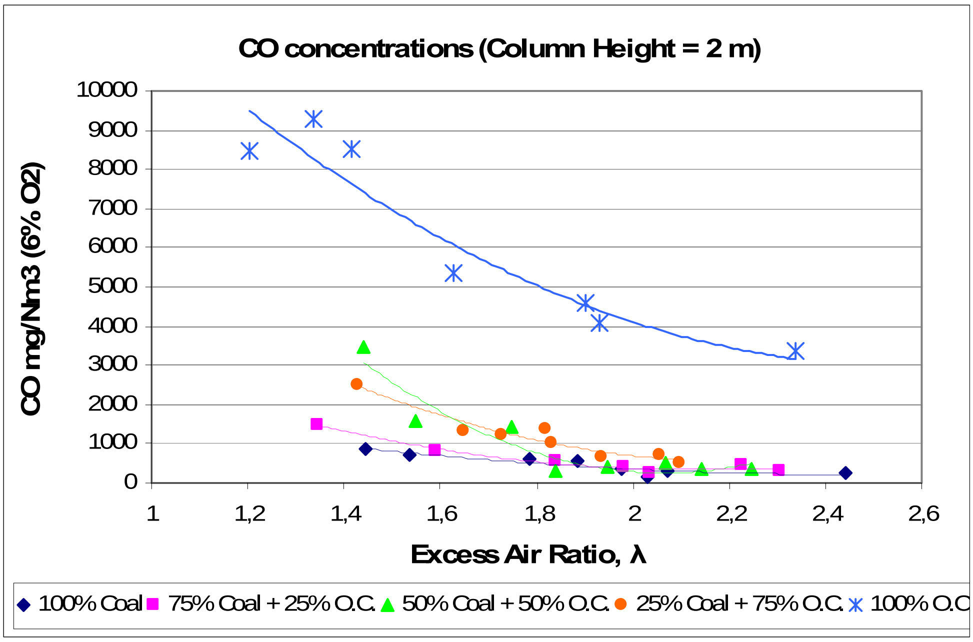

Figure 5.9 Effect of excess air ratio on CO emissions for the combustion and co-combustion of coal and olive cake in 2 m - combustion column

The effect of excess air ratio on **SO_2 emissions** for the combustion and co-combustion of coal and olive cake is given in Figure 5.10. SO_2 formation is much higher for lower excess air ratios (1.3-1.6) due to high temperatures (900-950 ^{o}C). As the excess air ratio is increased, emissions start to decrease because of dilution of flue gases and decrease in temperature. As it was mentioned before, SO_2 emissions are observed to decrease with increasing olive cake percentage since the sulfur content of olive cake is much lower than coal.

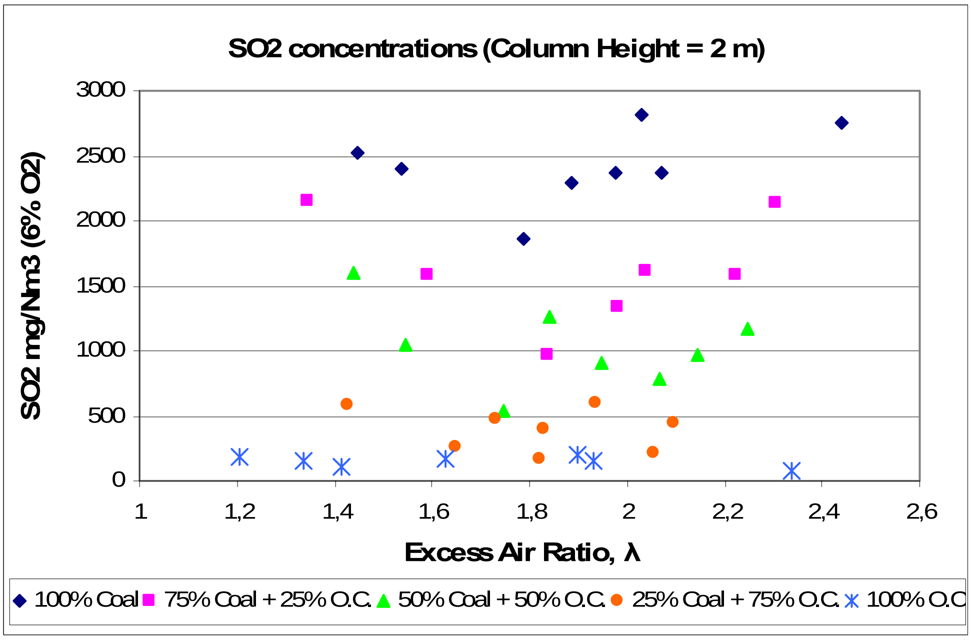

Figure 5.10 Effect of excess air ratio on SO_2 emissions for the combustion and co-combustion of coal and olive cake in 2 m - combustion column

The effect of excess air ratio on **NO_x emissions** for the combustion and co-combustion of coal and olive cake is given in Figure 5.11. Similarly, NO_x concentrations were observed to increase with the increase in excess air ratio both in 1 m and 2 m - combustion columns. This may be the result of better combustion of N in the fuel due to higher amount of O_2 supplied to the combustor. On the other hand, when λ is small, CO formation is large and a reducing atmosphere is formed in the combustor. This helps in reducing NO_x to N_2 and therefore NO_x emissions are expected to be lower. However, when CO emissions decrease with the increase in λ, NO_x emissions start to increase. It is also seen from the figure that with increasing olive cake percentage in the fuel mixture, NO_x concentrations decrease. As the olive cake percentage increases in the fuel mixture, high levels of hydrocarbon radicals and CO formation result in a reducing atmosphere in the freeboard region.

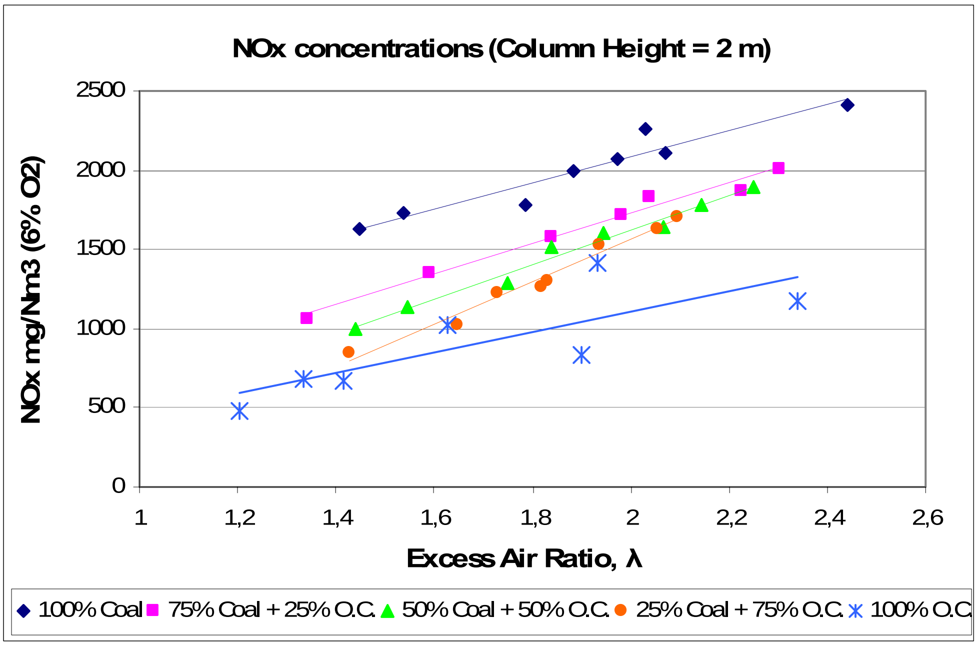

Figure 5.11 Effect of excess air ratio on NO_x emissions for the combustion and co-combustion of coal and olive cake in 2 m - combustion column

In order to see the degree of relevance between the variables (emission concentrations and excess air ratios), correlation coefficients (R^2) were calculated by using "Microsoft Excel" software program. The R^2 values below indicate how much percentage of the data fit the trend lines.

Table 5.6 R^2 values for the emission data obtained from combustion and co-combustion of coal and olive cake in 1 m and 2 m - combustion columns

	Fuel	**CO**	**NO_x**	**SO_2**
Set 1	Coal 100 wt%	0.9818	0.7220	0.7799
	Coal 75 wt% + Olive Cake 25 wt%	0.9172	0.9684	0.3966
	Coal 50 wt% + Olive Cake 50 wt%	0.9505	0.9907	0.6769
	Coal 25 wt% + Olive Cake 75 wt%	0.8056	0.8825	0.9336
	Olive Cake100 wt%	0.9182	0.9482	0.4206
Set 2	Coal 100 wt%	0.9284	0.9165	0.6302
	Coal 75 wt% + Olive Cake 25 wt%	0.8930	0.9824	0.8175
	Coal 50 wt% + Olive Cake 50 wt%	0.9297	0.9797	0.5303
	Coal 25 wt% + Olive Cake 75 wt%	0.9726	0.9722	0.2539
	Olive Cake100 wt%	0.8776	0.6380	0.7104

In addition to the R^2 values, "Statgraphics Plus 3.1" software program was used for goodness of fit information about the flue gas emission data. In order to check the fitting of the data to the models, confidence test was performed with this program. According to the regression analyses, there is a statistically significant relationship between CO and NO_x concentrations and excess air ratios at the 90% and higher confidence levels, since the P-values for these emissions are less than 0.10. However, there is not a statistically significant relationship between SO_2 concentrations with lower R^2 values and corresponding excess air ratios, because P-values for these SO_2 emissions are greater or equal to 0.10.

5.2.3. Combustion Efficiencies

As it was stated in previous section, combustion losses mostly originate from CO formation (L_{CO}), unburnt carbon in the fly ash and bottom ash ($L_{fly\ ash}$, $L_{bottom\ ash}$). The addition of these three values gives the total % loss in combustion. Therefore net combustion efficiency is $\eta = 100 - L_{total}$.

Combustion losses and efficiencies for the combustion of coal, olive cake and co-combustion of olive cake + coal mixtures are shown in Table 5.7. Losses due to fly ash have generally the largest portion in the total combustion loss. As can be seen from this table, combustion losses due to CO formation increases as the fuels shift from coal to olive cake. Just for 100 wt% olive cake combustion, the effect of L_{CO} is much higher than the other losses and it decreases the overall combustion efficiency. In addition to this, decrease in $L_{fly\ ash}$, $L_{bottom\ ash}$ decreases gradually with increasing olive cake percentage since olive cake has much lower ash content as compared to coal. Although these tendencies for combustion efficiencies are identical with 1 m - combustion column, the overall efficiencies increase for 2 m - combustion column. These improvements in efficiencies are examined in the next section.

Table 5.7 Combustion losses and efficiencies for the combustion and co-combustion of olive cake and coal in 2 m - combustion column

Run No	Fuel	L_{CO} (%)	$L_{bottom\ ash}$ (%)	$L_{fly\ ash}$ (%)	η (%)
r-6	Coal 100 wt%	**0.21**	**1.25**	**1.88**	**96.66**
r-7	Coal 75 wt% + O.C. 25 wt%	**0.27**	**0.93**	**1.58**	**97.22**
r-8	Coal 50 wt% + O.C. 50 wt%	**0.45**	**0.26**	**1.33**	**97.96**
r-9	Coal 25 wt% + O.C. 75 wt%	**0.51**	**0.21**	**0.49**	**98.79**
r-10	O.C. 100 wt%	**2.54**	**0.12**	**0.01**	**97.33**

Effect of excess air ratio on combustion efficiencies for the combustion and co-combustion of olive cake and coal is shown in Figure 5.12. As in the overall combustion efficiencies calculated in 1 m - combustion column, when the coal percentage increases in the fuel mixture, combustion efficiencies decrease due to $L_{fly\ ash}$. On the other hand, the effect of L_{CO} on the overall combustion efficiency also increases since CO emissions are higher for lower excess air ratios. This effect is especially observed as the olive cake percentage increases in the fuel mixture. After a certain λ value, overall efficiencies become almost stable for all fuel mixtures since CO emissions start to decrease.

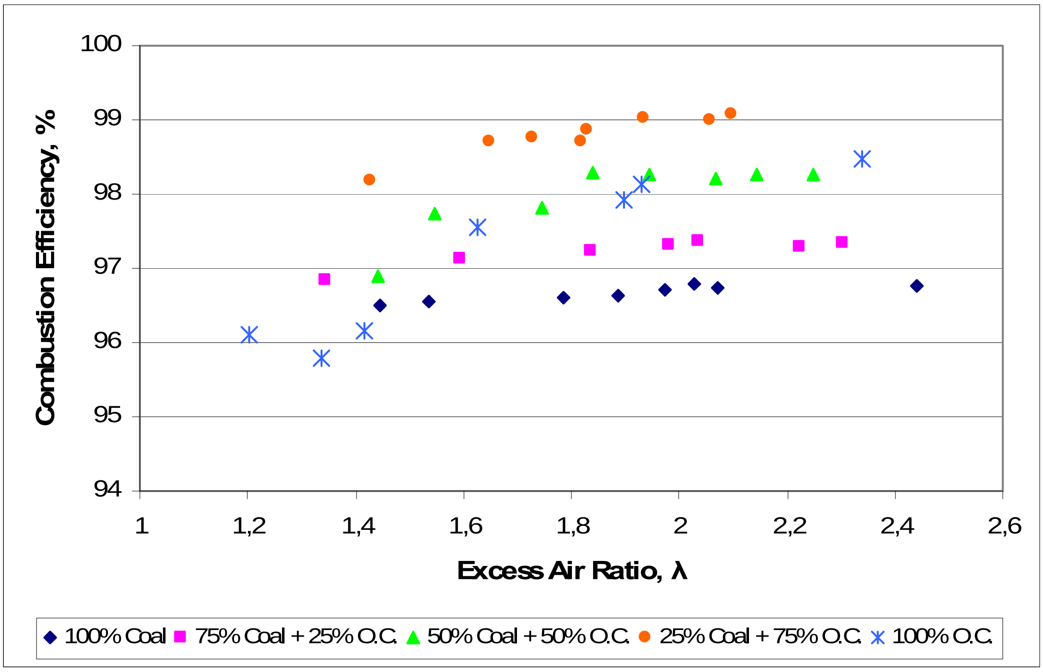

Figure 5.12 Effect of excess air ratio on combustion efficiencies for the combustion and co-combustion of olive cake and coal in 2 m - combustion column

5.2.4. Comparison of CO Emissions Obtained from Set 1 and Set 2

With the freeboard extension, a decrease in CO emissions and an increase in combustion efficiency is expected since the residence time of the fuel particles in combustion column increase.

Figure 5.13, 5.14, 5.15, 5.16 and 5.17 show the comparison of CO concentrations for different fuel compositions in 1 m and 2 m combustion columns. Decrease in CO concentrations is obvious for co-combustion of 50 wt% coal and 50 wt% olive cake, co-combustion of 25 wt% coal and 75 wt% olive cake, and combustion of olive cake. Although freeboard extension helps to decrease CO emissions, it is seen from the figures that it is hardly enough to decrease the emissions under the limit determined by Turkish Regulation.

For combustion of coal and co-combustion of 75 wt% coal and 25 wt% olive cake, freeboard extension does not seem to be advantageous. No decrease in CO emissions is observed with the freeboard extension for these experiments. However, CO emissions for λ ≥ 2 comply with the CO limits in RCAPIS.

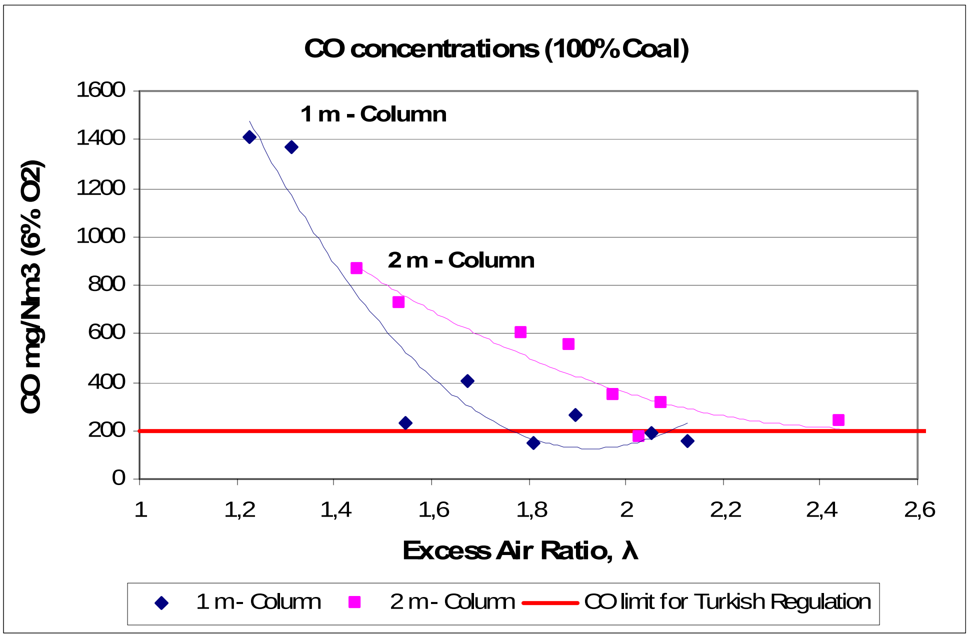

Figure 5.13 Comparison of CO concentrations in 1 m and 2 m - combustion columns for the combustion of coal

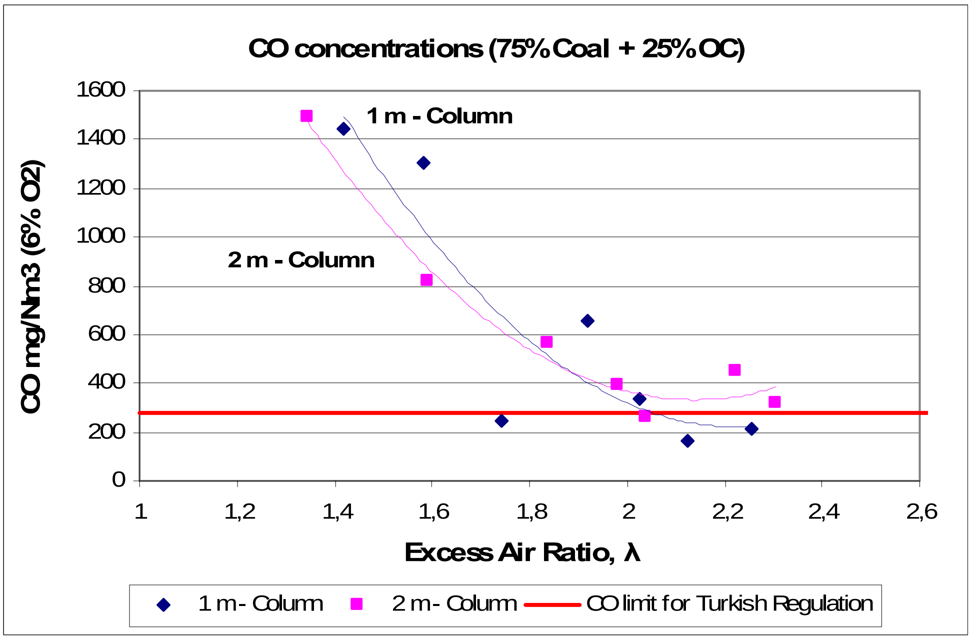

Figure 5.14 Comparison of CO concentrations in 1 m and 2 m - combustion columns for the co-combustion of 75 wt% coal and 25 wt% olive cake

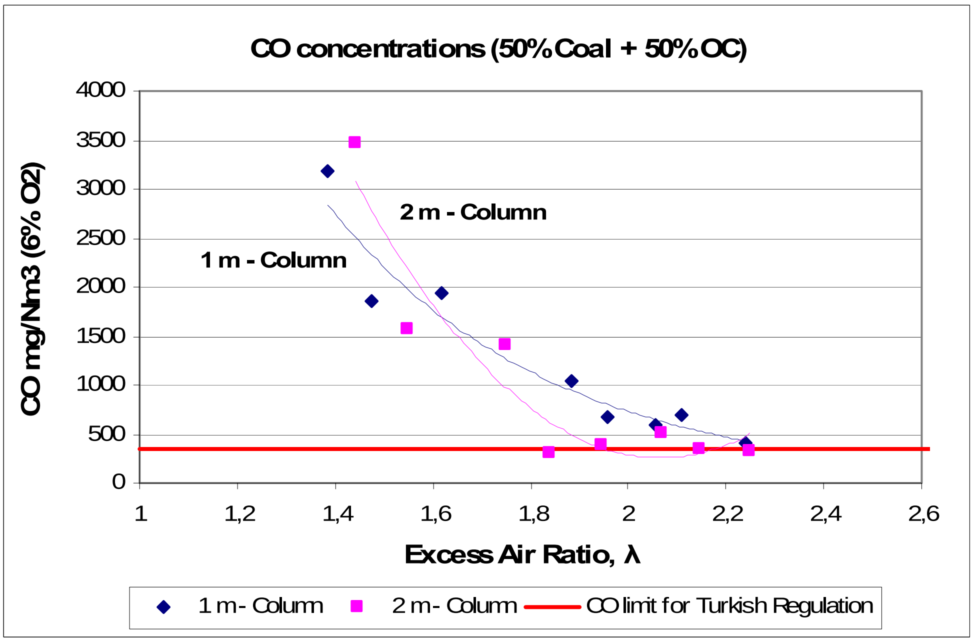

Figure 5.15 Comparison of CO concentrations in 1 m and 2 m - combustion columns for the co-combustion of 50 wt% coal and 50 wt% olive cake

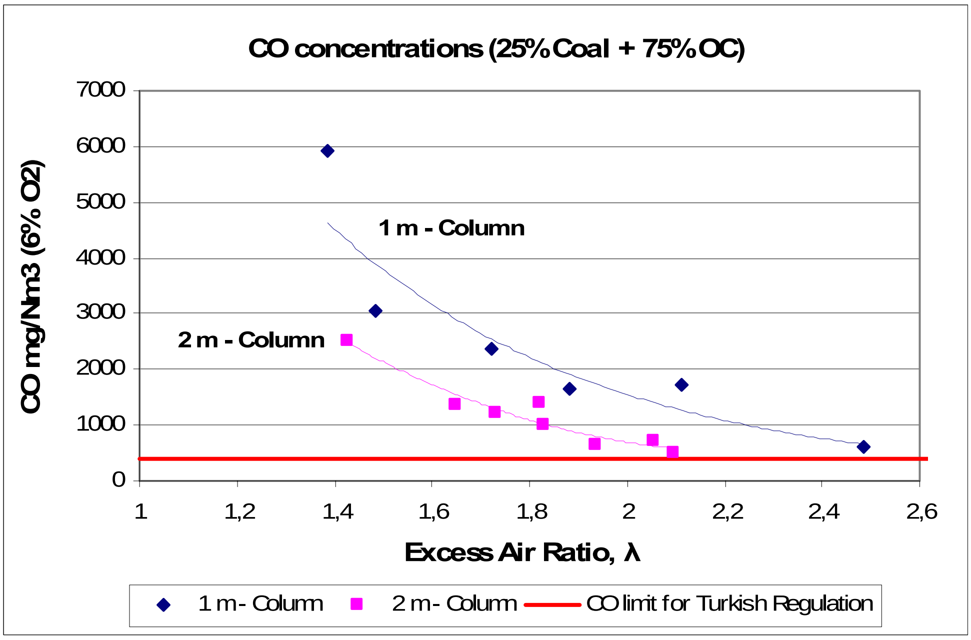

Figure 5.16 Comparison of CO concentrations in 1 m and 2 m - combustion columns for the co-combustion of 25 wt% coal and 75 wt% olive cake

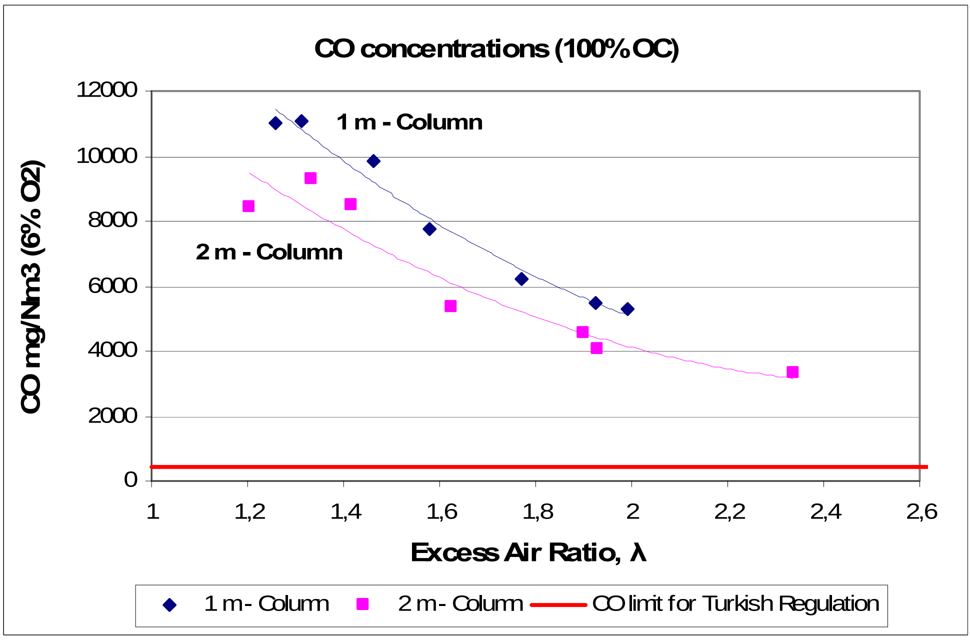

Figure 5.17 Comparison of CO concentrations in 1 m and 2 m - combustion columns for the combustion of olive cake

In Table 5.8, comparison of combustion efficiencies for the combustion and co-combustion of olive cake and coal in 1 m and 2 m combustion columns is presented. All efficiencies are found to increase slightly with the addition of 1 m - column. This can be explained with the increase in residence time of fuel particles in combustion medium which gives extra time for them to burn more efficiently. For the combustion and co-combustion experiments conducted in 1 m and 2 m - combustion columns, maximum efficiency (98.79%) was obtained for co-combustion of coal 25 wt% + olive cake 75 wt% while minimum efficiency (96.15%) was obtained for combustion of 100 wt% coal.

Table 5.8 Comparison of combustion efficiencies for the combustion and co-combustion of olive cake and coal in 1 m and 2 m combustion columns

Fuel	**η (%) (1m - column)**	**η (%) (2m - column)**
Coal 100 wt%	**96.15**	**96.66**
Coal 75 wt% + O.C. 25 wt%	**96.99**	**97.22**
Coal 50 wt% + O.C. 50 wt%	**97.81**	**97.96**
Coal 25 wt% + O.C. 75 wt%	**98.08**	**98.79**
O.C. 100 wt%	**96.32**	**97.33**

Thus, it is seen that freeboard extension is helpful for fuel mixtures where olive cake content ≥ 50 wt%, in other words when the biomass has higher percentage in the fuel mixture. When olive cake content is less than 50% by wt., no significant decrease in CO emissions is observed.

Rather than increasing the column height which has not proved to be very successful for certain fuel mixtures, injection of secondary air into the freeboard at certain locations might be more advantageous. Firstly, a reduction zone is created by providing small λ with the primary air and then an oxidation zone is created with secondary air injection (excess air) in order to complete combustion process.

5.3. Combustion and Co-combustion of Coal and Olive Cake with Limestone Addition in 1 m - Combustion Column

“Sulfur dioxide (SO_2) emissions are a major concern in combustion processes. Solid fuels contain sulfur in varying proportions, and SO_2 pollution originates from oxidation of this sulfur during combustion. Calcium sorbents (primarily limestones) are widely used for in situ SO_2 capture in fluidized-bed combustion” (Li et al., 2005). The most suitable temperature for this capture is 850 - 900 ^oC where limestone is calcined and $CaO + CO_2$ are formed. The CaO formed reacts with SO_2 in the bed and $CaSO_4$ formation occurs. The key reactions are commonly described as follows;

Calcination: $CaCO_3 \rightarrow CaO + CO_2$ – 183 kJ/g.mol (5-1)
Sulfation: $CaO + SO_2 + 1/2\ O_2 \rightarrow CaSO_4$ + 486 kJ/g.mol (5-2)

In this study, the lignite coal contains 1.19 wt% total S (on dry basis) and when coal is burned without any adsorbent about 4000 - 4500 mg/Nm^3 SO_2 is formed. This is way above the limit values. Therefore, an adsorbent should be added to capture SO_2 formed until the SO_2 concentration will come down to the limit values. Three different limestones were used as adsorbents namely Çan - Çanakkale, Çumra -Konya and Sedef - İstanbul. During these tests, the reactivity of these limestones and their sulfur removal efficiencies were also investigated for further use.

Calculation of amount of limestone needed in order to capture SO_2 emissions are given in Appendix D.

5.3.1. Combustion of Coal with Different Limestones

In this set of experiments, the effect of addition of three different limestones (Çan, Çumra and Sedef) on SO_2 emissions and combustion efficiency was examined for combustion of coal in 1 m - combustion column. Five different Ca/S ratios (1.5, 2.0, 2.5, 3.0 and 3.5) were tried for each limestone. Determination of the reactivities of the limestones and the optimum Ca/S ratio to decrease SO_2 concentrations in the flue gas were also among the objectives of this study.

5.3.1.1. SO_2 Emissions for Different Ca/S Ratios

During combustion of coal with three different limestones, it was observed that SO_2 emissions decrease with the increase in Ca/S ratios. The reason is that the calcination reaction occurs at an optimum temperature about 850 ^oC providing a maximum removal efficiency for limestone. Over and under this temperature, SO_2 emissions in the flue gas are higher since the calcination reactivity reduces at lower temperatures and $CaSO_4$ decomposes at higher temperatures (Basu, 2006). In the experiments of this set, this optimum temperature is provided with an excess air ratio of 1.9. Although almost each Ca/S ratio of limestone addition helps to decrease SO_2 emissions, Ca/S ratios of 2.5, 3 and 3.5 can decrease the emissions more efficiently under the limits determined by EU and Turkish Regulations, namely 2000 mg/Nm^3 (at 6% O_2).

5.3.1.2. SO_2 Removal Efficiencies for Different Ca/S Ratios

SO_2 emissions and % removals for the combustion of coal with different limestones are given in Table 5.9, Figure 5.18 and 5.19. Porosities (36.99% and 30.47%, respectively) and surface areas (41.87 m^2/g and 21.74 m^2/g, respectively) of Çumra and Sedef limestones are higher than those of Çan limestone (29.88%, 14.93 m^2/g) (all values given are for after calcination at 900 ^oC). However, it is clearly seen from Table 5.8, Figure 5.18 and 5.19 that Çan limestone is much more effective in SO_2 capturing as compared to other two limestones. This can be explained with the structural strength of Çan limestone. Although all limestones are fed into the bed between 1-2 mm size interval, Çan limestone particles are quickly powdered in the fuel mixture. Since Çan limestone particles become much smaller in fuel mixture their surface area increase inevitably. This possibly causes a much more efficient calcination of $CaCO_3$. Therefore SO_2 capturing efficiency increases accordingly. The effect of the particle size on SO_2 retention efficiency was displayed before by Atilgan (2004). According to his study, as the size of the limestone particle decreases, the rate of SO_2 sorption increases since the particle size of the limestone significantly affects the reaction rate and conversion rate (Atilgan, 2004).

Table 5.9 SO_2 emissions and removal efficiencies for the combustion of coal with different limestones (average bed temperature ≅ 850 °C and $\lambda \cong 1.9$)

	Çan Limestone		**Çumra Limestone**		**Sedef Limestone**	
Ca/S Ratio	**SO_2 Conc. (mg/Nm^3 based on 6% O_2)**	**SO_2 Removal (%)**	**SO_2 Conc. (mg/Nm^3 based on 6% O_2)**	**SO_2 Removal (%)**	**SO_2 Conc. (mg/Nm^3 based on 6% O_2)**	**SO_2 Removal (%)**
3.5	892.1	65	1388.4	45	1554.2	39
3	338.1	87	1342.8	47	1675.8	34
2.5	745.5	71	1601.6	37	1881.9	26
2	1625.0	36	1798.3	29	2059.3	19
1.5	1820.6	28	2140.4	16	2190.8	14

The highest SO_2 removal efficiencies of Çan, Çumra and Sedef limestones were found to be 87%, 47% and 39%, respectively. Additionally, it was identified in this set of experiments that Çan and Çumra limestones gave the highest SO_2 removal efficiency at Ca/S = 3. The worst limestone is obviously Sedef limestone.

Maximum SO_2 removal generally takes place at about 850 °C. Below this value calcination of limestone can not be completed whereas above 850 °C, $CaSO_4$ starts to decompose. The presented values in Table 5.9, Figure 5.18 and 5.19 are the maximum SO_2 removal efficiencies and the minimum SO_2 concentrations in the flue gas at optimum temperatures (average bed temperature ≅ 850 °C). A peculiar behavior is observed with Çan limestone for which a maximum SO_2 removal efficiency was obtained at Ca/S = 3. There is a pronounced maximum on the curve in Figure 5.18. The explanation given above could be more relevant for the Çan limestone. The effect is less pronounced for the Çumra limestone. A possible further explanation could be lowering of bed temperature below 850 °C when excess $CaCO_3$ is given to the combustor, like Ca/S = 3.5.

In a large scale system these conditions can be easily provided in order to obtain these removal efficiencies. As it is clearly seen from the Figure 5.19, standards set by both EU and Turkish regulations (2000 mg/Nm^3 at 6% O_2) can be satisfied with almost all limestones for each Ca/S ratio studied.

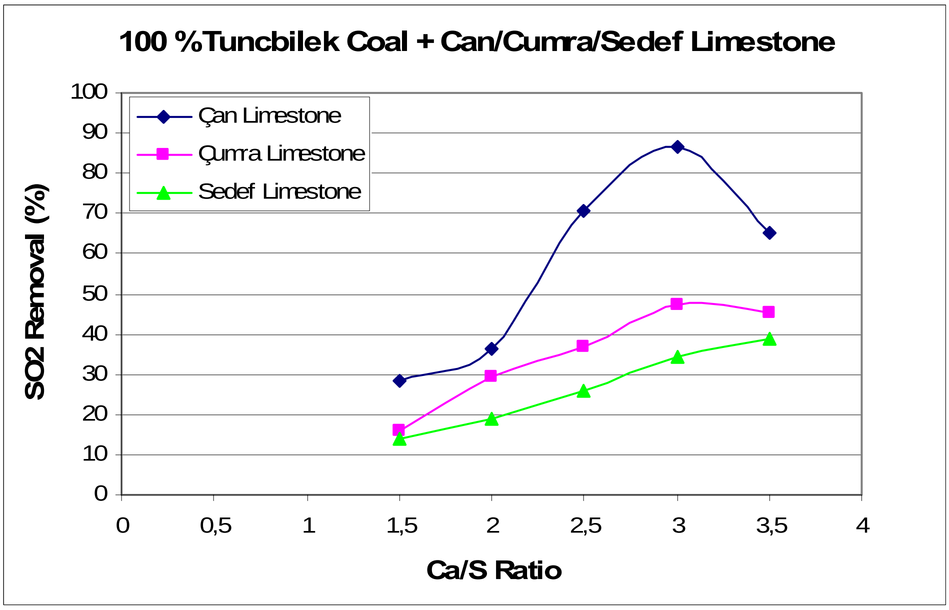

Figure 5.18 Effect of Ca/S ratio on SO_2 removal efficiency for combustion of coal with different limestones in 1 m - combustion column (avg. bed temperature ≅ 850 °C and $\lambda \cong 1.9$)

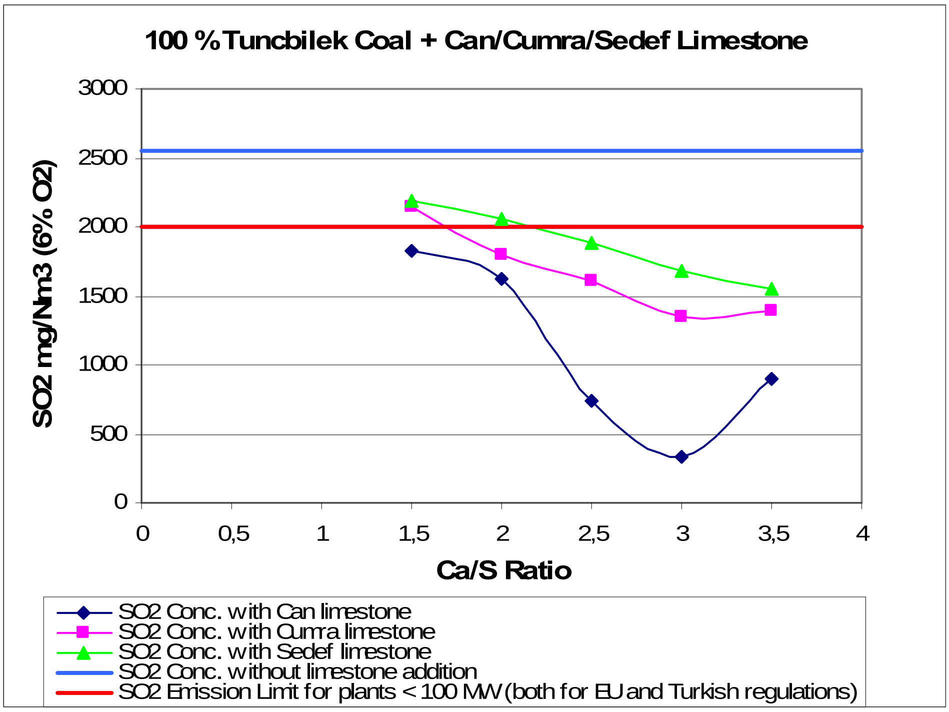

Figure 5.19 Effect of Ca/S ratio on SO_2 emissions for combustion of coal with different limestones in 1 m - combustion column (avg. bed temperature ≅ 850 ^{o}C and $\lambda \cong 1.9$)

5.3.1.3. Combustion Efficiencies

Combustion losses and efficiencies for the combustion of coal with different limestones in 1 m - combustion column are shown in Table 5.10. As it was observed in previous sets of experiments, combustion losses resulting from fly ash have the largest contribution in the total loss. Total of $L_{\text{fly ash}}$ and $L_{\text{bottom ash}}$ slightly increases with increasing limestone addition. This can be explained with that the addition of more limestone into the fuel mixture possibly decreases the temperature and the combustion rate. Besides calcination reaction is an endothermic reaction which takes up heat. It is clearly seen from Table 5.10 that combustion efficiencies of the experiments carried out with Çumra and Sedef limestones are found to be lower than the ones carried out with Çan limestone. This point may need further research.

Table 5.10 Combustion losses and efficiencies for the combustion of coal with different limestones in 1 m - combustion column

Run No	Fuel + Adsorbent	L_{CO} (%)	$L_{bottom\ ash}$ (%)	$L_{fly\ ash}$ (%)	η (%)
r-11	Coal 100 wt% + Çan Ls. (Ca/S=1.5)	**0.22**	**1.42**	**3.09**	**95.27**
r-12	Coal 100 wt% + Çan Ls. (Ca/S=2.0)	**0.16**	**3.66**	**1.97**	**94.21**
r-13	Coal 100 wt% + Çan Ls. (Ca/S=2.5)	**0.33**	**1.70**	**3.08**	**94.89**
r-14	Coal 100 wt% + Çan Ls. (Ca/S=3.0)	**0.10**	**0.60**	**5.14**	**94.16**
r-15	Coal 100 wt% + Çan Ls. (Ca/S=3.5)	**0.37**	**3.14**	**3.33**	**93.16**
r-16	Coal 100 wt% + Çumra Ls. (Ca/S=1.5)	**0.48**	**1.12**	**5.02**	**93.38**
r-17	Coal 100 wt% + Çumra Ls. (Ca/S=2.0)	**0.35**	**2.81**	**3.83**	**93.01**
r-18	Coal 100 wt% + Çumra Ls. (Ca/S=2.5)	**0.21**	**2.48**	**4.83**	**92.48**
r-19	Coal 100 wt% + Çumra Ls. (Ca/S=3.0)	**0.44**	**3.42**	**4.72**	**91.42**
r-20	Coal 100 wt% + Çumra Ls. (Ca/S=3.5)	**0.32**	**1.88**	**7.03**	**90.77**
r-21	Coal 100 wt% + Sedef Ls. (Ca/S=1.5)	**0.55**	**1.29**	**5.12**	**93.04**
r-22	Coal 100 wt% + Sedef Ls. (Ca/S=2.0)	**1.05**	**0.97**	**5.92**	**92.06**
r-23	Coal 100 wt% + Sedef Ls. (Ca/S=2.5)	**1.43**	**1.05**	**5.64**	**91.88**
r-24	Coal 100 wt% + Sedef Ls. (Ca/S=3.0)	**0.68**	**2.14**	**6.12**	**91.06**
r-25	Coal 100 wt% + Sedef Ls. (Ca/S=3.5)	**1.12**	**1.90**	**6.61**	**90.37**

5.3.2. Co-combustion of Coal and Olive Cake with Different Limestones

In this set of experiments, the effect of addition of three different limestones (Çan, Çumra and Sedef) on SO_2 emissions and combustion efficiency was examined for co-combustion of coal and olive cake in 1 m - combustion column. Four different Ca/S ratios (1.5, 2.0, 2.5 and 3.0) were tried for each limestone.

5.3.2.1. SO_2 Emissions for Different Ca/S Ratios

Similar to coal combustion experiments with different limestones, SO_2 emissions decrease with increasing Ca/S ratios for co-combustion of 50 wt% coal and 50 wt% olive cake, too. The calcination reaction occurs at an optimum temperature about 850 ^{o}C providing a maximum removal efficiency for limestone. Over and under this temperature, SO_2 emissions have higher values. In the experiments of this set, this optimum temperature is provided with an excess air ratio of 1.8. At this temperature, almost every Ca/S ratio can decrease the emissions efficiently under the limits determined by EU and Turkish Regulations, namely 987 mg/Nm^3 (at 6% O_2).

5.3.2.2. SO_2 Removal Efficiencies for Different Ca/S Ratios

SO_2 emissions and removal efficiencies for the co-combustion of 50 wt% coal and 50 wt% olive cake with different limestones are given in Table 5.11, Figure 5.20 and 5.21. Similar to the experiments of coal combustion with different limestones, it is seen from Table 5.11, Figure 5.20 and 5.21 that Çan limestone is much more effective in SO_2 capturing than the other limestones. The reason of higher removal efficiency of Çan limestone was explained in previous section in detail (see section 5.3.1.2).

Table 5.11 SO_2 emissions and removal efficiencies for co-combustion of 50 wt% coal and 50 wt% olive cake with different limestones (average bed temperature ≅ 850 °C and λ ≅ 1.8)

	Çan Limestone		**Çumra Limestone**		**Sedef Limestone**	
Ca/S Ratio	**SO_2 Conc. (mg/Nm^3 based on 6% O_2)**	**SO_2 Removal (%)**	**SO_2 Conc. (mg/Nm^3 based on 6% O_2)**	**SO_2 Removal (%)**	**SO_2 Conc. (mg/Nm^3 based on 6% O_2)**	**SO_2 Removal (%)**
3	184.3	88	572.1	64	765.8	51
2.5	476.5	70	718.1	54	853.7	46
2	530.0	66	1215.6	23	909.2	42
1.5	572.8	64	895.9	43	1062.4	32

Since it was identified in the experiments of coal combustion with different limestones that Çan and Çumra limestones gave the highest SO_2 removal efficiency at Ca/S = 3 and SO_2 concentrations below the limits are obtained, higher Ca/S ratios were not tried in these experiment series. Highest SO_2 removal efficiencies of Çan, Çumra and Sedef limestones were found to be 88%, 64% and 51%, respectively. Additionally, standards set by both EU and Turkish regulations

(987 mg/Nm^3 at 6% O_2) can be satisfied with almost all limestones for each Ca/S ratio studied (see Figure 5.21).

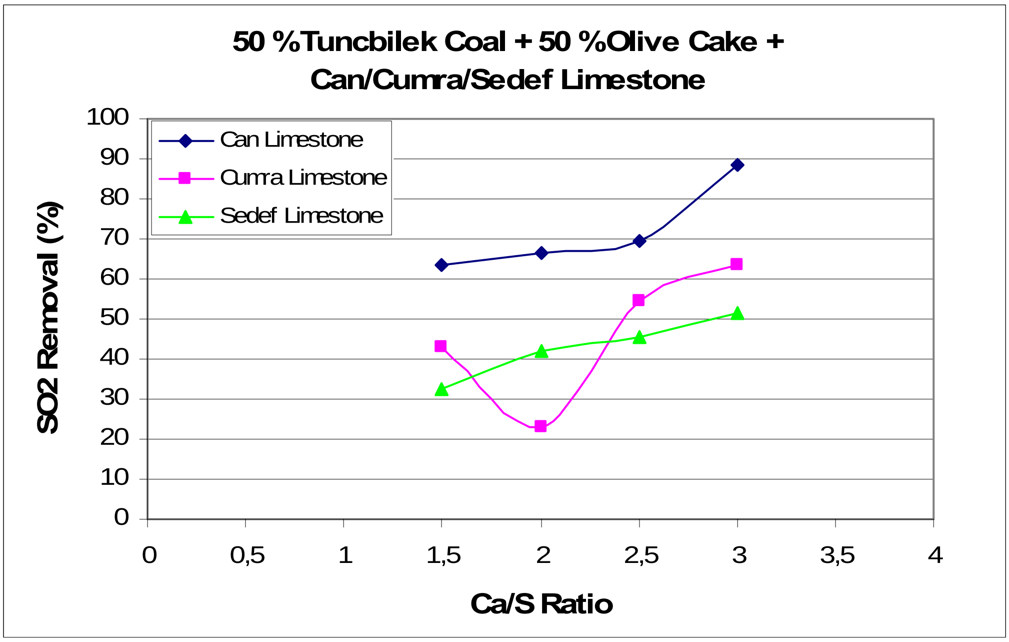

Figure 5.20 Effect of Ca/S ratio on SO_2 removal efficiency for co-combustion of 50 wt% coal and 50 wt% olive cake with different limestones in 1 m - combustion column (average bed temperature ≅ 850 °C and $\lambda \cong 1.8$)

Again in Figure 5.20 and 5.21, a peculiar situation was obtained with Çumra limestone which gave a minimum %SO_2 removal at Ca/S = 2. Then, the removal efficiency increased again with an increase in the Ca/S ratio. This abnormal behavior could not be explained at this point, although the experiment was repeated for a few times.

It is interesting to note that SO_2 emissions were 2544.1 mg/Nm^3 (@ average bed temperature ≅ 850 °C) when coal was burned alone. When coal is mixed with 50% by wt. olive cake, SO_2 emissions decreased to 1573.6 mg/Nm^3 (@ average bed temperature ≅ 850 °C) and when limestone was added, emissions were much lower than 1000 mg/Nm^3. If the limits are satisfied, then there is no need to use excess amount of limestone, because at the end it becomes a solid waste.

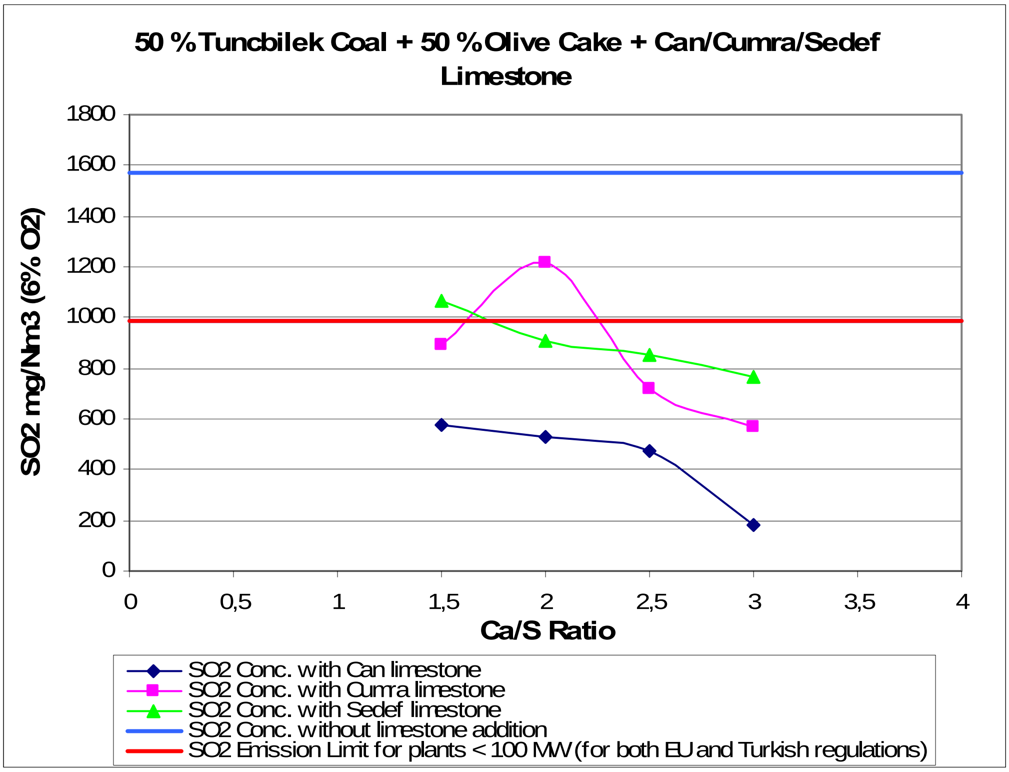

Figure 5.21 Effect of Ca/S ratio on SO_2 emissions for co-combustion of 50 wt% coal and 50 wt% olive cake with different limestones in 1 m - combustion column (average bed temperature ≅ 850 °C and $\lambda \cong 1.8$)

5.3.2.3. Combustion Efficiencies

Combustion losses and efficiencies for the co-combustion of 50 wt% coal and 50 wt% olive cake with different limestones in 1 m - combustion column are shown in Table 5.12. As it was observed in coal combustion with different limestones, total of $L_{\text{fly ash}}$ and $L_{\text{bottom ash}}$ slightly increases with increasing limestone addition. The reason of this increase and higher efficiencies of Çan limestone was explained in detail in previous section (see section 5.3.1.3).

It is clearly seen from Table 5.12 that overall efficiencies for co-combustion of 50 wt% coal and 50 wt% olive cake with different limestones are higher than combustion of coal with different limestones since losses originated from fly ash and bottom ash are lower for olive cake combustion.

Table 5.12 Combustion losses and efficiencies for the co-combustion of 50 wt% coal and 50 wt% olive cake with different limestones in 1 m - combustion column

Run No	Fuel + Adsorbent	L_{CO} (%)	$L_{bottom\ ash}$ (%)	$L_{fly\ ash}$ (%)	η (%)
r-26	Coal 50 wt% + Olive Cake 50 wt% + Çan Ls. (Ca/S=1.5)	**0.73**	**0.54**	**1.17**	**97.56**
r-27	Coal 50 wt% + Olive Cake 50 wt% + Çan Ls. (Ca/S=2.0)	**0.63**	**1.19**	**1.22**	**96.96**
r-28	Coal 50 wt% + Olive Cake 50 wt% + Çan Ls. (Ca/S=2.5)	**0.61**	**1.36**	**1.61**	**96.42**
r-29	Coal 50 wt% + Olive Cake 50 wt% + Çan Ls. (Ca/S=3.0)	**0.71**	**1.81**	**1.49**	**95.99**
r-30	Coal 50 wt% + Olive Cake 50 wt% + Çumra Ls. (Ca/S=1.5)	**0.65**	**0.24**	**2.17**	**96.94**
r-31	Coal 50 wt% + Olive Cake 50 wt% + Çumra Ls. (Ca/S=2.0)	**1.60**	**0.37**	**1.29**	**96.74**
r-32	Coal 50 wt% + Olive Cake 50 wt% + Çumra Ls. (Ca/S=2.5)	**0.67**	**0.99**	**1.67**	**96.67**
r-33	Coal 50 wt% + Olive Cake 50 wt% + Çumra Ls. (Ca/S=3.0)	**0.52**	**1.95**	**1.58**	**95.95**
r-34	Coal 50 wt% + Olive Cake 50 wt% + Sedef Ls. (Ca/S=1.5)	**1.62**	**0.28**	**1.30**	**96.80**
r-35	Coal 50 wt% + Olive Cake 50 wt% + Sedef Ls. (Ca/S=2.0)	**1.37**	**0.37**	**1.63**	**96.63**
r-36	Coal 50 wt% + Olive Cake 50 wt% + Sedef Ls. (Ca/S=2.5)	**1.21**	**0.44**	**1.89**	**96.46**
r-37	Coal 50 wt% + Olive Cake 50 wt% + Sedef Ls. (Ca/S=3.0)	**1.60**	**0.76**	**1.72**	**95.92**

5.3.3. Comparison of SO_2 Removal Efficiencies Obtained in Combustion and Co-combustion Experiments

If performances of limestones during combustion of coal and co-combustion of 50 wt% coal and 50 wt% olive cake are compared, an obvious improvement is seen with the addition of olive cake in fuel mixture. There are some results reported in the literature stating that herbaceous biomass fuels may have high chlorine content leading to the formation of salts such as KCl and NaCl (Van Loo and Koppejan, 2008). NaCl can improve the absorbency of $CaCO_3$ by promoting the calcination of limestone. This was also claimed by Shearer et al. (1979) and Liu et al. (2006). According to Shearer (1979), salts increase the pore diameters that allows sulfation to occur for a longer time.

For the olive cake used in this study, the ash analysis could not be performed. However, in the previous study carried out by Varol (2006), the olive cake used contained 19.5% by wt. K_2O, 2.4% by wt. Na_2O and 14.0% by wt. CaO. The alkaline content of the olive cake was high. Therefore, a synergistic effect between the biomass and limestone might promote the calcination of limestone.

Table 5.13 Comparison of SO_2 removal efficiencies obtained in combustion and co-combustion experiments

	Çan Limestone		**Çumra Limestone**		**Sedef Limestone**	
Ca/S Ratio	**SO_2 removal in combustion (%)**	**SO_2 removal in co-combustion (%)**	**SO_2 removal in combustion (%)**	**SO_2 removal in co-combustion (%)**	**SO_2 removal in combustion (%)**	**SO_2 removal in co-combustion (%)**
3.5	65	-	45	-	39	-
3	87	88	47	64	34	51
2.5	71	70	37	54	26	46
2	36	66	29	23	19	42
1.5	28	64	16	43	14	32

5.4. Co-combustion of Coal and Olive Cake with Limestone Addition in 2 m - Combustion Column

In this set of experiments, effect of addition of Çan limestone on SO_2 emissions and combustion efficiency was examined for co-combustion of coal in 2 m -

combustion column. Three different Ca/S ratios (2.0, 2.5, and 3.0) were tried for Çan limestone.

5.4.1. SO_2 Emissions for Different Ca/S Ratios

The same trend in 1 m - combustion column on SO_2 emissions is seen again in 2 m - combustion column. SO_2 emissions are observed to decrease with increasing Ca/S ratios. The reason is probably that calcination reaction occurs at an optimum temperature about 850 °C providing a maximum removal efficiency for limestone. Over and under this temperature, SO_2 emissions have higher values. In the experiments of this set, this optimum temperature is provided with an excess air ratio of 1.7. At this temperature, especially Ca/S = 3 can decrease the emissions efficiently under the limits determined by EU and Turkish Regulations (987 mg/Nm^3 at 6% O_2).

5.4.2. SO_2 Removal Efficiencies for Different Ca/S Ratios

SO_2 emissions and removal efficiencies for the co-combustion of 50 wt% coal and 50 wt% olive cake with Çan limestone are given in Table 5.14, Figure 5.22 and 5.23. Since it was identified in the experiments of coal combustion with Çan limestone that this limestone gave the highest SO_2 removal efficiency at Ca/S = 3 and lowest SO_2 efficiency at Ca/S = 1.5, these Ca/S ratios were not tried in these experiment series. As it was expected highest removal efficiency was observed at Ca/S = 3 for Çan limestone. Additionally, standards set by both EU and Turkish regulations (987 mg/Nm^3 at 6% O_2) can also be satisfied with each Ca/S ratio studied of Çan limestone (see Figure 5.22).

Table 5.14 SO_2 emissions and removal efficiencies for the co-combustion of 50 wt% coal, 50 wt% olive cake with Çan limestone in 2 m - combustion column (average bed temperature ≅ 850 °C and $\lambda \cong 1.7$)

Ca/S Ratio	SO_2 Concentration (mg/Nm^3 based on 6% O_2)	SO_2 Removal (%)
3	407.8	74
2,5	515.8	67
2	893.3	43

According to Table 5.14 maximum SO_2 removal efficiency was calculated as 74% at Ca/S = 3. However, performance of Çan limestone is not observed to improve with the extension of freeboard. SO_2 removal efficiencies for the co-combustion of 50 wt% coal + 50 wt% olive cake with Çan limestone in 1 m - combustion column and 2 m - combustion column were found to be close to each other.

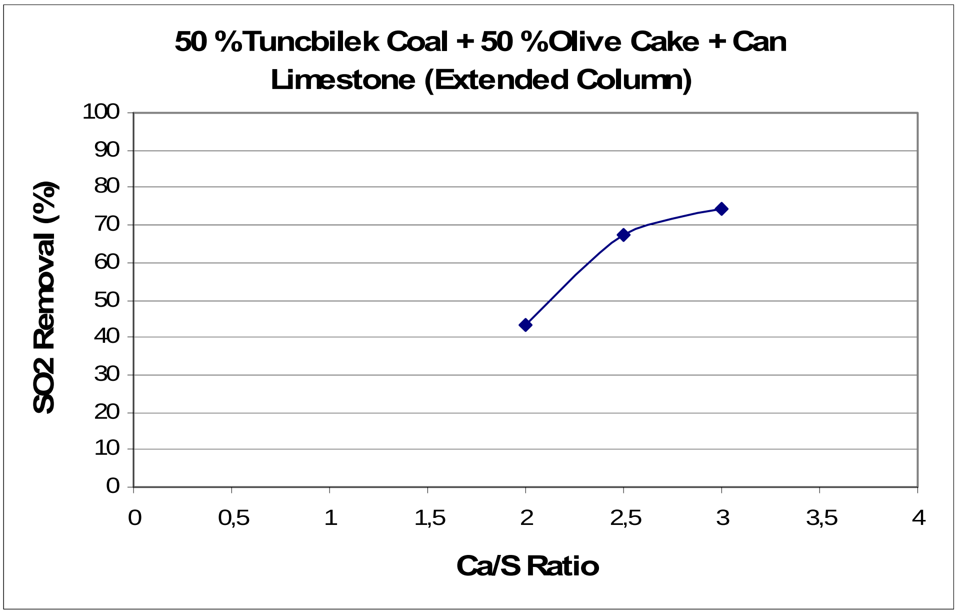

Figure 5.22 Effect of Ca/S ratio on SO_2 removal efficiency for co-combustion of 50 wt% coal and 50 wt% olive cake with Çan limestone in 2 m - combustion column (average bed temperature ≅ 850 °C and $\lambda \cong 1.7$)

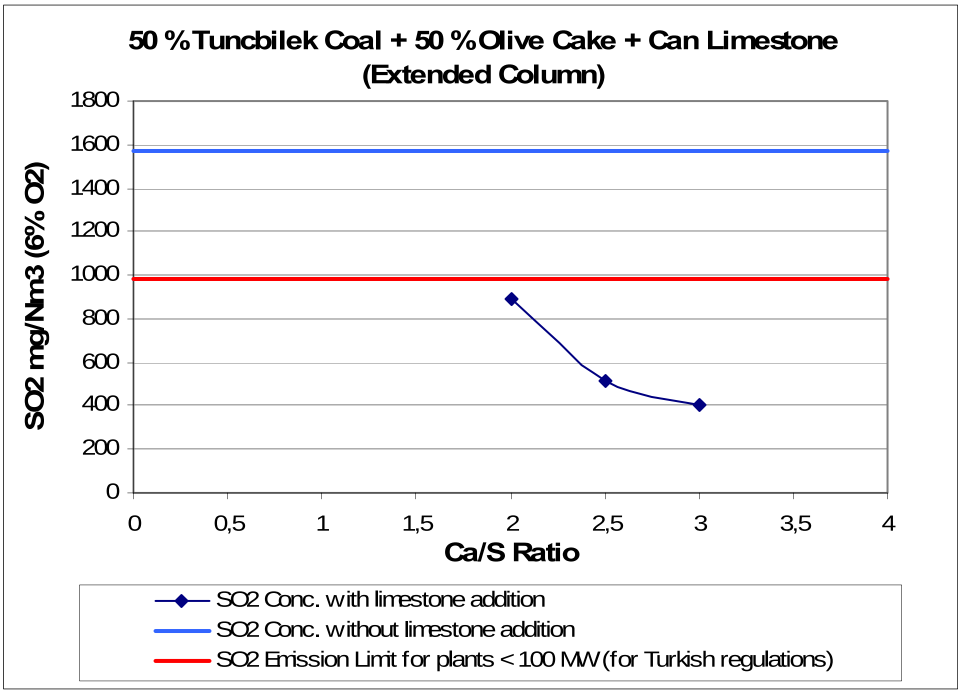

Figure 5.23 Effect of Ca/S ratio on SO_2 emissions for co-combustion of 50 wt% coal and 50 wt% olive cake with Çan limestone in 2 m - combustion column (average bed temperature $\cong$ 850 °C and $\lambda \cong 1.7$)

5.4.3. Combustion Efficiencies

Table 5.15 shows combustion losses and efficiencies for the co-combustion of 50 wt% coal and 50 wt% olive cake with Çan limestone in 2 m - combustion column. Overall efficiencies for co-combustion of 50 wt% coal and 50 wt% olive cake with Çan limestone in 2 m - column is higher in comparison with in 1 m - column. All efficiencies are found to increase with the addition of 1000 mm column on top the 900 mm column. As it was explained before, increase in residence time of fuel particles in combustion column gives extra time for them to burn more efficiently.

Table 5.15 Combustion losses and efficiencies for the co-combustion of 50 wt% coal and 50 wt% olive cake with Çan limestone in 2 m - combustion column

Run No	Fuel + Adsorbent	L_{CO} (%)	$L_{bottom\ ash}$ (%)	$L_{fly\ ash}$ (%)	H (%)
r-38	Coal 50 wt% + Olive Cake 50 wt% + Çan Ls. (Ca/S=2.0)	**1.48**	**0.37**	**1.06**	**97.09**
r-39	Coal 50 wt% + Olive Cake 50 wt% + Çan Ls. (Ca/S=2.5)	**1.36**	**0.55**	**1.46**	**96.64**
r-40	Coal 50 wt% + Olive Cake 50 wt% + Çan Ls. (Ca/S=3.0)	**1.18**	**0.38**	**1.87**	**96.57**

5.5. Comparison of the Emissions with Standards and Literature

5.5.1. Comparison of the Emissions with Standards

Although there are few emission limitations including lab-scale systems with small thermal capacity (like the one used in this study), most suitable limit values were taken into consideration in order to compare them with the flue gas emissions. Emission limits for coal, olive cake and their mixtures and their calculations according to the mixing rules of 2001-80-EC and RCAPIS were listed before in Chapter 2. Comparison of these limit values and flue gas emissions obtained from the experiments performed during this study are listed in Table 5.16 and 5.17. Highlighted values are the concentrations over the limits while the other values are the concentrations under the limits.

As it is seen from Table 5.16, it is seen that almost each concentration obtained from Set 1 is over the limits, except for CO emissions for combustion of 100 wt% coal and co-combustion of 75 wt% coal + 25 wt% olive cake. However as the combustion column was extended, SO_2 emissions for co-combustion of 50 wt% coal + 50 wt% olive cake and 25 wt% coal + 75 wt% olive cake and combustion of 100 wt% olive cake could be decreased under the limits. Although NO_x and CO emissions could not be decreased under the limits of these two regulations, with the freeboard extension an obvious reduction can be observed in NO$_x$ and CO emissions (see Table 5.5).

Table 5.16 Comparison of the emissions with the limit values in EU Directive 2001-80-EC and Turkish Regulation (RCAPIS) (Set 1 and Set 2)

Set 1 (Combustion Column Height = 1 m)		**SO$_2$ (mg/Nm^3)**		**NO$_x$ (mg/Nm^3)**		**CO (mg/Nm^3)**	
Run No.	**Fuel**	**EU**	**Turkish**	**EU**	**Turkish**	**EU***	**Turkish**
r-1	C 100 wt%	2000	2000	600	800	NL	200
r-2	C 75 wt% + OC 25 wt%	1475	1459	542	744	NL	278
r-3	C 50 wt% + OC 50 wt%	1005	987	489	695	NL	346
r-4	C 25 wt% + OC 75 wt%	583	570	443	652	NL	407
r-5	OC 100 wt%	200	200	400	613	NL	460
Set 2 (Combustion Column Height = 2 m)		**SO$_2$ (mg/Nm^3)**		**NO$_x$ (mg/Nm^3)**		**CO (mg/Nm^3)**	
Run No.	**Fuel**	**EU**	**Turkish**	**EU**	**Turkish**	**EU**	**Turkish**
r-6	C 100 wt%	2000	2000	600	800	NL	200
r-7	C 75 wt% + OC 25 wt%	1475	1459	542	744	NL	278
r-8	C 50 wt% + OC 50 wt%	1005	987	489	695	NL	346
r-9	C 25 wt% + OC 75 wt%	583	570	443	652	NL	407
r-10	OC 100 wt%	200	200	400	613	NL	460

*NL - There is no limit for CO emissions.

On the other hand, with limestone addition SO$_2$ concentrations could be easily reduced under the limits. As it is seen from Table 5.17 addition of almost each Ca/S of three different limestones could decrease the SO$_2$ emissions under the limit. Only Ca/S ratios that can not comply with the standards are combustion of 100 wt% coal + Çumra limestone (Ca/S=1.5), combustion of 100 wt% coal + Sedef limestone (Ca/S=1.5 and 2.0), co-combustion of 50 wt% coal + 50 wt% olive cake + Çumra limestone (Ca/S=2.0) and 50 wt% coal + 50 wt% olive cake + Sedef limestone (Ca/S=1.5).

Table 5.17 Comparison of the emissions with the limit values in EU Directive 2001-80-EC and Turkish Regulation (RCAPIS) (Set 3 and Set 4)

Set 3 (Combustion Column Height = 1 m)		**SO$_2$ (mg/Nm^3)**	
Run No.	**Fuel + Adsorbent**	**EU**	**Turkish**
r-11	C 100 wt% + Çan Ls. (Ca/S=1.5)	2000	2000
r-12	C 100 wt% + Çan Ls. (Ca/S=2.0)	2000	2000
r-13	C 100 wt% + Çan Ls. (Ca/S=2.5)	2000	2000
r-14	C 100 wt% + Çan Ls. (Ca/S=3.0)	2000	2000
r-15	C 100 wt% + Çan Ls. (Ca/S=3.5)	2000	2000
r-16	C 100 wt% + Çumra Ls. (Ca/S=1.5)	2000	2000
r-17	C 100 wt% + Çumra Ls. (Ca/S=2.0)	2000	2000
r-18	C 100 wt% + Çumra Ls. (Ca/S=2.5)	2000	2000
r-19	C 100 wt% + Çumra Ls. (Ca/S=3.0)	2000	2000
r-20	C 100 wt% + Çumra Ls. (Ca/S=3.5)	2000	2000
r-21	C 100 wt% + Sedef Ls. (Ca/S=1.5)	2000	2000
r-22	C 100 wt% + Sedef Ls. (Ca/S=2.0)	2000	2000
r-23	C 100 wt% + Sedef Ls. (Ca/S=2.5)	2000	2000
r-24	C 100 wt% + Sedef Ls. (Ca/S=3.0)	2000	2000
r-25	C 100 wt% + Sedef Ls. (Ca/S=3.5)	2000	2000
r-26	C 50 wt% + OC 50 wt% + Çan Ls. (Ca/S=1.5)	1005	987
r-27	C 50 wt% + OC 50 wt% + Çan Ls. (Ca/S=2.0)	1005	987
r-28	C 50 wt% + OC 50 wt% + Çan Ls. (Ca/S=2.5)	1005	987
r-29	C 50 wt% + OC 50 wt% + Çan Ls. (Ca/S=3.0)	1005	987
r-30	C 50 wt% + OC 50 wt% + Çumra Ls. (Ca/S=1.5)	1005	987
r-31	C 50 wt% + OC 50 wt% + Çumra Ls. (Ca/S=2.0)	1005	987
r-32	C 50 wt% + OC 50 wt% + Çumra Ls. (Ca/S=2.5)	1005	987
r-33	C 50 wt% + OC 50 wt% + Çumra Ls. (Ca/S=3.0)	1005	987
r-34	C 50 wt% + OC 50 wt% + Sedef Ls. (Ca/S=1.5)	1005	987
r-35	C 50 wt% + OC 50 wt% + Sedef Ls. (Ca/S=2.0)	1005	987
r-36	C 50 wt% + OC 50 wt% + Sedef Ls. (Ca/S=2.5)	1005	987
r-37	C 50 wt% + OC 50 wt% + Sedef Ls. (Ca/S=3.0)	1005	987
Set 4 (Combustion Column Height = 2 m)		**SO$_2$ (mg/Nm^3)**	
Run No.	**Fuel + Adsorbent**	**EU**	**Turkish**
r-38	C 50 wt% + OC 50 wt% + Çan Ls. (Ca/S=2.0)	1005	987
r-39	C 50 wt% + OC 50 wt% + Çan Ls. (Ca/S=2.5)	1005	987
r-40	C 50 wt% + OC 50 wt% + Çan Ls. (Ca/S=3.0)	1005	987

5.5.2. Comparison of the Results with Literature

Anthony et al. (2007) investigated the reactivation of limestone sorbents in a bubbling fluidized bed combustor for SO_2 capture. Moreover, they studied addition of inorganic salts to improve sorbent utilization. They used a coal having a sulfur content of 7.2% by wt. and a limestone having a $CaCO_3$ content of 98.2% by wt. During the test runs, Cl was added in the form of $CaCl_2$ in order to promote removal efficiencies. At a bed temperature of 850 ^{o}C, Ca/S ratios of 3.0, 3.2 and 4.0 were tried several times and highest SO_2 removal efficiencies of 90%, 88% and 92% were obtained, respectively. In order to compare the results, Ca/S = 3 of Çan limestone is selected for combustion of coal and co-combustion of coal and olive cake. The sulfur content of Tunçbilek lignite coal used in the experiments is 1.19% by wt. and $CaCO_3$ content of Çan limestone is 91.11% by wt. In this study, SO_2 removal efficiency of Çan limestone during combustion of coal is 87% while during co-combustion of coal and olive cake is 88% (@ average bed temperature $\cong$ 850 ^{o}C).

Pisani and Moraes (2004) studied removal of SO_2 from a fluidized bed reactor using hydrated lime. Effects of different superficial velocities (0.8, 1.0 and 1.2 m/s) and Ca/S molar ratios (1, 2 and 3) on the SO_2 removal efficiency were investigated for an initially static bed height of 10.0 cm (size of sand particles 0.5-0.6 mm). The SO_2 removal efficiency was proved to depend on the temperature and the velocity of the gaseous flow and was strongly influenced by the Ca/S molar ratio. The maximum efficiency of 97.7% was achieved at a temperature of 700 ^{o}C, a Ca/S ratio of 3 and a superficial velocity of 0.8 m/s. On the other hand, SO_2 removal efficiency of 85.0% at a temperature of 800 ^{o}C, a Ca/S ratio of 3 and a superficial velocity of 1.0 m/s is comparable with the results obtained in this study. As it was stated above SO_2 removal efficiency of Çan limestone during combustion of coal is 87% while during co-combustion of coal and olive cake is 88% (@ average bed temperature $\cong$ 850 ^{o}C and Ca/S = 3). Additionally, superficial velocity was 1.03 m/s for average bed temperature of 850 ^{o}C and initial static bed height was 10.0 cm (size of sand particles 0.5-2.0 mm).

Kose (1996) compiled some results from several studies about utilization of low rank coals and control of SO_2 emissions. According to this study, SO_2 removal efficiencies over 90% are possible with limestone addition during combustion of coal in fluidized bed combustors. Maximum SO_2 removal efficiencies were obtained with Ca/S ratios of 2.5 and 3.0. It was proved that higher increase in Ca/S ratio does not affect SO_2 emissions. Additionally, it was stated that SO_2 removal efficiency increases with increasing bed temperature up to a certain point. Then, with the further increase in bed temperature SO_2 removal efficiency starts to decrease. Maximum SO_2 removal was obtained between 815 ^{o}C and 855 ^{o}C. When the bed temperature is lower, calcination reaction can not be completed. In addition to Ca/S ratio and bed temperature, size of the limestone particles was claimed to be another factor affecting SO_2 removal efficiency. Smaller limestone particles having higher surface areas per unit volume are more suitable to react. Similarly, in this study maximum SO_2 removal efficiency during combustion of coal (87%) was obtained for Çan limestone with Ca/S = 3 at an average bed temperature of 850 ^{o}C. Additionally, since Çan limestone particles become much smaller in fuel mixture their surface area increase as expected. This probably promotes calcination efficiency of $CaCO_3$. Therefore, SO_2 removal efficiency increases.

CHAPTER 6

CONCLUSIONS

As a result of this study, it has been shown that co-combustion of coal and olive cake in a bubbling fluidized bed with limestone addition and freeboard extension is quite applicable. Temperature profiles measured along the combustion column showed that coal combustion occurs at lower parts of the combustion column for a long period of time whereas olive cake combustion takes place more in the freeboard region. As olive cake percentage in the fuel mixture was increased, temperatures in the dense bed decreased while temperatures in the freeboard increased. Maximum temperatures in the column shift from bed to freeboard as the volatile matter content in the fuel mixture increases.

For the combustion and co-combustion experiments, SO_2 emissions decreased with increasing olive cake percentage since sulfur content of olive cake is low. On the other hand, as olive cake percentage in the fuel mixture was increased, CO emissions increased due to higher volatile matter content of olive cake in comparison with coal. Most of this volatile matter leaves the combustor as CO without burning completely. NO_x concentrations are observed to decrease with increasing olive cake percentage in the fuel mixture due to formation of reducing atmosphere in the column. Therefore, combustion of coal with biomass can be an option for NO_x control.

In this study, combustion losses resulted from fly ash has the largest portion in the total combustion loss. Combustion losses due to CO formation increases as the fuels shift from coal to olive cake. Just for 100 wt% olive cake combustion, L_{CO} is the highest and it decreases the overall combustion efficiency. Additionally, $L_{fly\ ash}$

and $L_{bottom\ ash}$ decrease gradually with increasing olive cake percentage in the fuel mixture since olive cake has a lower ash content as compared to coal. For the combustion and co-combustion experiments conducted, maximum efficiency of 98.79% was obtained for co-combustion of coal with 75 wt% olive cake addition while minimum efficiency of 96.15% was obtained for combustion of 100 wt% coal.

With the freeboard extension, noticeable decreases were observed for co-combustion of 50 wt% coal and 50 wt% olive cake mixture and co-combustion of 25 wt% coal and 75 wt% olive cake mixture. Additionally, all efficiencies were found to increase slightly with the addition of 1 m - column. It has been seen that freeboard extension is helpful for fuel mixtures containing 50 wt% or more olive cake. In other words when the biomass has higher percentage in fuel mixture, increasing the freeboard height is advantageous. However, for fuel mixtures containing less than 50 wt% olive cake no significant decrease is observed for CO emissions and combustion losses. Rather than increasing the freeboard height which has not proved to be very effective for certain fuel mixtures, secondary air injection into the freeboard might be more advantageous.

During coal combustion in 1 m - combustion column, different Ca/S ratios (1.5, 2.0, 2.5, 3.0 and 3.5) were tried for three limestones, namely Çan, Çumra and Sedef. As it was expected, SO_2 emissions decreased with the increase in Ca/S ratio. At an optimum bed temperature of 850 ^{o}C, maximum SO_2 removal efficiencies of Çan, Çumra and Sedef limestones were found to be 87%, 47% and 39%, respectively. Since it was identified in the experiments of **coal combustion** with different limestones that Çan and Çumra limestones gave the maximum SO_2 removal efficiency at Ca/S = 3, higher Ca/S ratios were not tried. For co-combustion of coal and olive cake, maximum SO_2 removal efficiencies of Çan, Çumra and Sedef limestones were found to be 88%, 64% and 51%, respectively. With the addition of olive cake in the fuel mixture, obvious increases were observed in SO_2 removal efficiencies. Additionally, it was identified that Ca/S of

2.5 is the optimum value to comply with the SO_2 limit values given in EU and Turkish regulations.

Lastly, during co-combustion of coal and olive cake in 2 m - combustion column different Ca/S ratios (2.0, 2.5and 3.0) were tried for Çan limestone. As it was expected highest removal efficiency (74%) was observed at Ca/S = 3 for Çan limestone. However, performance of Çan limestone was not observed to improve with the extension of freeboard.

In conclusion, olive cake which has a high production potential in Turkey can be used as a substitute fuel in fluidized bed combustion systems for clean energy production due to its high heating value, low sulfur and low ash content. Therefore, the results of this work can be used for local and regional heating, cogeneration and disposal of biowastes which otherwise create environmental problems.

Suggestions for Future Studies

The following improvement ideas are for possible future studies that can be a continuation of the work performed in this thesis:

- The system can be modified to a circulating fluidized bed in order to increase the detention time, decrease the CO emissions and increase combustion efficiencies.
- Size of the bed material can be selected smaller to be able to decrease the fluidization air supplied to the system and the amount of flue gas emissions.
- Different bed materials with smaller densities such as perlite or dolomite can be chosen in order to prevent segregation of biomass/coal mixture and increase combustion efficiency.
- Improvement of SO_2 removal efficiency with the addition of olive cake in the fuel mixture may be due to the salts in the olive cake. According to

various studies in literature, salts can improve the absorbency of $CaCO_3$ by promoting the calcination of limestone or increase the pore diameters that allows sulfation to occur for a longer time. Therefore, this point needs further investigation.

REFERENCES

Afacan M.O., 2005. Mathematical modeling of NO_x emissions in bubbling fluidized bed combustors, MSc. Thesis, Chemical Engineering, METU.

Anthony E. J., et. al, 2007. Reactivation of limestone sorbents in FBC for SO_2 capture, *Progress in Energy and Combustion Science*, 33, 171-210.

Armesto L., et. al, 2003. Co-combustion of coal and olive oil industry residues in fluidized bed, *Fuel*, 82, 993-1000.

Atılgan İ, 2004. Investigation of the effect of particle size of limestone added to lignite on emission behavior in a fluidized bed combustion system, *G.U. Journal of Science*, 17, 89-101.

Basu P., 2006. Combustion and Gasification in Fluidized Beds, Taylor and Francis Group, USA.

Cliffe K.R., Patumsawad S., 2001. Co-combustion of waste from olive oil production with coal in a fluidised bed, *Waste Management*, 21, 49-53.

Clini C., et. al, 2008. Sustainable Development and Environmental Management: Experiences and Case Studies, Springer, USA.

Directive 2000/76/EC of the European Parliament and of the Council of December 4, 2000, on the Incineration of Waste.

Directive 2001/80/EC of the European Parliament and of the Council of 23 October 2001, on the Limitation of Emissions of Certain Pollutants into the Air from Large Combustion Plants.

FAO (Food and Agriculture Organization of the United Nations), 2008. ProdStat, http://faostat.fao.org/site/567/default.aspx#ancor, (Last accessed date: 10.12.2008).

Fiorentino M., Miccio F., 2000. On the relevance of segregation phenomena during bubbling fluidized bed combustion and desulfurization of ebonite, *Combustion Science and Technology*, 159, 57-86.

Ghani W., et. al., 2009. Co-combustion of agricultural residues with coal in a fluidised bed combustor, *Waste Management*, 29, 767–773.

Gogebakan Z., et. al., 2008. Co-Firing of Olive Residue with Lignite in Bubbling FBC, *Combustion Science and Technology*, 180, 854–868.

ICRE (International Conference for Renewable Energies), 2004. The Potentials of Renewable Energy, Thematic Background Paper, http://www.renewables2004.de/pdf/tbp/TBP10-potentials.pdf, (Last accessed date: 12.03.2009).

IEA (International Energy Agency), 2009. Biomass Combustion and Co-firing: An Overview, http://www.ieabcc.nl/, (Last accessed date: 10.03.2009).

IP (Integrated Publishing), 2009. Saturation mixing ratio, http://www.tpub.com/weather3/6a-4.htm, (Last accessed date: 01.08.2009).

Junginger M., et. al, 2006. Technological learning in bioenergy systems, *Energy Policy*, 34, 4024–4041.

Kayali C. A., et. al, 2008. Development potential of olive production establishments in Akhisar-Manisa-Turkey, *Asian Journal of Scientific Research*, 1, 103-112.

Khan A. A., et. al, 2009. Biomass combustion in fluidized bed boilers: Potential problems and remedies, *Fuel Processing Technology*, 90, 21-50.

Khraisha Y. H., et. al., 1999. Direct Combustion of Olive Cake Using Fluidized Bed Combustor, *Energy Sources*, 21, 319-327.

Klass D.L., 2004. Biomass for Renewable Energy and Fuels, *Encyclopedia of Energy*, 1, 193-212.

Koornneef J., et. al, 2007. Development of fluidized bed combustion - An overview of trends, performance and cost, *Progress in Energy and Combustion Science*, 33, 19–55.

Kose R., 1996. Utilization of low rank coals and control of SO_2 emissions (in Turkish), *10. Kömür Kongresi Bildiriler Kitabı*, 51-58.

Kunii D., Levenspiel O., 1991. Fluidization Engineering, 2nd Edition, Butterworth-Heinemann, USA.

LCP BREF, 2006. Integrated Pollution Prevention and Control, Reference Document on Best Available Techniques for Large Combustion Plants, Spain.

Leckner B., 2007. Co-combustion – A Summary of Technology, *Thermal Science*, 11, 5-40.

Li Y., et. al, 2005. SO_2 Removal and CO_2 Capture by Limestone Resulting from Calcination/Sulfation/Carbonation Cycles. *Fuel&Energy*, 19, 1927-1934.

Liu H., Gibbs B. M., 1998. The influence of limestone addition at different positions on gaseous emissions from a coal-fired circulating fluidized bed combustor, *Fuel*, 77, 1569-1577.

Liu Y., et. al, 2006. Effects of NaCl on the capture of SO_2 by $CaCO_3$ during coal combustion, *Fuel*, 85, 524-531.

Llorente M.J., et. al., 2006. Combustion in bubbling fluidised bed with bed material of limestone to reduce the biomass ash agglomeration and sintering, *Fuel*, 85, 2081-2092.

LMNO Engineering, Research, and Software, Ltd., 2008. Gas Viscosity Calculator, http://www.lmnoeng.com/Flow/GasViscosity.htm, (Last accessed date: 26.09.2008).

Lutgens F. K., et. al., 1997. The atmosphere: An Introduction to Meteorology, 7th edition, Prentice Hall, USA.

McKendry P., 2002. Energy production from biomass (part 1): overview of biomass, *Bioresource Technology*, 83, 37-46.

MENR (Ministry of Energy and Natural Resources), 2009. Birincil Enerji Kaynaklari Üretim-Tüketim Gerçekleşmeleri ve Hedefleri (in Turkish), http://www.enerji.gov.tr/istatistik.asp, (Last accessed date: 15.08.2009).

Muncaster R., 1993. A-Level Physics (4th Edition), Nelson Thornes, UK.

Nowak W., Kobylecki R., 2009. Biomass Combustion and Gasification, http://www.6pr.pl/images/prezentacje/info/energy-conf/prezentacje/Wojciech_Nowak_Abstract.doc,
(Last accessed date: 01.04.2009).

OGRI (Olive Growing Research Institute), 2008. Zeytinyağı Teknolojisi (in Turkish), http://www.zae.gov.tr/zeytinyagi/7.asp, (Last accessed date: 27.12.2008).

Ozgur M. A., 2008. Review of Turkey’s renewable energy potential, *Renewable Energy*, 33, 2345–2356.

Özkan G., Doğu G., 2002. Combustion of a high ash and sulfur containing lignite in a pilot circulating fluidized bed combustor and its pollution characteristics *Chemical Engineering and Processing*, 41, 11-15.

Patumsawad S., 2001. Coal combustion studies in a fluidised bed, *The Journal of KMITNB*, 11(2).

Perry R. H., 2007. Chemical Engineers' Handbook, 8th edition, McGraw Hill Professional.

Pisani R. Jr., de Moraes D. Jr., 2004. Removal of sulfur dioxide from a continuously operated binary fluidized bed reactor using inert solids and hydrated lime, *Journal of Hazardous Materials*, B109, 183-189.

RCAPIS, 2009. Turkish Regulation for Control of Air Pollution from Industrial Sources, Republic of Turkey Ministry of Environment and Forestry.

REC (Regional Environmental Center), 2009. http://www.rec.org/REC/Announcements/PressReleases/2009_turkey_accedes_kyoto_protocol.html, (Last accessed date: 13.03.2009).

REC Turkey, Regional Environmental Center, 2008. http://www.rec.org.tr/climate.htm, (Last accessed date: 17.09.2008).

Scala F., Chirone R., 2006. Characterization and Early Detection of Bed Agglomeration during the Fluidized Bed Combustion of Olive Husk, *Energy & Fuels*, 20, 120-132.

Shearer J. A., et. al, 1979. Effects of Sodium Chloride on Limestone Calcination and Sulfation in Fluidized-Bed Combustion, *American Chemical Society*, 13, 1113-1118.

Suksankraisorn K., et. al., 2003. Combustion studies of high moisture content waste in a fluidised bed, *Waste Management*, 23, 433-439.

SYW (South Yorkshire Woodfuel), 2009. The Carbon Cycle, http://www.wood-fuel.org.uk/why_global.php, (Last accessed date: 13.03.2009).

Thomas I., 2007. The Pros and Cons of Biomass Power. The Rosen Publishing Group, USA.

Toraman O. Y., et. al., 2004. Emission Characteristics of Co-combustion of Sewage Sludge with Olive Cake and Lignite Coal in a Circulating Fluidized Bed, *Journal of Environmental Science and Health*, A39, 973-986.

TSI (Turkish Statistical Institute), 2009. Crop Production Statistics, http://www.turkstat.gov.tr/PreIstatistikTablo.do?istab_id=1073, (Last accessed date: 15.08.2009).

Van Loo S., Koppejan J., 2008. The handbook of biomass combustion and co-firing, Earthscan, UK.

Varol M., 2006. Combustion and co-combustion of olive cake and coal in a fluidized bed, MSc. Thesis, Environmental Engineering, METU.

Varol M., Atimtay A. 2007. Combustion of olive cake and coal in a bubbling fluidized bed with secondary air injection, *Fuel*, 86, 1430-1438.

Varol M., Atimtay A. 2009. Investigation of co-combustion of coal and olive cake in a bubbling fluidized bed with secondary air injection, *Fuel*, 88, 1000-1008.

VGB Powertech, 2008. Advantages and Limitations of Biomass Co-combustion in Fossil Fired Power Plants, http://www.vgb.org/en/news_biomass_co_combustion_march2008.html, (Last accessed date: 17.09.2008).

Werther J., et. al, 2000. Combustion of agricultural residues, *Progress in Energy and Combustion Science*, 26, 1–27.

Xie J., et. al., 2007. Emissions of SO_2, NO and N_2O in a circulating fluidized bed combustor during co-firing coal and biomass, *Journal of Environmental Science*s, 19, 109-117.

APPENDIX A

CALCULATIONS AND CALIBRATION CURVES FOR THE FUEL FEEDING SYSTEM

Operational principle of the fuel feeding system is like that; solid fuel is carried into the combustor by the screw feeder with “on mode” and held in the fuel hopper with “off mode”. In order to control the feeding rate, ten control steps are placed on each of these two modes. These steps divide one minute into ten equal segments having six seconds of time interval. For example; 2 (on) – 1 (off) mode of the screw feeder means that the feeder works for twelve seconds, stops six seconds and then works twelve seconds again.

Calibration of the feeding system was carried out for olive cake and coal. The feeding rate calibration curves for olive cake and coal are given in Figure A.1 and Figure A.2, respectively. The calibration was done with 10 (on) – 5 (off) mode meaning that the feeder operates for one minute (10*6) and stops to feed for thirty seconds (5*6). In Table A.1, the feeding rates for both olive cake and coal were calculated using the formula of the calibration curves. In order to find the feeding rates of other three mixtures, feeding rates of olive cake and coal were multiplied with the weight fraction of each fuel in the mixture for the same on-off mode and then summed up.

For instance, let’s go over an example for 4-2 mode. For 4-2 mode, screw feeder works 4*6=24 sec and stops 2*6=12 sec. Thus in a 36 seconds time interval, screw feeder feeds fuel for 24 sec. When operation time is calculated for one minute, it is found that screw feeder feeds fuel for 40 sec in a 60 sec time interval.

Equations of feeding rate calibration curves for olive cake and coal are given below.

$y = 23.164\ x + 2.1552$ for olive cake (O.C.)

$y = 37.897\ x - 2.8958$ for coal (C)

where x represents operation time in “min” and y represents fuel feeding rate in “g/min”.

In this way, fuel feeding rates of coal and olive cake for 4-2 mode are calculated as following:

$x = (24/36)*1\ \text{min} = 0.666\ \text{min}$

$y_{O.C} = 23.164\ (0.666) + 2.1552 = 17{,}598\ \text{g/min}$ for O.C.

$y_C = 37.897\ (0.666) - 2.8958 = 22{,}369\ \text{g/min}$ for C

Feeding rates of different mixtures are calculated by the weight fraction of the solid fuel in mixture

$y = y_C * wf_C + y_{O.C} * wf_{O.C.}$

where “$wf_{O.C.}$” represents weight fraction of olive cake in mixture and “wf_C” represents weight fraction of coal in mixture.

As an example, fuel feeding rate of 75% coal and 25% olive cake mixture for 4-2 mode are calculated as following:

$y = 22{,}369\ \text{g/min} * 0.75 + 17{,}598\ \text{g/min} * 0.25 = 21{,}176\ \text{g/min}$

Table A.1 Feeding rates for coal, olive cake and their different mixtures

		Feeding Rate, g/min				
On	**off**	**Olive Cake (OC)**	**Coal (C)**	**%25 OC +%75 C**	**%50 OC +%50 C**	**%75 OC +%25 C**
1	**1**	13,737	16,053	15,474	14,895	14,316
1	**2**	9,877	9,737	9,772	9,807	9,842
1	**3**	7,946	6,578	6,920	7,262	7,604
2	**1**	17,598	22,369	21,176	19,983	18,791
2	**2**	13,737	16,053	15,474	14,895	14,316
2	**3**	11,421	12,263	12,052	11,842	11,631
2	**5**	8,773	7,932	8,142	8,353	8,563
3	**1**	19,528	25,527	24,027	22,528	21,028
3	**4**	12,083	13,346	13,030	12,714	12,398
3	**5**	10,842	11,316	11,197	11,079	10,960
4	**2**	17,598	22,369	21,176	19,983	18,791
4	**4**	13,737	16,053	15,474	14,895	14,316
4	**7**	10,578	10,885	10,808	10,732	10,655
4	**8**	9,877	9,737	9,772	9,807	9,842
5	**1**	21,459	28,685	26,878	25,072	23,265
5	**3**	16,633	20,790	19,751	18,711	17,672
5	**8**	11,064	11,680	11,526	11,372	11,218
6	**3**	17,598	22,369	21,176	19,983	18,791
6	**6**	13,737	16,053	15,474	14,895	14,316
6	**8**	12,083	13,346	13,030	12,714	12,398
7	**4**	16,896	21,220	20,139	19,058	17,977
7	**5**	15,668	19,211	18,325	17,439	16,553
7	**9**	12,289	13,684	13,335	12,987	12,638
8	**3**	19,002	24,666	23,250	21,834	20,418
8	**4**	17,598	22,369	21,176	19,983	18,791
8	**5**	16,410	20,425	19,422	18,418	17,414
9	**1**	23,003	31,212	29,159	27,107	25,055
9	**7**	15,185	18,421	17,612	16,803	15,994
9	**10**	13,128	15,055	14,573	14,092	13,610
10	**4**	18,701	24,173	22,805	21,437	20,069
10	**6**	16,633	20,790	19,751	18,711	17,672
10	**8**	15,024	18,158	17,375	16,591	15,808

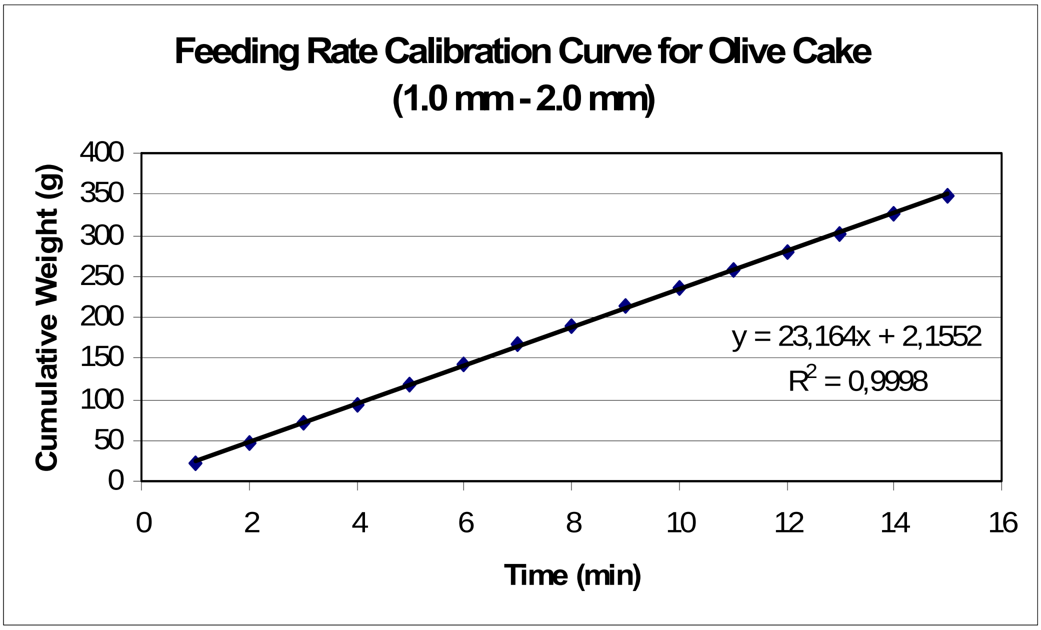

Figure A.1 Feeding rate calibration curve for olive cake

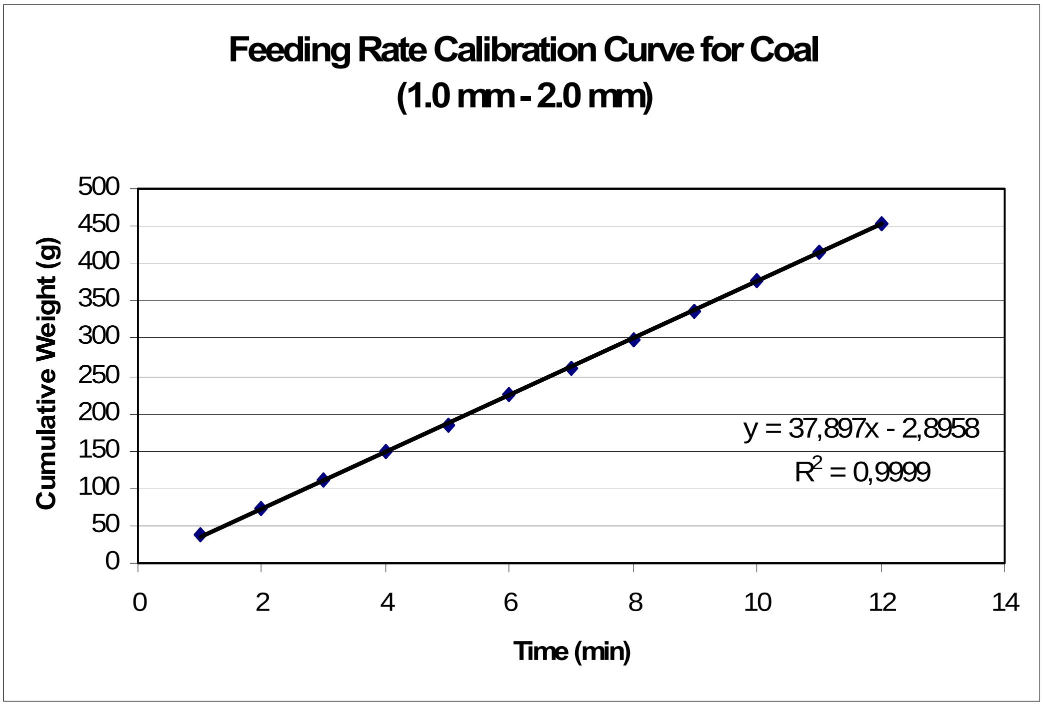

Figure A.2 Feeding rate calibration curve for Tunçbilek Lignite

APPENDIX B

DETERMINATION OF MINIMUM FLUIDIZATION VELOCITY

Theoretical Determination of Minimum Fluidization Velocity

According to Kunii and Levenspiel (1991), the formula below can be used in order to calculate minimum fluidization velocity if Re (Reynolds number) is less than 20.

$$u_{mf} = [d_p^2 * (\rho_s - \rho_f) * g * \varepsilon_{mf}^3 * \phi_s^2] / [150 * \mu * (1-\varepsilon_{mf})] \qquad ; Re<20 \qquad (B.1)$$

where;

d_p: average particle diameter (0.067 cm)

ρ_s: solid (sand) density, experimentally found as 2.557 g/cm^3

ρ_f: air density at 20^{o}C (0.0012 g/cm^3) (Muncaster, 1993)

g: gravitational acceleration (981 cm/s^2) (Muncaster, 1993)

ε_{mf}: void fraction at minimum fluidization, calculated as 0.418

ϕ_s: sphericity of an average sand particle (0,75) (Basu, 2006)

μ: viscosity of air at 20^{o}C (0.00018 g/cm-s) (LMNO, 2008).

Void fraction at minimum fluidization can be calculated from the formula below given by Kunii and Levenspiel (1991).

$$L_m * (1-\varepsilon_m) = L_{mf} * (1-\varepsilon_{mf}) \qquad (B.2)$$

where;

L_m : height of fixed bed (10 cm)

ε_m : void fraction of fixed bed experimentally found as 0.36

L_{mf} : height at minimum fluidization (11cm)

ε_{mf} : void fraction at minimum fluidization

$\varepsilon_{mf} = 0.418$

Finally by the formula B.1, minimum fluidization velocity at 20 ^oC can be calculated as;

$u_{mf} = 29{,}472$ cm/sec

Re (Reynolds number) = $d_p * u_{mf} * \rho_f / \mu$ (B.3)

Re = 0.067 * 35.694 * 0.0012 / 0.00018 = 13,164 < 20

Since the Reynolds number was found less than 20, calculation of u_{mf} by the formula B.1 is acceptable.

Experimental Determination of Minimum Fluidization Velocity

Determination of the minimum fluidization velocity was also performed experimentally in order to compare with the theoretically calculated u_{mf} value.

Initially, orifice was calibrated in order to see the pressure drops corresponding to different velocities. Air velocities in the orifice were measured by using pitot tube. After the measurement of the velocities in the orifice, equivalent velocities in the column were calculated. Orifice calibration curve is given in Figure B.1.

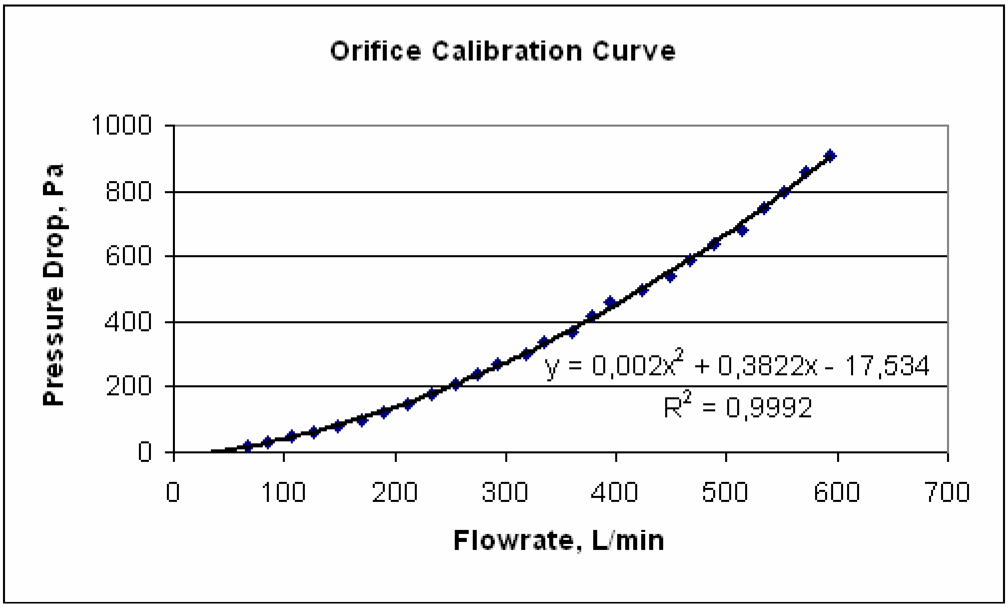

Figure B.1 Orifice calibration curve

After the orifice calibration, the pressure drops at the orifice and the distributor plate were measured for both empty and loaded column. Firstly while the column was empty, control valve of the compressor was opened gradually starting from minimum flow. The pressure drops at the orifice and the distributor plate were recorded and matched with the correlated velocity values obtained from the orifice calibration. Secondly, 1339 g of sand (corresponding to 10 cm-bed height) was loaded into the combustor column and same procedure was carried out for loaded column.

Pressure drops through the bed was calculated by subtracting the pressure drops caused by distributor plate (empty bed) from the pressure drops caused by distributor plate + bed (loaded bed). Pressure drops through the bed and corresponding velocities are given in Table B.1.

Table B.1 Pressure drops through the bed and corresponding velocities

Gas velocity m/sec	**Δp @ distributor mmH_2O**	**Δp @ distributor+bed mmH_2O**	**Δp @ bed mm H_2O**
0,01	1,00	1,50	0,50
0,07	1,14	36,00	34,86
0,08	4,37	77,00	72,63
0,10	10,20	168,00	157,80
0,12	15,52	189,50	173,98
0,14	20,52	236,00	215,48
0,16	27,61	261,00	233,39
0,17	31,02	265,50	234,48
0,32	88,00	214,00	126,00
0,34	101,71	222,00	120,29
0,38	120,00	243,00	123,00
0,45	156,40	270,00	113,60
0,50	184,05	310,00	125,95
0,54	207,94	343,00	135,06
0,55	214,99	350,00	135,01
0,59	244,87	368,00	123,13
0,61	249,00	383,00	134,00
0,58	236,10	350,00	113,90
0,55	217,63	342,00	124,37
0,51	189,37	312,00	122,63
0,49	183,16	307,00	123,84
0,46	160,88	270,00	109,12
0,39	127,50	243,00	115,50
0,34	101,71	218,00	116,29
0,30	82,86	190,00	107,14
0,26	63,42	158,00	94,58
0,20	41,93	111,00	69,07
0,15	25,29	67,00	41,71
0,10	10,20	36,00	25,80
0,08	4,37	17,00	12,63
0,01	0,00	0,10	0,10

Finally, in order to find the minimum fluidization velocity, the pressure drop versus air velocity was plotted (Figure B.2). According to Kunii and Levenspiel

(1991), the pressure drop is approximately proportional to the gas velocity for the relatively low flow rates in a fixed bed and this pressure drop reaches to the maximum (Δp_{max}) with increasing air velocity. Since the voidage of the bed material increases from ε_m (void fraction in the fix bed) to ε_{mf} (void fraction of the bed at minimum fluidization), the pressure drop starts to decrease. The dashed line in Figure B.2 refers to the static pressure of the bed (W/A) which is slightly less then the maximum pressure drop (Δp_{max}). Minimum fluidization velocity is the x-axis value perpendicular to the point where W/A (weight of particles / cross sectional area of the column) intersects the pressure drop versus velocity curve. From curve plotted the velocity at minimum fluidization was found as 0.27 m/sec. So, it can be seen that this measured value is very close to the theoretically calculated u_{mf} = 0.29 m/sec. Experimentally obtained u_{mf} value is comparable with some values in the literature. In the experiments performed with a bench-scale bubbling fluidized bed reactor by Fiorentino and Miccio (2000), u_{mf} was found as 0.22 m/sec using silica sand between 0.6-0.85 mm as bed material. As it was stated above, in this study u_{mf} was experimentally found as 0.27 m/sec using silica sand as bed material with an average particle diameter 0.67 mm.

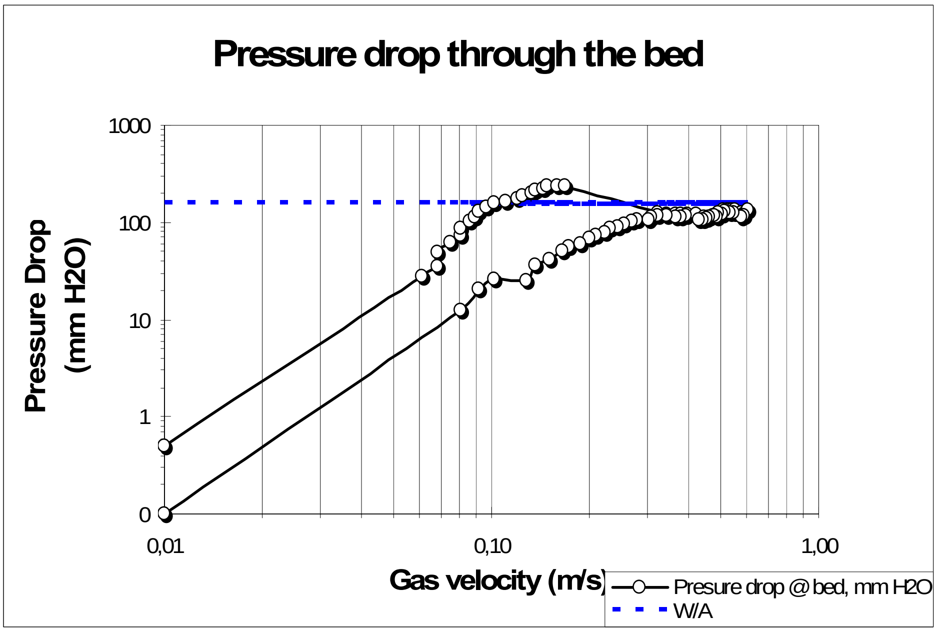

Figure B.2 Pressure drop versus the superficial gas velocity across the bed

APPENDIX C

SAMPLE CALCULATIONS FOR THEORETICAL AIR REQUIREMENT, TOTAL FLUE GAS AND COMBUSTION EFFICIENCY

Calculation of Theoretical Air Requirement:

Table C.1 Ultimate analysis of Tunçbilek lignite coal and Edremit olive cake

Ultimate Analysis, on wet basis (wt%)		
	Tunçbilek lignite coal	**Edremit olive cake**
C	33.32	43.35
H	2.64	5.15
N	1.02	1.29
O	7.98	30.40
S (comb.)	0.59	0.00
Ash	44.30	6.32
Moisture	10.15	13.49
Total	100.00	100.00

Initially, 100 g fuel is taken as a base value in order to calculate theoretical oxygen requirement and total amount of flue gas. Following calculations are the ones for theoretical oxygen requirement and total flue gas in Nm^3/kg of "Tunçbilek lignite coal".

$n_C = m_C / MW_C$ (C-1)

$= 33.32 / 12 = 2.777$ mole/100 g fuel

$n_H = m_H / MW_H$ (C-2)

$= 2.64 / 1 = 2.640$ mole/100 g fuel

$n_N = m_N / MW_N$ (C-3)

$= 1.02 / 14 = 0.073$ mole/100 g fuel

$n_S = m_S / MW_S$ (C-4)

$= 0.59 / 32 = 0.018$ mole/100 g fuel

$n_O = m_O / MW_O$ (C-5)

$=7.98 / 16 = 0.499$ mole/100 g fuel

$n_{H2O} = m_{H2O} / MW_{H2O}$ (C-6)

$=10.15 / 18 = 0.564$ mole/100 g fuel

where;

m_X: Amount of X in 100 g of fuel, g/100g fuel

MW_X: Molecular weight of X, g/mole

n_X: Mole of X for 100 g of fuel, mole X/100g fuel

Following reactions are complete combustion reactions in order to calculate theoretical oxygen requirement and total amount of flue gas.

$C + O_2 \rightarrow CO_2$ (C.7)

$H_2 + ½ O_2 \rightarrow H_2O$ (C.8)

$N_2 + O_2 \rightarrow 2NO$ (C.9)

$S + O_2 \rightarrow SO_2$ (C.10)

Following molar calculations is done using the reactions above:

- 1 mole oxygen (O_2) is needed to burn 1 mole carbon (C). Therefore 2.777 mole O_2/100 g fuel is needed to burn 2.777 mole C/100 g fuel.
- 0.5 mole O_2 is needed to burn 1 mole hydrogen (H_2). Therefore 0.660 mole O_2/100 g fuel is needed to burn 1.320 mole H_2/100 g fuel.
- 1 mole O_2 is needed to burn 1 mole nitrogen (N_2). Therefore 0.036 mole O_2/100 g fuel is needed to burn 0.036 mole N_2/100 g fuel.
- 1 mole O_2 is needed to burn 1 mole sulphur (S). Therefore 0.018 mole O_2/100 g fuel is needed to burn 0.018 mole S/100 g fuel.
- 0.249 mole O_2 is supplied for 100 g fuel.
- 0.564 mole water vapor (H_2O) is supplied for 100 g fuel.

Therefore, mole of total theoretical oxygen requirement for the combustion of 100 g of Tunçbilek coal is;

$n_{O2,th} = 2.777 + 0.660 + 0.036 + 0.018 - 0.249 = 3.242$ mole O_2/100 g fuel

Atmospheric oxygen percentage ($O_{2,atm}$) is assumed to be 20.9%.

$n_{air,th} = (n_{O2,th} / O_{2,atm}) * 100$ (C.11)

$= (3.242 / 20.9) * 100 = 15.513$ mole air/100 g fuel

where;

$n_{air,th}$: Mole of air theoretically required for the combustion of 100 g of fuel

$n_{O2,th}$: Mole of oxygen theoretically required for the combustion of 100 g of fuel

$O_{2,atm}$: Atmospheric oxygen percentage (20.9%)

The actual amount of air to be supplied is calculated by taking the excess air also into consideration. According to Van Loo and Koppejan (2008) excess air ratio of 1.2 is an optimum value for bubbling fluidized beds, theoretically.

$n_{air,actual} = n_{air,th} * \lambda$ (C.12)

$= 15.513 * 1.2 = 18.615$ mole air/100 g fuel

where;

$n_{air,actual}$: Actual mole of air required for the combustion of 100 g of fuel

λ : Excess air ratio, (1.2)

In order to burn the fuel completely, more air should be supplied to the system than theoretical air requirement to have sufficient volume of combustion air surrounding all fuel particles completely. Share of this additional air supplied to the system is called "excess air ratio (λ)". For example, λ =1.30 means that 30 percent more than the required stoichiometric air is used. Stoichiometric condition refers to the condition where theoretical oxygen demand of fuel for complete combustion is met. λ =1 means that no excess air is supplied to the system. In other words combustion takes place on stoichiometric condition.

From the ideal gas law;

Volume of actual air ($V_{air,actual}$) = $n_{air,actual} * R * T / P$

$n_{air,actual} = 18.615$ mole air/100 g fuel

$R = 8.205 * 10^{-5}$ atm-m^3/mole-K

$T = 273$ K

$P = 1$ atm

Volume of actual air required = 4.170 Nm^3/kg of Tunçbilek coal @ NTP (Normal Temperature and Pressure)

Calculation of Theoretical Total Flue Gas:

Total amount of theoretical flue gas formed from the combustion process is calculated on wet basis.

- 1 mole CO_2 is formed from combustion of 1 mole carbon (C). Therefore 2.777 mole CO_2/100 g fuel is formed from combustion of 2.777 mole C/100 g fuel.
- 1 mole H_2O is formed from combustion of 1 mole hydrogen (H_2). Therefore 1.320 mole H_2O/100 g fuel is formed from combustion of 1.320 mole H_2/100 g fuel.
- 2 mole NO is formed from combustion of 1 mole nitrogen (N_2). Therefore 0.073 mole NO/100 g fuel is formed from combustion of 0.036 mole N_2/100 g fuel.
- 1 mole SO_2 is formed from combustion of 1 mole sulphur (S). Therefore 0.018 mole SO_2/100 g fuel is formed from combustion of 0.018 mole S/100 g fuel.
- 0.564 mole water vapor (H_2O) is supplied for 100 g fuel. (see C-6)

The amount of N_2 supplied to the combustor with O_2 is calculated as below:

$$n_{N2} = (n_{air,th} * N_{2,atm}) / 100 \qquad \text{(C.13)}$$

$= (18.615 * 79.1) / 100 = $ 14.725 mole N_2/100 g fuel

where;

n_{N2}: The mole of N_2 supplied for 100 g of fuel

$N_{2,atm}$: Atmospheric nitrogen percentage (79.1%)

Excess O_2 supplied to the system is calculated with the following formula:

$$n_{O2,ex} = n_{O2,th} * (\lambda - 1) \qquad \text{(C.14)}$$

$= 3.242 * (1.2 - 1) = $ 0.648 mole O_2/100 g fuel

Moisture in air is found with calculations below:

Saturation mixing ratio (W_s) is the theoretical maximum amount of water vapor that air at a specific temperature and pressure can hold. Relative humidity (RH) is a ratio, expressed in percent, of the amount of water vapor in the air (actual mixing ratio (W)) proportional to the amount of water vapor the air can hold (saturation mixing ratio) (IP, 2009).

According to Lutgens et al. (1997), saturation mixing ratio at room temperature (20 ^oC) is 14 g H_2O/kg of air. Relative humidity is assumed to be 75%.

$W = (W_s * RH) / 100$ (C.15)
$= (14 * 75) / 100 = 10.5$ g H_2O/kg of air

where;

W_s: Saturation Mixing Ratio, g H_2O/kg of air
W: Actual Mixing Ratio, g H_2O/kg of air
RH: Relative Humidity, %

Mixing ratio (X) is the ratio of amount of water vapor in dry air by mole.

$X = (W / 1000) * (MW_{air} / MW_{H2O}) * 100$ (C.16)
$= (10.5 / 1000) * (28.84 / 18) * 100 = 1.682\%$ mole H_2O/mole dry air

where;

$MW_{air} = 28.84$ g/mole (20.9% of O_2 and 79.1% of N_2)
$MW_{H2O} = 18$ g/mole

$n_{H2O,air} = (X * n_{air,actual}) / 100$ (C.17)
$= (1.682 * 18.615) / 100 =$ $\underline{0.313 \text{ mole } H_2O/100 \text{ g fuel}}$

Therefore, mole of theoretical total flue gas coming from the combustion of 100 g of Tunçbilek coal is;

$n_{fluegas,th(w.b)} = n_{CO2} + n_{H2O} + n_{NO} + n_{SO2} + n_{H2O,fuel} + n_{N2} + n_{O2,ex} + n_{H2O,air}$ (C.18)
$= 2.777 + 1.320 + 0.073 + 0.018 + 0.564 + 14.725 + 0.648 + 0.313$
$= 20.438$ mole/100 g fuel

From the ideal gas law;

Volume of theoretical total flue gas ($V_{fluegas,th(w.b)}$) = $n_{fluegas,th(w.b)}$ * R * T / P

$n_{fluegas,th(w.b)}$ = 20.438 mole/100 g fuel

R = 8.205 * 10^{-5} atm-m^3/mole-K

T = 273 K

P = 1 Atm

Volume of theoretical total flue gas = 4.578 Nm^3/kg of Tunçbilek coal @ NTP (Normal Temperature and Pressure)

Calculation of Combustion Efficiency:

As it was stated before combustion losses mostly originate from CO formation (L_{CO}) and unburnt carbon in the fly ash and bottom ash ($L_{fly\ ash}$, $L_{bottom\ ash}$). Therefore, combustion efficiency of the system is calculated by using flue gas analysis and ash analysis in order to find losses resulted from CO formation and unburnt carbon in the ash.

CO emissions and unburnt carbon formed as a result of the incomplete combustion cause heat loss from flue gas.

Combustion loss originating from CO emissions is calculated with the formula below:

L_{CO} = CO * $V_{fluegas,\ actual}$ * H_{L_CO} / H_{L_fuel} / 10,000 (C.19)

= 416 * 6.366 * 12.63 / 12.138 / 10,000 = 0.23%

where,

L_{CO}: Total C loss resulted from CO formation, %

CO: Average CO concentration measured in flue gas, 416 ppm

H_{L_CO}: Lower heating value of CO (ΔH_c^0, Heat of combustion), 12.63 MJ/Nm^3 CO (Perry, 2007)

H_{L_fuel}: Lower heating value of the fuel used, 12.138 MJ/kg Tunçbilek coal

$V_{fluegas,\ actual}$: Volume of actual total flue gas, calculated as 6.366 Nm^3/kg of Tunçbilek coal

The actual amount of flue gas ($V_{fluegas,\ actual}$) is calculated by taking the excess air ratio as 1.71. Average oxygen concentration in the flue gas during combustion of Tunçbilek coal is measured as 8.7 %. Excess air ratio is calculated according to this measured concentration of O_2 by using the formula below.

$$\lambda = 20.9 / (20.9 - O_{2,measured}) \tag{C.20}$$

$$= 20.9 / (20.9 - 8.7) = 1.71$$

At the end of the combustion of Tunçbilek coal, 496.16 g of bottom ash and 909.64 g of fly ash was collected from combustion column and ash hopper, respectively. Elapsed time for the combustion was 2.73 hours. In order to find the unburnt carbon content of the ash samples, they were burned in a furnace at 950 ^oC. The difference in weight after burning at 950 ^oC, gave the unburnt amount of carbon in the ash samples. The unburnt carbon amounts were found as 1.6 wt% and 6.8 wt% for bottom ash and fly ash, respectively.

Therefore;

Ash_{bottom} = (909.64 g / 2.73 h) * (10^{-3} kg/g) = 0.333 kg ash/h

C_{bottom} = 0.016 kg C/ kg ash

Ash_{fly}: (496.16 g / 2.73 h) * (10^{-3} kg/g) = 0.182 kg ash/h

C_{fly} = 0.068 kg C/ kg ash

M_f = 22 g fuel/min = 1.32 kg fuel/h

Combustion loss originating from unburnt carbon in bottom ash is calculated with the formula below:

$$L_{bottom} = Ash_{bottom} * C_{bottom} * H_{L\_Char} / M_f / H_{L\_fuel} * 100 \qquad (C.21)$$
$$= 0.333 * 0.016 * 32.79 / 1.32 / 12.138 * 100 = 1.09\%$$

where,

L_{bottom}: Total C loss resulted from carbon in bottom ash, %

Ash_{bottom}: Amount of bottom ash formed during combustion, kg ash/h

C_{bottom}: Unburnt carbon content in the bottom ash, kg C/ kg ash

H_{L_Char}: Lower heating value of char (ΔH_c^0, Heat of combustion), 32.79 MJ/kg char (Perry, 2007)

M_f: Fuel feeding rate, kg fuel/h

Combustion loss originating from unburnt carbon in fly ash is calculated with the formula below:

$$L_{fly}= Ash_{fly} * C_{fly} * H_{L\_Char} / M_f / H_{L\_fuel} * 100 \qquad (C.22)$$
$$= 0.182 * 0.068 * 32.79 / 1.32 / 12.138 * 100 = 2.53\%$$

where,

L_{fly}: Total C loss resulted from carbon in fly ash, %

Ash_{fly}: Amount of fly ash formed during combustion, kg ash/h

C_{fly}: Unburnt carbon content in the fly ash, kg C/ kg ash

Finally, overall combustion efficiency (η) is calculated with the formula below:

$$\eta = 100 - (L_{CO} + L_{bottom} + L_{fly}) \qquad (C.23)$$
$$= 100 - (0.23 + 1.09 + 2.53) = 96.15\%$$

$$\boxed{\text{Overall combustion efficiency } (\eta) = 96.15\%}$$

Total thermal capacity of the system is calculated with the formula below (assuming that there is no heat loss):

$$Q_f = M_f * H_{L\_fuel} * (\eta/100) * (1\ h/3600\ sec) * (10^3\ kW/1\ MW) \qquad (C.24)$$

$$= 1.32 * 12.138 * (96.15 / 100) / 3600 * 1000 = 4.3\ kW$$

APPENDIX D

SAMPLE CALCULATION FOR LIMESTONE NEED TO REMOVE SO_2 EMISSIONS

The overall removal reaction of sulfur dioxide with limestone is:

$CaCO_3 + SO_2 + 1/2\ O_2 \rightarrow CaSO_4 + CO_2$ (D-1)

“However reaction (D-1) does not take place in one step. The first step is calcination, where the limestone decomposes into CaO and CO_2 through an endothermic reaction”:

$CaCO_3 \rightarrow CaO + CO_2$ – 183 kJ/g.mol (D-2)

“The second step in sulfur capture during fluidized bed combustion is sulfation, where the calcium oxide absorbs sulfur dioxide, forming calcium sulfate. Calcium sulfate is a relatively inert and stable solid that is disposed of easily. The overall reaction is as follows”:

$CaO + SO_2 + 1/2\ O_2 \rightarrow CaSO_4$ + 486 kJ/g.mol (D-3)

“The carbon dioxide released during the calcination creates and enlarges many pores in the limestone (Figure D.1), which exposes greater surface area for the subsequent sulfation reactions” (Basu 2006).

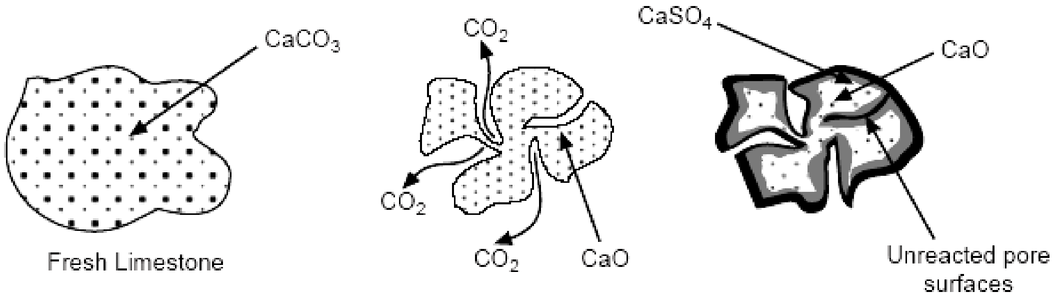

Figure D.1 Absorption of sulfur dioxide by limestone (Basu, 2006)

Following calculations are a sample for theoretical Çan limestone need (Ca/S ratio of 3) to capture SO_2 emissions originated from combustion of 1 kg of Tunçbilek lignite coal.

Calcination efficiency is assumed to be 100%, in other words all $CaCO_3$ is assumed to turns into CaO since limestone is easily calcined at operating temperatures of fluidized bed combustors (800 - 900 °C) (Basu, 2006).

$m_S = m_{coal} * S\% / 100$ (D-4)

$= 1000 * 1.07 / 100 = 10.7$ g

where;

m_S: Amount of Sulfur (S) in 1000 g of Tunçbilek coal, g

m_{coal}: Amount of Tunçbilek coal (1000 g)

S% : S percentage in Tunçbilek coal (1.07 wt%) (see Table 4.2)

$n_S = m_S / MW_S$ (D-5)

$= 10.7 / 32 = 0.334$ mole S

where;

n_S: Mole of S in 1000 g of Tunçbilek coal

MW_S: Molecular weight of S (32 g/mole)

$n_{Ca} = n_S * Ca/S$ (D-6)

$= 0.334 * 3 = 1.002$ mole Ca

where;

n_{Ca}: Mole of Ca to capture S in 1000 g of Tunçbilek coal (for Ca/S=3)
Ca/S: Calcium to sulfur ratio (Ca/S=3)

1 mole Ca is needed to form 1 mole $CaCO_3$. Therefore, 1.002 mole Ca is needed to form 1.002 mole $CaCO_3$.

$m_{CaCO3} = n_{CaCO3} * MW_{CaCO3}$ (D-7)

$= 1.002 * 100 = 100.2$ g

where;

m_{CaCO3}: Amount of $CaCO_3$ to capture SO_2 originated from combustion of 1000 g of Tunçbilek coal, g
n_{CaCO3}: Mole of $CaCO_3$ to capture SO_2 originated from combustion of 1000 g of Tunçbilek coal, g
MW_{CaCO3}: Molecular weight of $CaCO_3$, (100 g/mole)

$m_{Limestone} = m_{CaCO3} / CaCO_3\% * 100$ (D-8)

$= 100.2 / 91.11 * 100 = \underline{110.0 \text{ g}}$

where;

$m_{Limestone}$: Amount of Çan limestone to capture SO_2 originated from combustion of 1000 g of Tunçbilek coal, g
$CaCO_3\%$: $CaCO_3$ percentage in Çan limestone (91.11 wt%) (see Table 4.5)

Amount of Çan limestone need (Ca/S = 3) to capture SO_2 emissions originated from combustion of 1 kg of Tunçbilek lignite coal = 110.0 g

Additionally, amount of $CaSO_4$ formed at the end of the overall removal reaction of SO_2 is calculated below:

1 mole CaO is formed from calcination of 1 mole $CaCO_3$ and 1 mole $CaSO_4$ is formed from sulfation of 1 mole CaO. Therefore, 1.002 mole CaO is formed from calcination of 1.002 mole $CaCO_3$ and 1.002 mole $CaSO_4$ is formed from sulfation of 1.002 mole CaO.

$m_{CaSO4} = n_{CaSO4} * MW_{CaSO4}$ (D-9)

$= 1.002 * 136 = \underline{136.3\ g}$

where;

m_{CaSO4}: Amount of $CaSO_4$ formed at the end of the overall removal reaction of SO_2 originated from combustion of 1000 g of Tunçbilek coal, g

n_{CaSO4}: Mole of $CaSO_4$ formed at the end of the overall removal reaction of SO_2 originated from combustion of 1000 g of Tunçbilek coal, g

MW_{CaSO4}: Molecular weight of $CaSO_4$ (136 g/mole)

APPENDIX E

EFFECT OF BIOMASS CONTENT ON SO_2 AND NO EMISSIONS

Calculation of theoretical SO_2 and NO emissions from combustion of Tunçbilek coal:

Theoretical SO_2 and NO emission concentrations from combustion of Tunçbilek lignite coal were calculated by following ways.

1. Way:

Combustible sulfur content of Tunçbilek lignite coal is 0.59% by weight. Therefore, 1 kg of Tunçbilek lignite coal contains 5.9 g of sulfur.

$n_S = m_S/MW_S$ (E-1)

$= 5.9 / 32 = 0.1844$ mole S/kg of coal

where;

m_S: Amount of S, g/kg coal
MW_S: Molecular weight of S, g/mole
n_S: Mole of S for 1 kg of coal, mole S/kg coal

1 mole SO_2 is formed from combustion of 1 mole of sulphur (S). Therefore 0.1844 mole SO_2/kg coal is formed from combustion of 0.1844 mole S/kg coal.

$m_{SO2} = n_{SO2} * MW_{SO2}$ (E-2)

= 0.1844 * 64 = **11.8 g SO_2/kg of coal**

where;

m_{SO2}: Amount of SO_2 coming from the combustion of 1 kg of coal, g

MW_{SO2}: Molecular weight of SO_2, g/mole

n_{SO2}: Mole of SO_2 coming from the combustion of coal, mole SO_2/kg coal

Nitrogen content of Tunçbilek lignite coal is 1.02% by weight. Therefore, 1 kg of Tunçbilek lignite coal contains 10.2 g of nitrogen.

$n_N = m_N/MW_N$ (E-3)

= 10.2 / 14 = 0.7286 mole N/kg of coal

where;

m_N: Amount of N, g/kg coal

MW_N: Molecular weight of N, g/mole

n_N: Mole of N for 1 kg of coal, mole N/kg coal

2 mole NO is formed from combustion of 1 mole nitrogen (N_2). Therefore 0.7286 mole NO/kg fuel is formed from combustion of 0.3643 mole N_2/kg fuel.

$m_{NO} = n_{NO} * MW_{NO}$ (E-4)

= 0.7286 * 30 = **21.9 g NO/kg of coal**

where;

m_{NO}: Amount of NO coming from the combustion of 1 kg of coal, g

MW_{NO}: Molecular weight of NO, g/mole

n_{NO}: Mole of NO coming from the combustion of coal, mole NO/kg coal

In Appendix D, volume of theoretical total flue gas was calculated as 4.578 Nm^3/kg of Tunçbilek lignite coal for an optimum excess air ratio of 1.2.

Therefore, theoretical SO_2 and NO emission concentrations from combustion of Tunçbilek lignite coal:

$C_{SO2,th} = m_{SO2} / V_{fluegas,th} * 1000$ (E-5)
$= 11.8 / 4.578 =$ **2577.5 mg/Nm^3**

where;

$C_{SO2,th}$: Theoretical SO_2 emission concentration from combustion of Tunçbilek lignite coal, mg/Nm^3
$V_{fluegas,th}$: Volume of theoretical total flue gas @ NTP, Nm^3/kg Tunçbilek lignite coal

$C_{NO,th} = m_{NO} / V_{fluegas,th} * 1000$ (E-6)
$= 21.9 / 4.578 =$ **4774.4 mg/Nm^3**

where;

$C_{NO,th}$: Theoretical NO emission concentration from combustion of Tunçbilek lignite coal, mg/Nm^3

2. Way:

In Appendix D, volume of total air flow was calculated as 4.170 Nm^3/kg of Tunçbilek lignite coal for an optimum excess air ratio of 1.2.

Therefore, theoretical SO_2 and NO emission concentrations from combustion of Tunçbilek lignite coal was found as:

$C_{SO2,th} = m_{SO2} / V_{air,\ actual} * 1000$ (E-7)
$= 11.8 / 4.170 =$ **2829.9 mg/Nm^3**

$C_{NO,th} = m_{NO} / V_{air,\ actual} * 1000$ (E-8)
$= 21.9 / 4.170 =$ **5241.5 mg/Nm^3**

These two SO_2 concentration values calculated (2577.5 mg/Nm^3, 2829.9 mg/Nm^3) and the SO_2 concentration measured in the experiments (2544.1 mg/Nm^3) are close to each other. However, there is an obvious difference between two NO concentration values calculated (4774.4 mg/Nm^3, 5241.5 mg/Nm^3) and the NO concentration measured in the experiments (1318.8 mg/Nm^3). This can be explained with complex conversion of coal nitrogen into NO. Nitrogen oxide formation and reduction do not occur in a straightforward manner.

In order to see the effect of biomass content in the fuel mixture, measured and expected concentrations of SO_2 and NO are compared in Table E.1 and Table E.2. Expected concentrations were calculated by taking the emission values of 100% by wt. coal combustion as a base. The SO_2 concentrations obtained during co-combustion coal and olive cake in 1 m - column are close to the expected values. On the other hand, the SO_2 concentrations obtained during co-combustion coal and olive cake in 2 m - column are lower than the expected values. This result shows that there is a synergistic effect between coal and olive cake in the SO_2 emission. The SO_2 emissions have decreased more than it should due to mixing of coal and olive cake together. This can be explained either by absorption of SO_2 by olive cake or by coal and olive cake ash. This effect has been seen more clearly in 2 m - column because of higher reaction time.

Additionally, positive effect of olive cake addition into the fuel mixture is obvious for NO emission. As it was stated before, this can be explained with the release of volatiles in olive cake particles leading to the high levels of hydrocarbon radicals and CO formation. Therefore, this causes a reducing atmosphere in the freeboard region. On the other hand, N in biomass can form NH_3 first. This formation can also help NO reduction due to some complex chain of reactions as referred in Afacan (2005).

Table E.1 SO_2 and NO emissions for the combustion and co-combustion of coal and olive cake in 1 m - combustion column

	Fuel	**1 m - column**		
		Measured	**Expected**	**% decrease**
SO_2 conc. (mg/Nm^3)	Coal 100 wt%	2544.1	-	-
	Coal 75 wt% + Olive Cake 25 wt%	2064.9	1908.1	-
	Coal 50 wt% + Olive Cake 50 wt%	1573.6	1272.1	-
	Coal 25 wt% + Olive Cake 75 wt%	703.7	636.0	-
	Olive Cake 100 wt%	442.0	0	-
NO conc. (mg/Nm^3)	Coal 100 wt%	1318.8	-	-
	Coal 75 wt% + Olive Cake 25 wt%	1211.3	1406.1	13.9
	Coal 50 wt% + Olive Cake 50 wt%	844.6	1493.3	43.4
	Coal 25 wt% + Olive Cake 75 wt%	672.3	1580.6	57.5
	Olive Cake 100 wt%	593.7	1667.9	64.4

Table E.2 SO_2 and NO emissions for the combustion and co-combustion of coal and olive cake in 2 m - combustion column

	Fuel	**2 m - column**		
		Measured	**Expected**	**% decrease**
SO_2 conc. (mg/Nm^3)	Coal 100 wt%	2371.8	-	-
	Coal 75 wt% + Olive Cake 25 wt%	1616.5	1778.1	9.1
	Coal 50 wt% + Olive Cake 50 wt%	909.8	1185.4	23.2
	Coal 25 wt% + Olive Cake 75 wt%	261.0	592.7	56.0
	Olive Cake 100 wt%	193.1	0	-
NO conc. (mg/Nm^3)	Coal 100 wt%	1215.8	-	-
	Coal 75 wt% + Olive Cake 25 wt%	1074.2	1296.3	17.1
	Coal 50 wt% + Olive Cake 50 wt%	941.8	1376.7	31.6
	Coal 25 wt% + Olive Cake 75 wt%	603.2	1457.2	58.6
	Olive Cake 100 wt%	492.4	1533.8	67.9

APPENDIX F

TEMPERATURE DATA AND CORRESPONDING EXCESS AIR RATIOS

Table F.1 Temperature data for the combustion of coal and olive cake in 1 m - column

Fuel	λ	TC1	TC2	TC3	TC4	TC5	TC6
% wt.		**°C**					
100% Coal	1.23	687.0	959.7	970.1	965.9	905.1	822.3
	1.31	633.4	944.5	950.0	950.4	903.1	818.0
	1.55	909.1	953.9	950.3	912.4	849.7	780.9
	1.67	821.4	908.4	910.7	912.4	859.4	788.6
	1.81	880.6	888.2	889.4	874.1	822.1	760.7
	1.90	868.6	873.4	848.0	804.2	764.2	709.8
	2.05	846.7	850.3	848.8	827.0	785.3	728.9
	2.13	838.6	842.7	846.6	841.3	799.6	742.5
100% Olive cake	1.26	816.3	906.9	870.2	929.4	905.0	839.1
	1.31	805.1	840.9	829.2	932.7	905.2	842.4
	1.46	817.9	842.2	850.5	920.2	900.4	835.2
	1.58	789.5	807.2	826.1	884.9	875.8	827.0
	1.77	815.5	830.9	847.0	905.9	893.5	836.3
	1.93	785.5	795.8	817.5	882.4	869.1	821.5
	1.99	800.9	815.2	835.1	889.9	878.0	825.9

Table F.2 Temperature data for the co-combustion of coal and olive cake in 1 m - column

Fuel	λ	TC1	TC2	TC3	TC4	TC5	TC6
% wt.		^{o}C					
75% Coal + 25% Olive cake	1.42	815.3	899.5	943.1	913.3	873.4	803.8
	1.58	921.6	976.5	838.7	850.0	810.0	748.3
	1.74	869.0	937.6	911.3	882.8	845.3	781.2
	1.92	876.2	876.9	781.9	792.7	766.7	714.0
	2.03	874.8	881.9	867.3	853.2	821.7	761.0
	2.12	848.7	850.3	856.5	864.1	839.6	780.2
	2.25	826.0	827.8	836.7	844.7	825.9	771.8
50% Coal + 50% Olive cake	1.39	896.5	945.8	850.7	891.7	857.6	790.1
	1.48	921.7	941.8	852.6	902.5	877.4	815.3
	1.62	913.0	937.9	812.7	848.0	819.5	760.0
	1.89	855.3	862.2	771.6	813.6	793.0	739.2
	1.96	878.4	888.2	829.7	863.6	838.3	778.9
	2.06	846.0	854.2	801.8	833.6	809.1	753.8
	2.11	836.6	841.3	835.5	856.7	838.6	784.5
	2.24	838.7	843.3	850.2	863.2	847.6	794.7
25% Coal + 75% Olive cake	1.39	740.6	940.0	901.1	949.2	916.6	849.6
	1.48	862.7	907.2	841.7	900.9	879.8	819.9
	1.72	794.0	865.8	808.5	868.1	847.4	787.5
	1.88	808.5	811.7	789.4	861.1	846.8	793.5
	2.11	758.9	775.3	759.8	824.5	807.8	748.2
	2.49	792.9	793.2	827.4	883.3	876.6	825.9

Table F.3 Temperature data for the combustion of coal and olive cake in 2 m - column

Fuel	λ	TC1	TC2	TC3	TC4	TC5	TC6	TC7	TC8	TC9
% wt.		^{o}C								
100 % Coal	1.45	910.2	917.4	919.4	893.0	847.9	786.3	708.8	663.7	581.8
	1.54	904.3	910.9	913.7	878.7	827.1	766.4	695.3	642.3	560.6
	1.79	852.9	862.1	864.7	803.6	757.6	704.7	645.8	579.5	505.3
	1.89	851.9	861.8	865.1	824.1	772.1	718.1	659.7	603.2	527.6
	1.97	849.3	858.0	862.4	837.3	783.5	728.1	669.5	620.4	544.2
	2.03	878.5	884.8	888.2	887.7	840.1	780.1	707.7	676.0	598.7
	2.07	844.7	853.7	857.7	845.1	792.3	737.0	678.1	637.4	561.2
	2.44	837.2	843.1	848.0	853.1	808.6	751.4	687.7	661.4	588.3
100 % Olive cake	1.20	826.09	865.2	860.7	932.0	927.4	874.0	776.5	726.5	631.8
	1.34	805.62	821.7	841.2	902.4	904.3	857.4	758.5	706.9	610.6
	1.42	831.49	850.7	861.1	916.8	917.9	869.9	770.7	719.4	622.0
	1.63	827.14	838.8	854.3	909.0	909.9	868.4	777.8	730.9	637.2
	1.90	805.33	819.0	838.6	899.1	891.1	835.0	722.3	665.7	553.2
	1.93	810.44	819.5	834.4	906.3	900.4	860.8	774.7	732.6	641.4
	2.34	794.17	805.3	822.6	886.7	879.9	834.4	732.0	683.3	578.2

Table F.4 Temperature data for the co-combustion of coal and olive cake in 2 m - column

Fuel	λ	**TC1**	**TC2**	**TC3**	**TC4**	**TC5**	**TC6**	**TC7**	**TC8**	**TC9**
% wt.		**^{o}C**								
75% Coal + 25% Olive cake	1.34	904.1	924.0	923.8	905.5	861.9	803.7	718.8	668.9	580.8
	1.59	897.0	906.2	904.6	852.1	813.3	761.5	690.8	642.3	561.4
	1.84	847.7	858.8	853.1	801.3	762.8	715.7	654.5	601.9	528.9
	1.98	828.2	839.1	841.1	808.9	769.2	721.7	661.5	618.6	546.5
	2.04	847.0	856.1	861.0	846.7	810.7	763.7	699.4	668.1	593.7
	2.22	812.4	822.9	828.0	808.4	771.4	726.2	669.0	634.8	564.5
	2.30	827.7	837.3	842.3	832.4	793.6	747.1	686.3	658.2	586.6
50% Coal + 50% Olive cake	1.44	877.4	890.0	893.8	896.9	860.5	809.4	727.2	691.1	603.4
	1.55	905.3	915.6	907.5	890.4	850.5	797.9	715.5	673.0	584.1
	1.75	858.8	868.3	860.7	851.8	803.1	748.4	675.3	621.1	535.4
	1.84	885.0	892.1	894.6	895.1	860.6	813.8	737.2	705.4	622.8
	1.95	845.1	855.0	855.3	863.6	822.0	771.1	697.1	658.9	575.9
	2.07	826.3	836.6	836.4	843.2	798.1	746.0	676.0	635.0	553.3
	2.14	813.6	823.4	828.3	850.3	814.2	766.3	696.8	666.0	586.9
	2.25	811.8	820.0	826.7	856.5	825.4	781.4	713.1	688.2	611.5
25% Coal + 75% Olive cake	1.43	868.7	884.2	869.1	863.9	848.4	796.0	715.4	668.0	598.2
	1.65	847.9	850.9	839.7	829.7	812.3	759.2	689.7	635.8	568.4
	1.73	859.3	875.4	867.1	874.7	858.9	815.2	736.1	701.3	633.6
	1.82	822.6	831.4	823.4	801.3	787.5	735.9	676.0	615.6	556.0
	1.83	829.9	841.5	840.6	834.0	817.0	766.9	697.7	652.0	589.4
	1.94	827.9	841.7	845.4	862.5	838.1	790.4	715.7	682.0	621.7
	2.06	789.2	799.9	807.9	808.2	787.6	736.1	676.2	627.3	571.7
	2.10	800.1	812.7	821.1	865.2	839.7	794.8	722.2	692.3	630.8